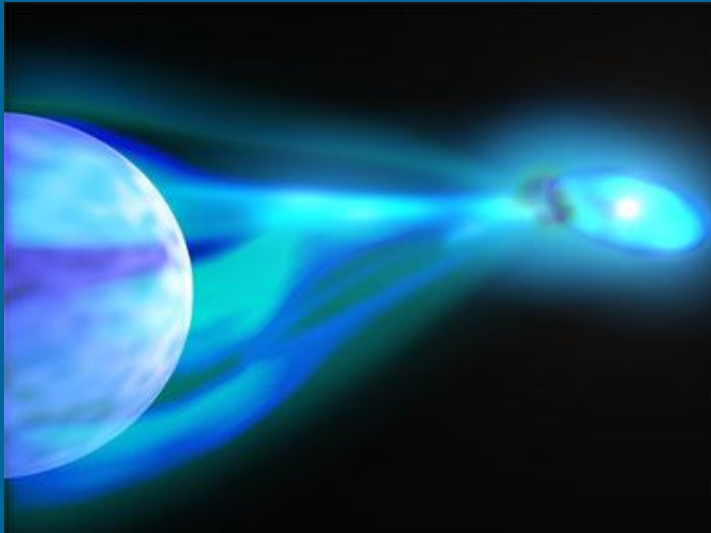
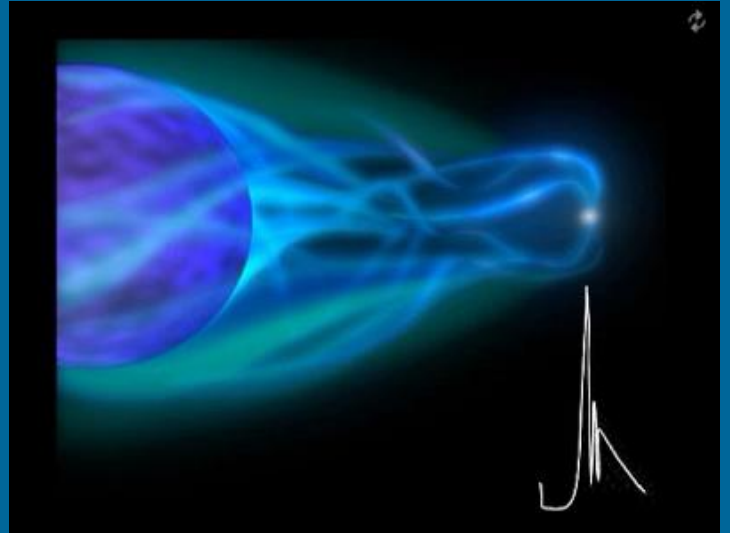


BH binaries

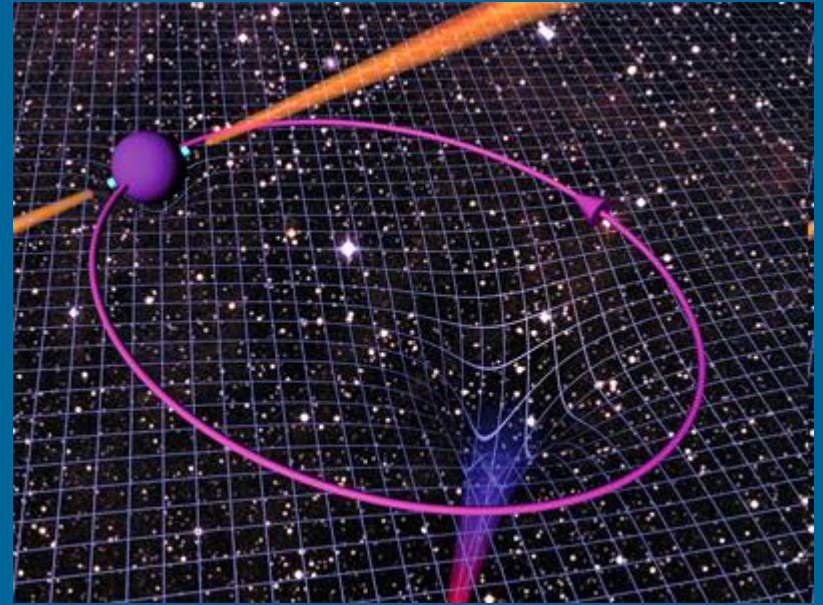
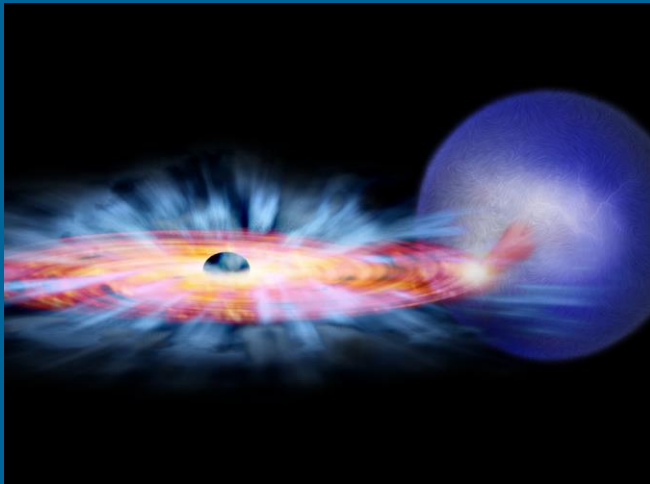


Black hole binaries

- High mass (few)
- Low-mass (majority)
- ULX – ultraluminous X-ray sources

Most of low-mass are transients.

Microquasars.



A hope for PSR+BH binary

- Either due to evolution
(one per several thousand normal PSRs)
- Either due to capture
(then – few in the central pc,
see arXiv: 1012.0573)

X-ray observations: Cyg X-1



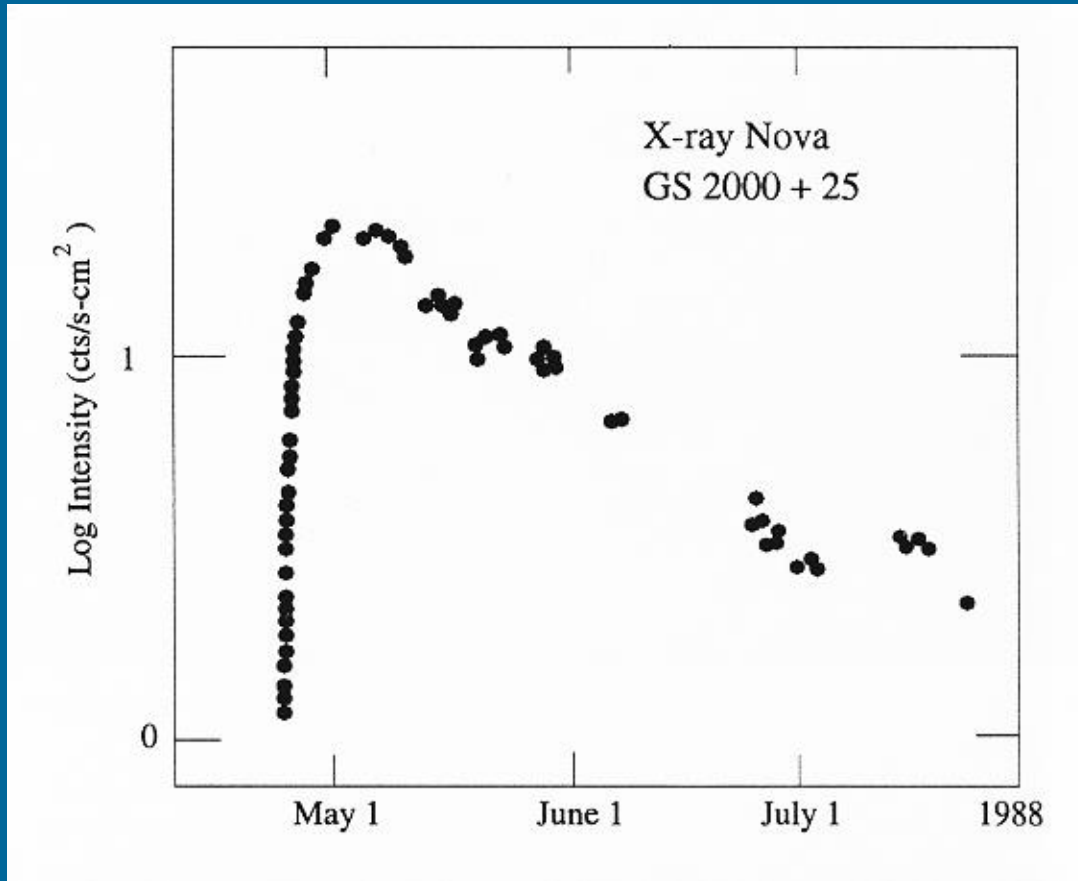
“In the case of Cyg X-1
black hole – is the most
conservative hypothesis”

Edwin Salpeter

The history of exploration
of binary systems with BHs
started about 40 years ago...

Recent mass measurement
for Cyg X-1 can be found in
[arXiv:1106.3689](https://arxiv.org/abs/1106.3689)

X-ray novae



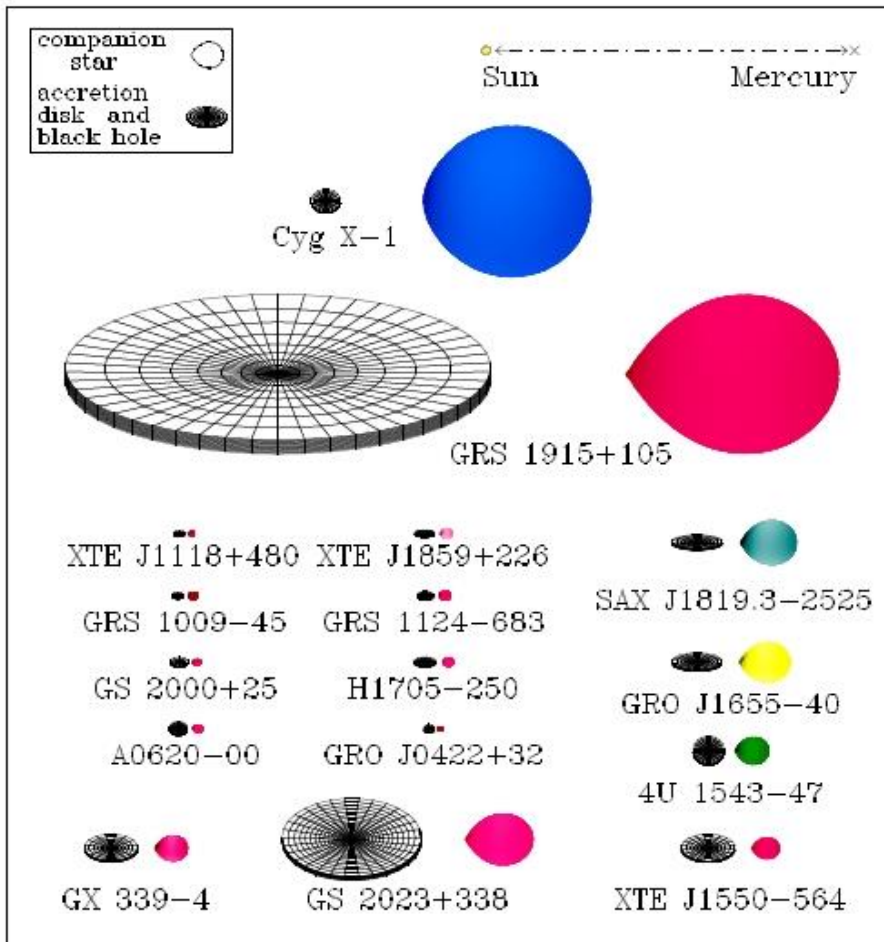
Low-mass binaries
with BHs

One of the best candidates

In the minimum it is
possible to see the
secondary companion,
and so to get a good mass
estimate for a BH.

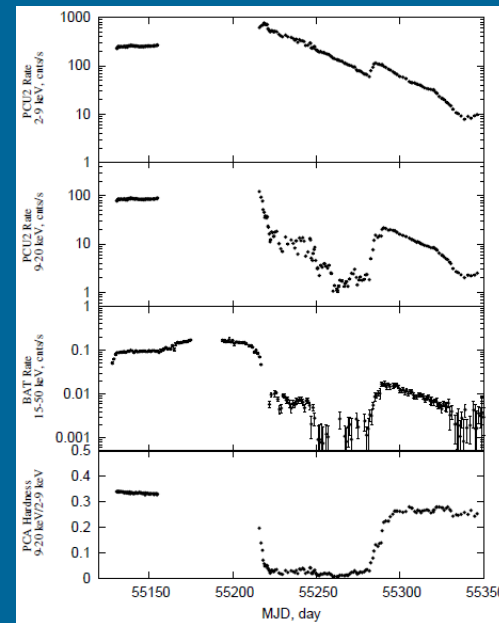
BH candidates

Black Hole Binaries in the Milky Way



Among 20 good galactic candidates
17 are X-ray novae.
3 belong to HMXBs
(Cyg X-1, LMC X-3, GRS 1915+105).

New candidates still appear.



Candidates properties

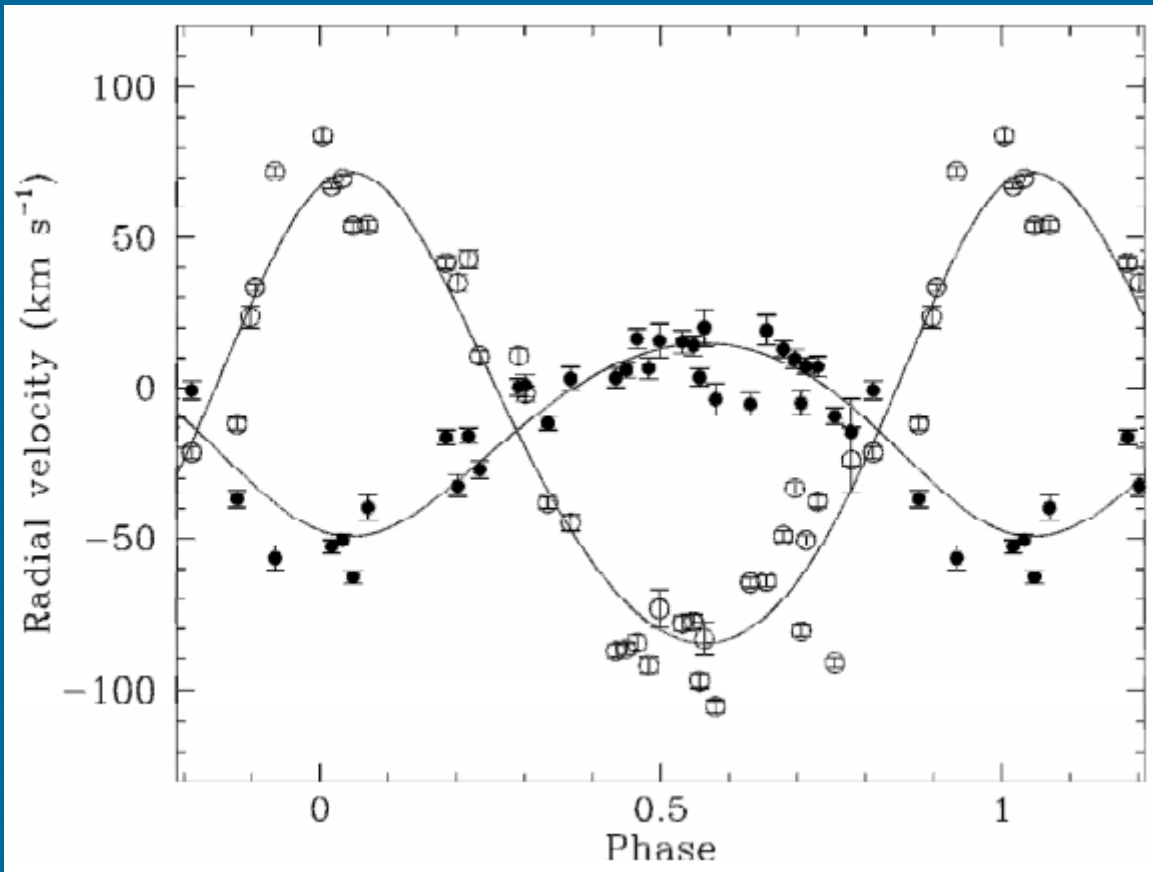
Table 1: Twenty confirmed black holes and twenty black hole candidates^a

Coordinate Name	Common ^b Name/Prefix	Year ^c	Spec.	P _{orb} (hr)	f(M) (M _⊙)	M ₁ (M _⊙)
0422+32	(GRO J)	1992/1	M2V	5.1	1.19±0.02	3.7–5.0
0538–641	LMC X–3	–	B3V	40.9	2.3±0.3	5.9–9.2
0540–697	LMC X–1	–	O7III	93.8 ^d	0.13±0.05 ^d	4.0–10.0: ^e
0620–003	(A)	1975/1 ^f	K4V	7.8	2.72±0.06	8.7–12.9
1009–45	(GRS)	1993/1	K7/M0V	6.8	3.17±0.12	3.6–4.7: ^e
1118+480	(XTE J)	2000/2	K5/M0V	4.1	6.1±0.3	6.5–7.2
1124–684	Nova Mus 91	1991/1	K3/K5V	10.4	3.01±0.15	6.5–8.2
1354–64 ^g	(GS)	1987/2	GIV	61.1 ^g	5.75±0.30	–
1543–475	(4U)	1971/4	A2V	26.8	0.25±0.01	8.4–10.4
1550–564	(XTE J)	1998/5	G8/K8IV	37.0	6.86±0.71	8.4–10.8
1650–500 ^h	(XTE J)	2001/1	K4V	7.7	2.73±0.56	–
1655–40	(GRO J)	1994/3	F3/F5IV	62.9	2.73±0.09	6.0–6.6
1659–487	GX 339–4	1972/10 ⁱ	–	42.1 ^{j,k}	5.8±0.5	–
1705–250	Nova Oph 77	1977/1	K3/7V	12.5	4.86±0.13	5.6–8.3
1819.3–2525	V4641 Sgr	1999/4	B9III	67.6	3.13±0.13	6.8–7.4
1859+226	(XTE J)	1999/1	–	9.2: ^e	7.4±1.1: ^e	7.6–12.0: ^e
1915+105	(GRS)	1992/Q ^l	K/MIII	804.0	9.5±3.0	10.0–18.0
1956+350	Cyg X–1	–	O9.7Iab	134.4	0.244±0.005	6.8–13.3
2000+251	(GS)	1988/1	K3/K7V	8.3	5.01±0.12	7.1–7.8
2023+338	V404 Cyg	1989/1 ^f	K0III	155.3	6.08±0.06	10.1–13.4

(astro-ph/0606352) Also there are about 20 “candidates to candidates”.

Detector MAXI recently added several new BH candidates

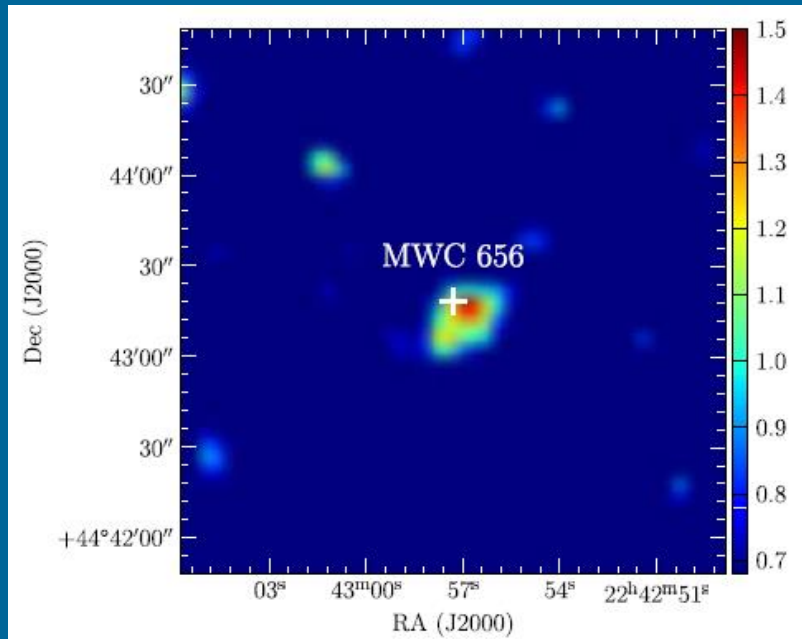
The first Be-BH binary in MWC 656



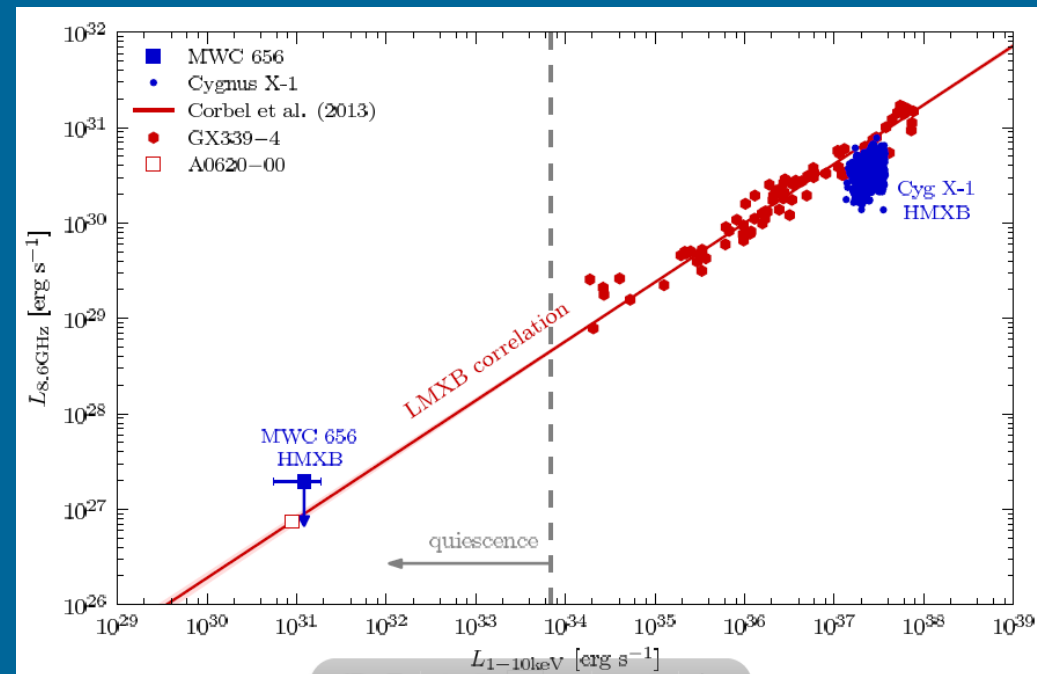
Compact object has a mass
3.8 – 6.9 Msolar.

X-ray luminosity is low

X-rays from MWC656

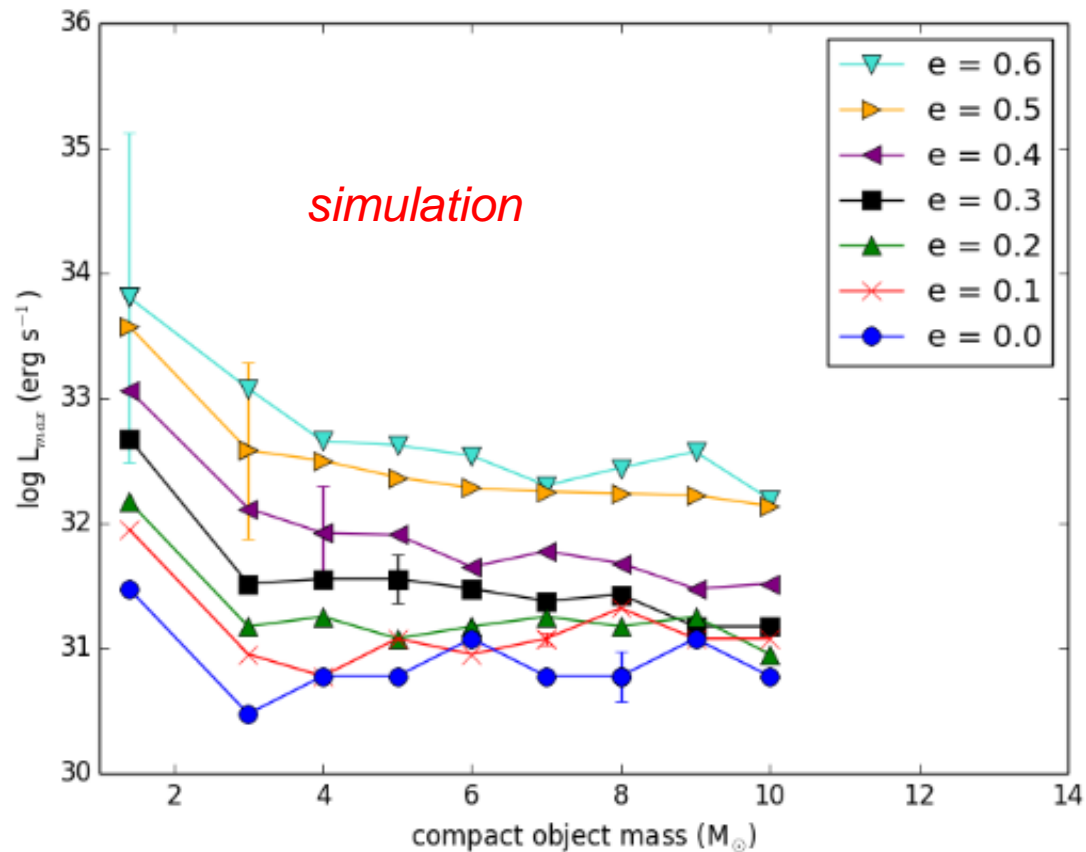


XMM-Newton

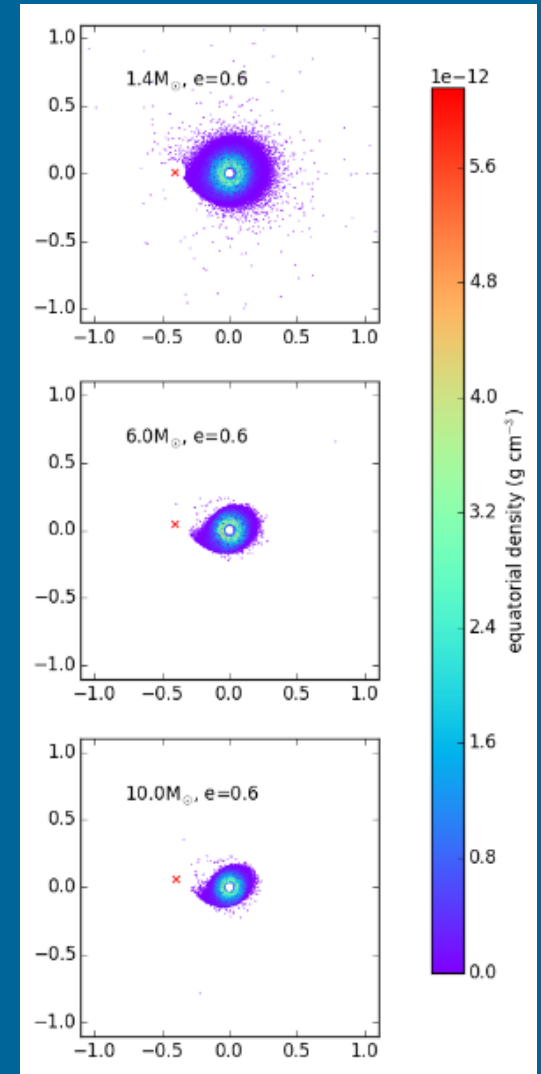


Became fainter since 2014.

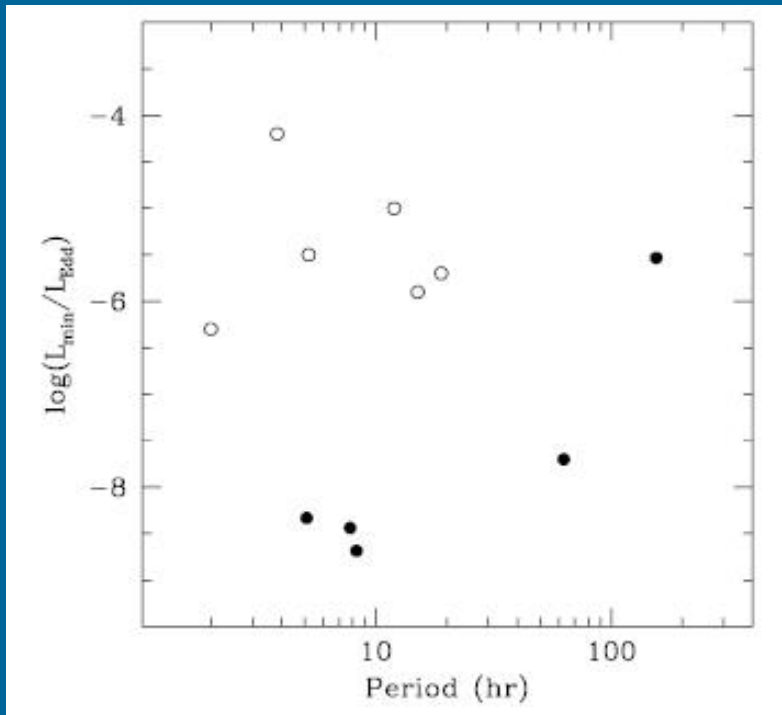
BH/Be are fainter than NS/Be



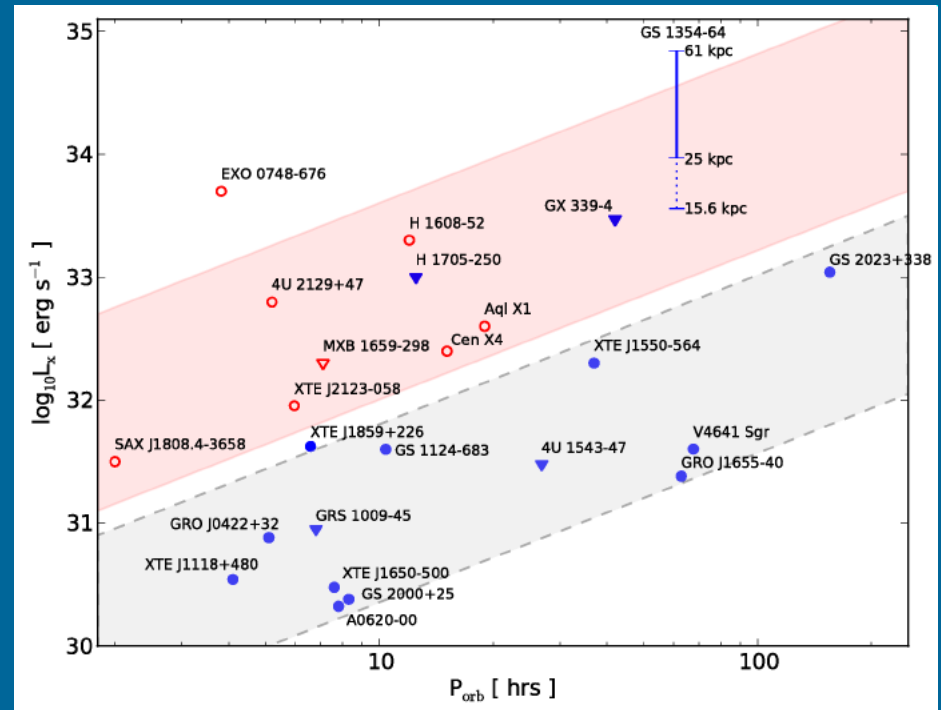
BH systems are fainter even for the same efficiency due to disc truncation. Lower efficiency can help to explain better why BH/Be systems are rarer than NS/Be.



Quescent luminosity vs. Orbital period

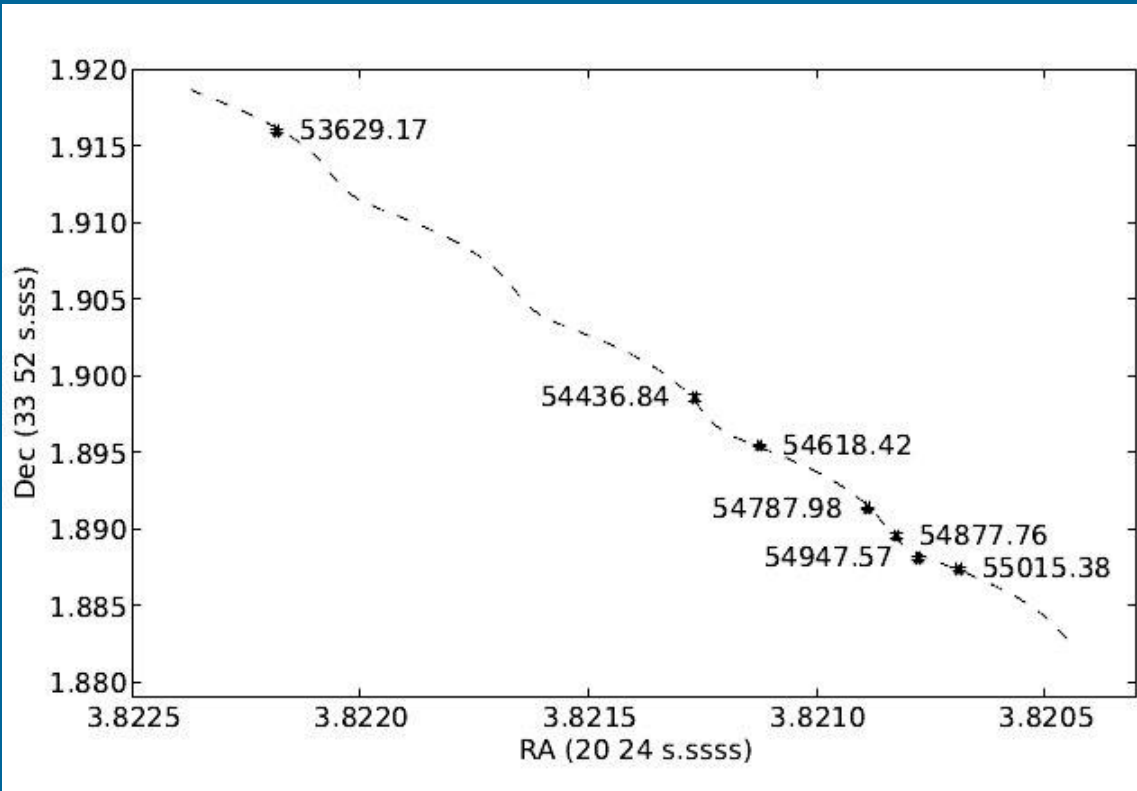


Open symbols – neutron stars
black symbols – black holes.



Red – NS systems.
Blue – BHs.
arXiv: 1105.0883

Distance to V404 Cyg



The parallax was measured.
The new distance estimate is 2.25-2.53 kpc.
It is smaller than before.
Correspondently, flares luminosity is lower, and so they are subEddington.

arXiv:0910.5253

Parallax is also measured for Cyg X-1 (arXiv:1106.3688)

Mass determination

$$f_v(m) \frac{m_x^3 \sin^3 i}{(m_x + m_v)^2} = 1,038 \cdot 10^{-7} K_v^3 P (1 - e^2)^{3/2},$$

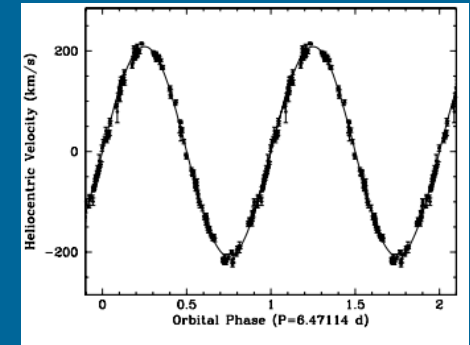
here m_x, m_v - masses of a compact object and of a normal (in solar units), K_v – observed semi-amplitude of the line of sight velocity of the normal star (in km/s), P – orbital period (in days), e – orbital eccentricity, i – orbital inclination (the angle between the line of sight and the normal to the orbital plane).

As one can see, the mass function of the normal star is the absolute lower limit for the mass of the compact object.

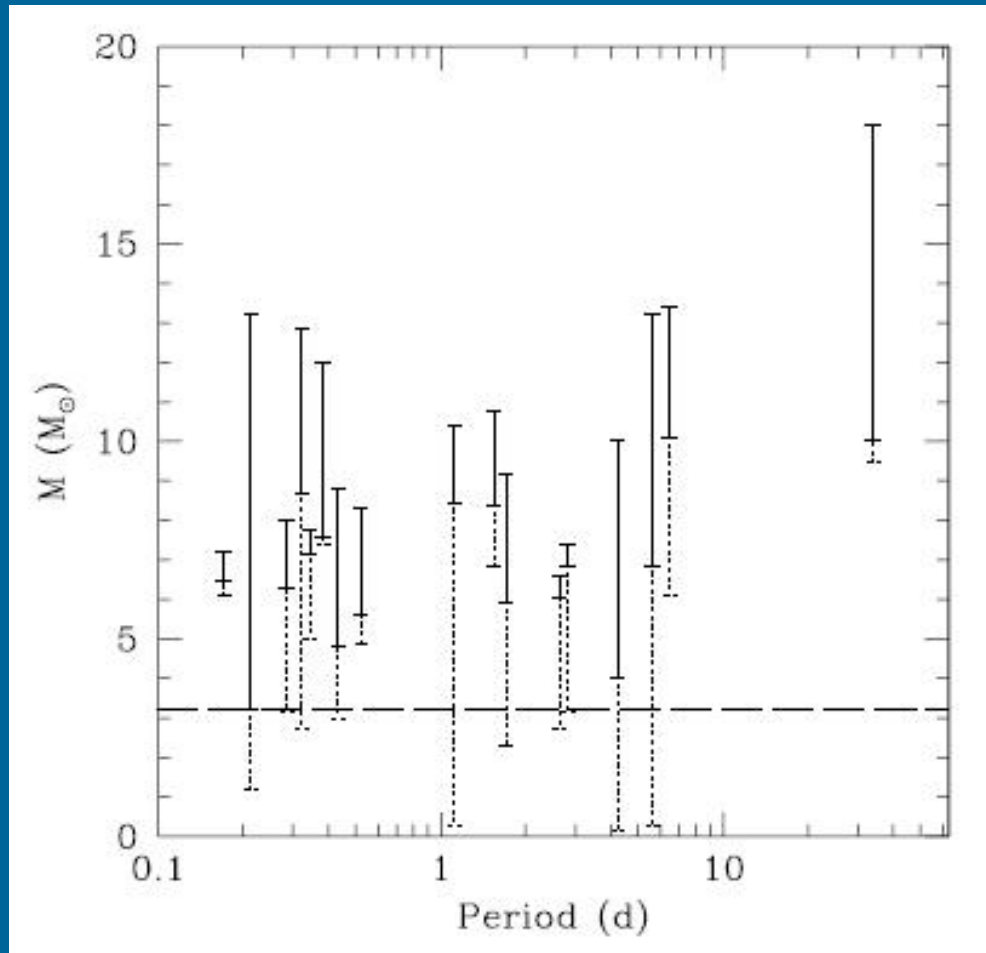
The mass of the compact object can be calculated as:

$$m_x = f_v(m) \left(1 + \frac{m_v}{m_x}\right)^2 \frac{1}{\sin^3 i}.$$

So, to derive the mass of the compact object in addition to the line of sight velocity it is necessary to know independently two more parameters: the mass ratio $q = m_x/m_v$, and the orbital inclination i .



Black hole masses



The horizontal line corresponds to the mass equal to 3.2 solar.

New technics are used to determine BH masses in binaries. For example, reverberation mapping was used for Cyg X-1 (1906.08266). The result ($16 \pm 5 M_{\text{sun}}$) is compatible with dynamical measurements.

Some more results on masses

Paredes
arXiv: 0907.3602

System	P_{orb} [days]	$f(M)$ [M_{\odot}]	Donor Spect. Type	Classification	M_x [M_{\odot}]
GRS 1915+105	33.5	9.5 ± 3.0	K/M III	LMXB/Transient	14 ± 4
V404 Cyg	6.471	6.09 ± 0.04	K0 IV	"	12 ± 2
Cyg X-1	5.600	0.244 ± 0.005	09.7 Iab	HMXB/Persistent	10 ± 3
M33 X-7 ^a	3.453	—	O7 III	—	15.65 ± 1.45
LMC X-1	4.229	0.14 ± 0.05	07 III	"	> 4
XTE J1819-254	2.816	3.13 ± 0.13	B9 III	IMXB/Transient	7.1 ± 0.3
GRO J1655-40	2.620	2.73 ± 0.09	F3/5 IV	"	6.3 ± 0.3
BW Cir	2.545	5.74 ± 0.29	G5 IV	LMXB/Transient	> 7.8
GX 339-4	1.754	5.8 ± 0.5	—	"	—
LMC X-3	1.704	2.3 ± 0.3	B3 V	HMXB/Persistent	7.6 ± 1.3
XTE J1550-564	1.542	6.86 ± 0.71	G8/K8 IV	LMXB/Transient	9.6 ± 1.2
IC 10 X-1 ^b	1.455	7.64 ± 1.26	—	Wolf-Rayet	32.7 ± 2.6
4U 1543-475	1.125	0.25 ± 0.01	A2 V	IMXB/Transient	9.4 ± 1.0
H1705-250	0.520	4.86 ± 0.13	K3/7 V	LMXB/Transient	6 ± 2
GS 1124-684	0.433	3.01 ± 0.15	K3/5 V	"	7.0 ± 0.6
XTE J1859+226	0.382	7.4 ± 1.1	—	"	—
GS2000+250	0.345	5.01 ± 0.12	K3/7 V	"	7.5 ± 0.3
A0620-003	0.325	2.72 ± 0.06	K4 V	"	11 ± 2
XTE J1650-500	0.321	2.73 ± 0.56	K4 V	"	—
GRS 1009-45	0.283	3.17 ± 0.12	K7/M0 V	"	5.2 ± 0.6
GRO J0422+32	0.212	1.19 ± 0.02	M2 V	"	4 ± 1
XTE J1118+480	0.171	6.3 ± 0.2	K5/M0 V	"	6.8 ± 0.4

M33 X-7 $15.65 \pm 1.45 M_{\text{Solar}}$ (Orosz et al. 2007).

Eclipsing binary IC10 X-1 32 ± 2.6 (Silverman and Filippenko 2008)

Systems BH + radio pulsar: a Holy Grail

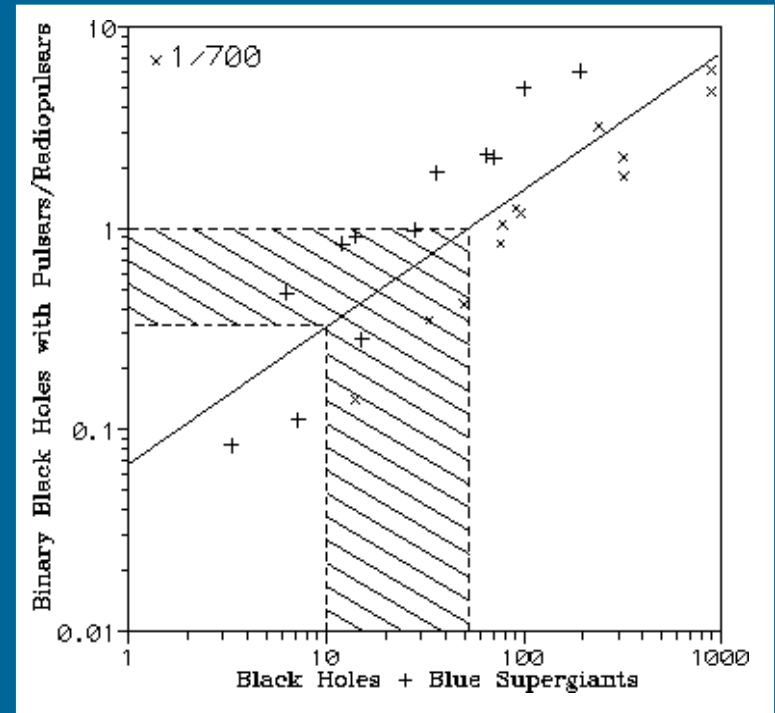
The discovery of a BH in pair with a radio pulsar can provide the most direct proof of the very existence of BHs.

Especially, it would be great to find a system with a millisecond pulsar observed close to the orbital plane.

Computer models provide different estimates of the abundance of such systems.

Lipunov et al (1994) give an estimate about one system (with a PSR of any type) per 1000 isolated PSRs.

Pfahl et al. (astro-ph/0502122) give much lower estimate for systems BH+mPSR: about 0.1-1% of the number of binary NSs. This is understandable, as a BH should be born by the secondary (i.e. initially less massive) component of a binary system.



What can be done with such systems if they are detected by SKA was studied recently in 1409.3882. Mainly related to gravity tests.

BH+pulsar binaries and FAST

Birth rate of NS+BH binaries $\sim 0.6\text{--}13 \text{ Myr}^{-1}$

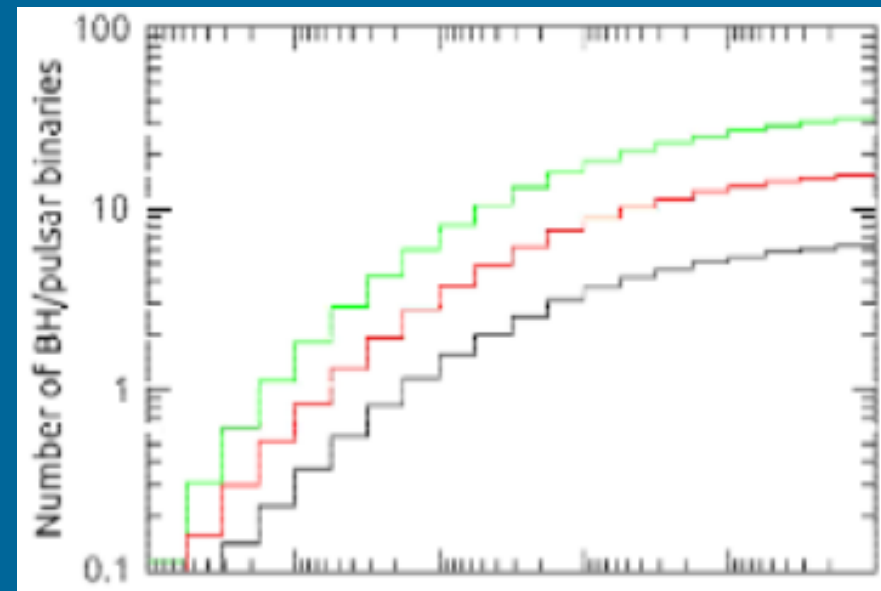
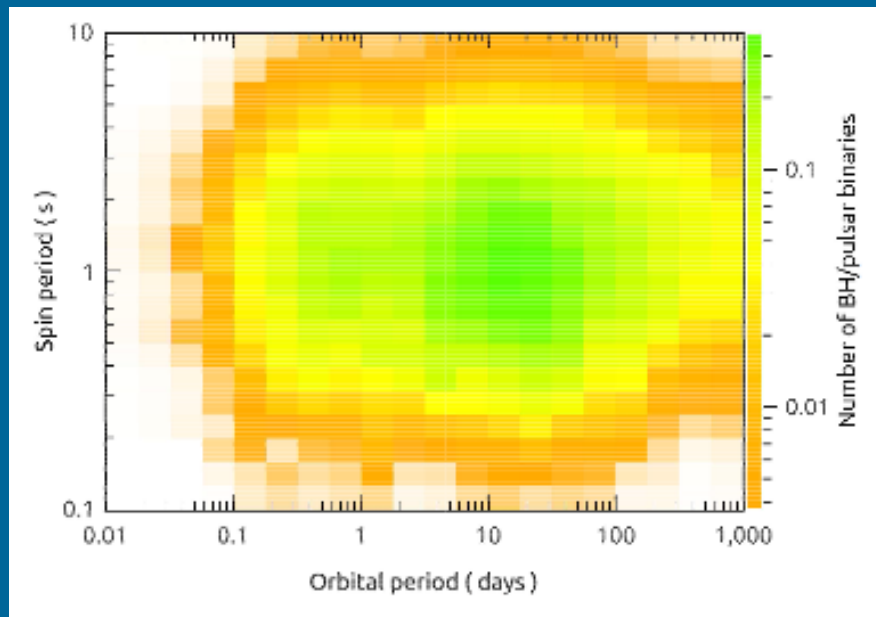
Thus, $\sim 10^4\text{--}10^5$ in the Galaxy.

Difficult to have a msecPSR.

Thus, typical spin periods $\sim 1 \text{ s}$.

3-80 BH+PSR binaries.

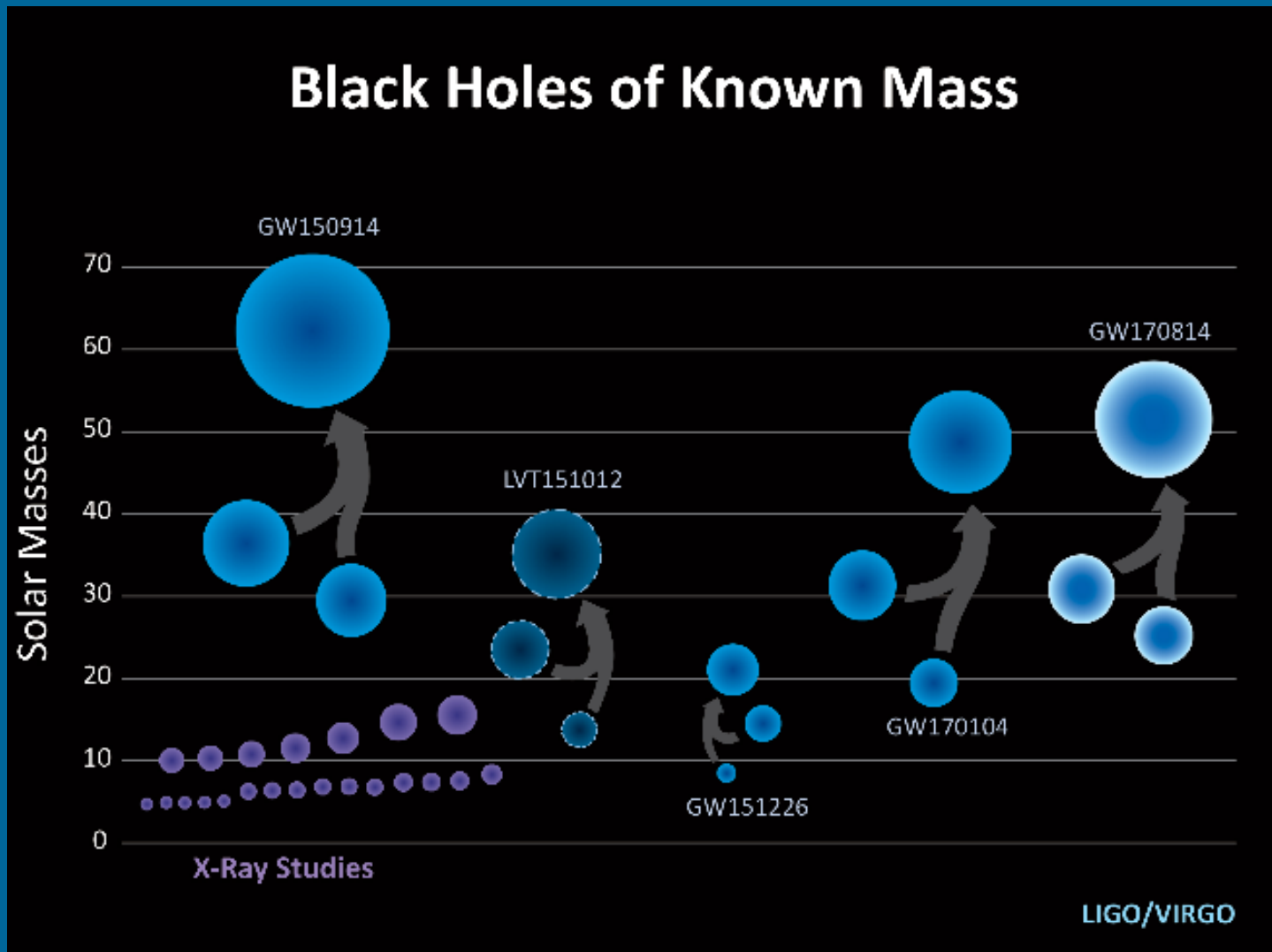
$\sim 10\%$ of them can be detected by FAST.



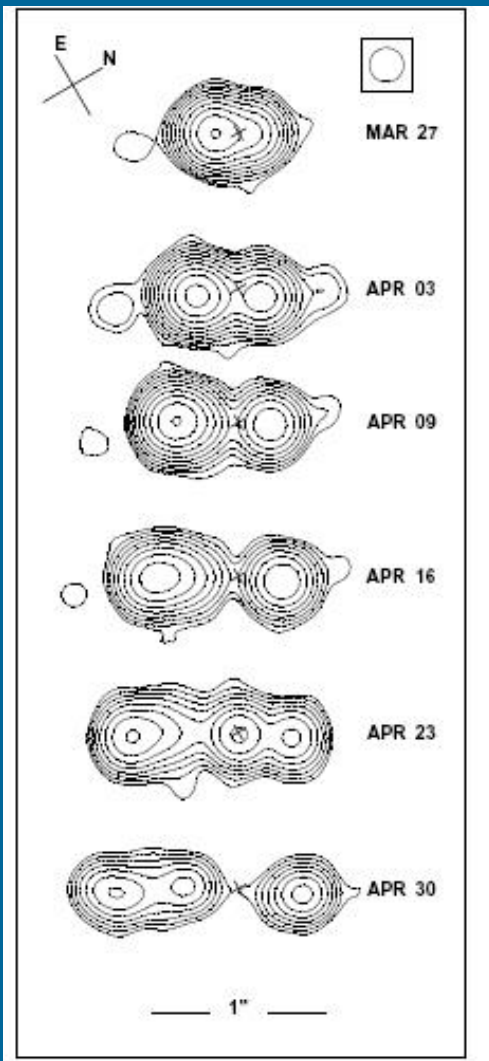
Flux density at 1.4 GHz (mJy)

$$\sigma_{\text{NS_kick}} = 150 \text{ km/s}$$

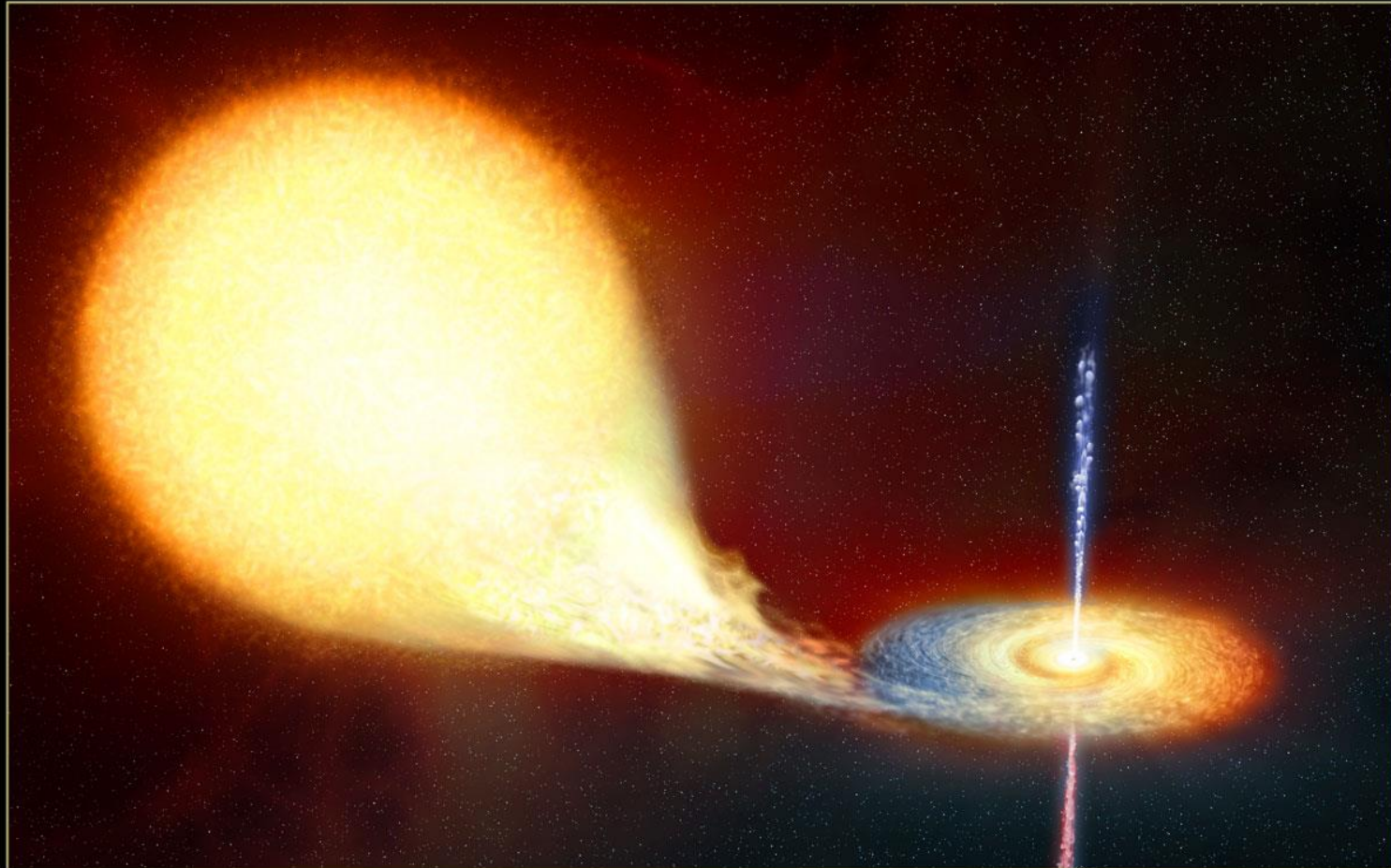
BH+BH. Coalescence.



Jet from GRS 1915+105



VLA data. Wavelength 3.5 cm.



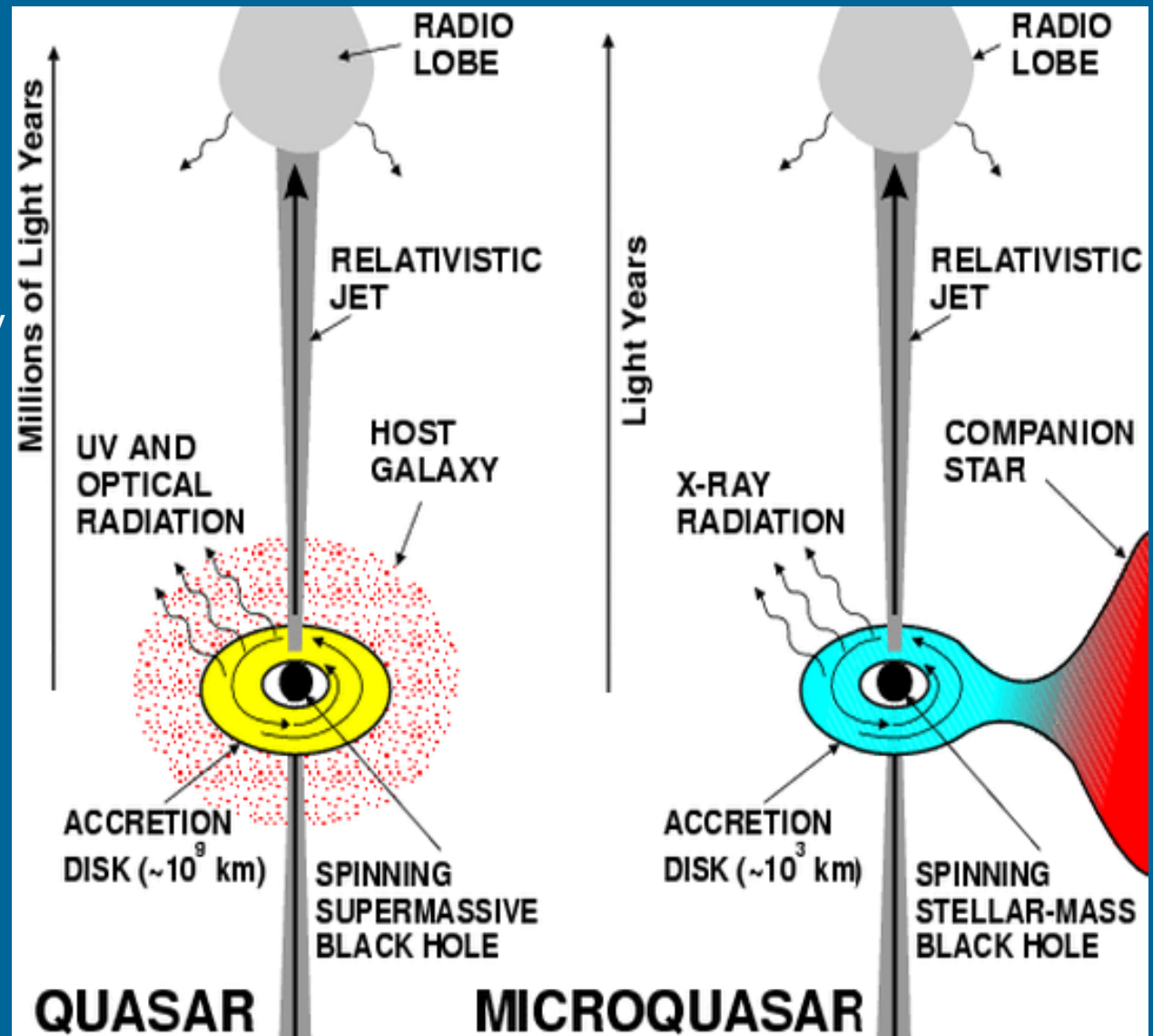
MICROQUASAR

©2004 European Space Agency
www.esa.int/sci/msp

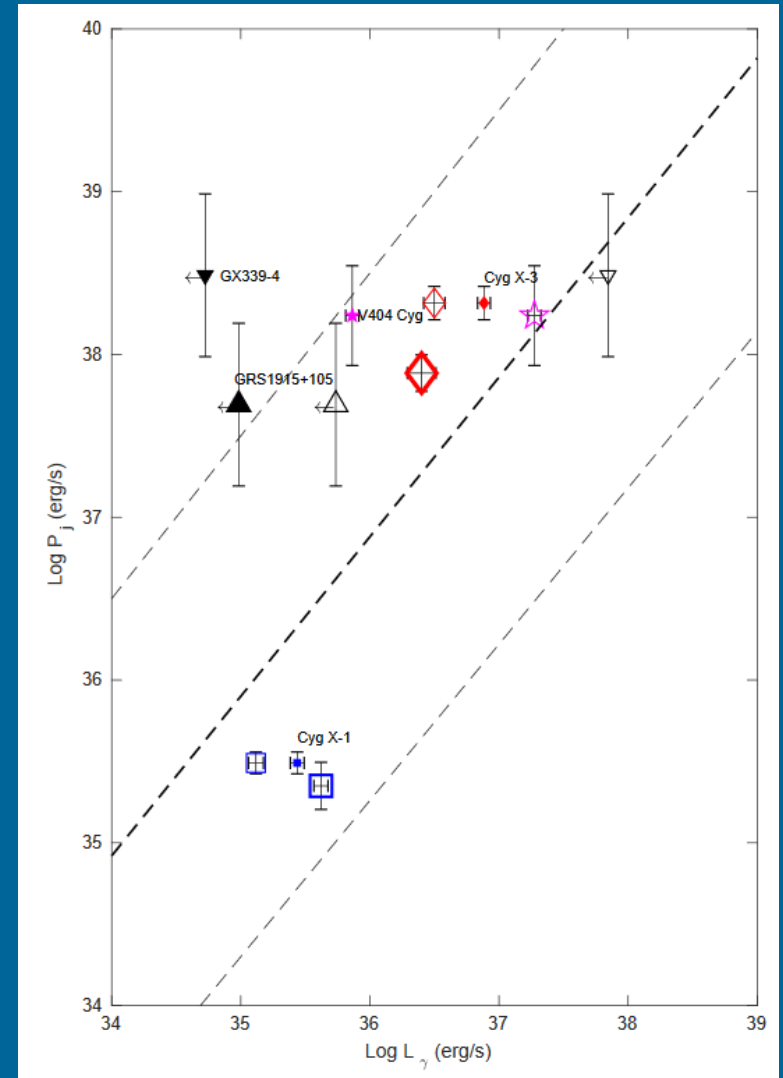
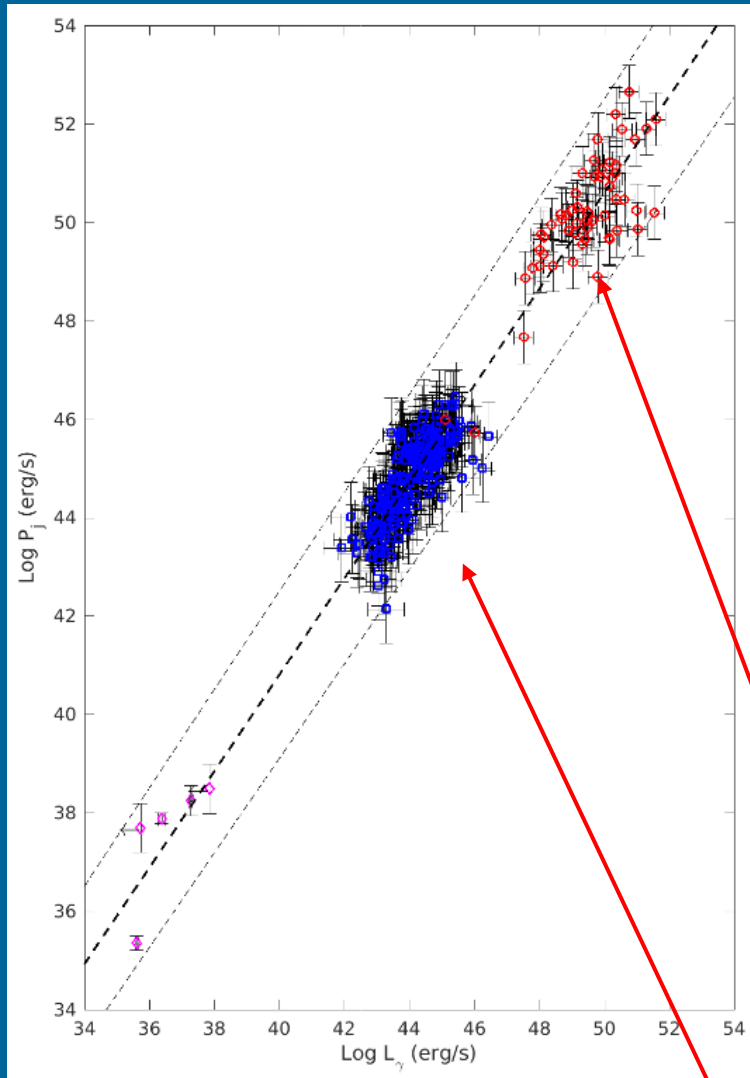
See a brief review in 1106.2059

$T \sim 10^7 \text{ K M}^{-1/4}$ —
last stable orbit
temperature at
Eddington luminosity

Optics/UV – QSO
X-ray - μ QSO



Jet-luminosity relation

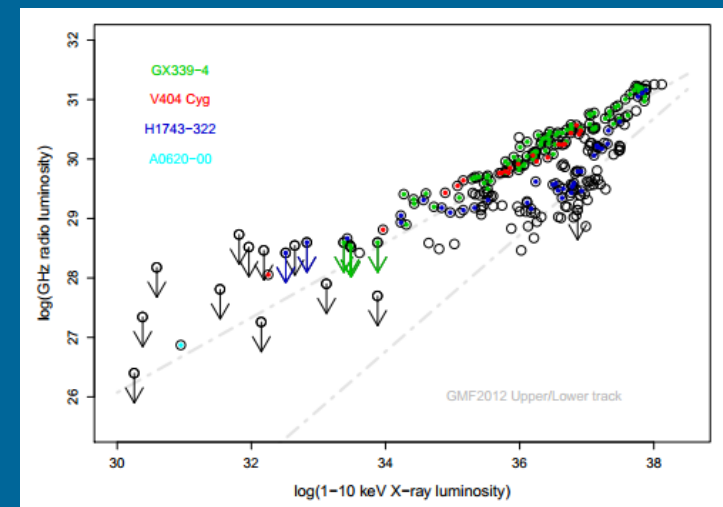
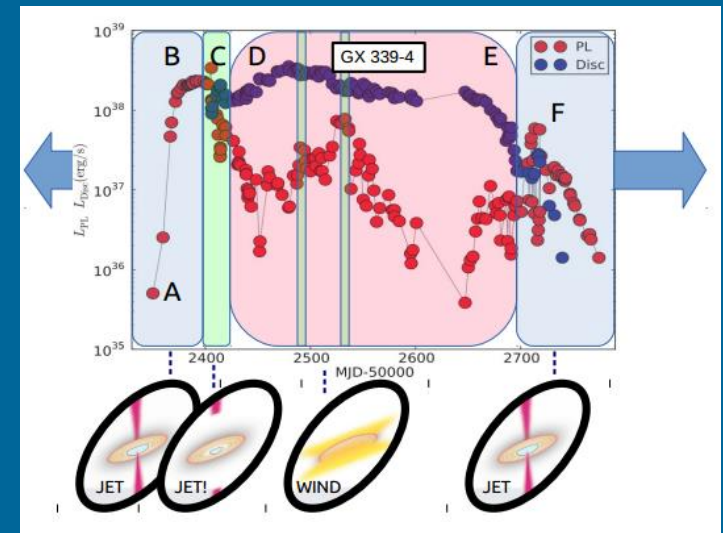
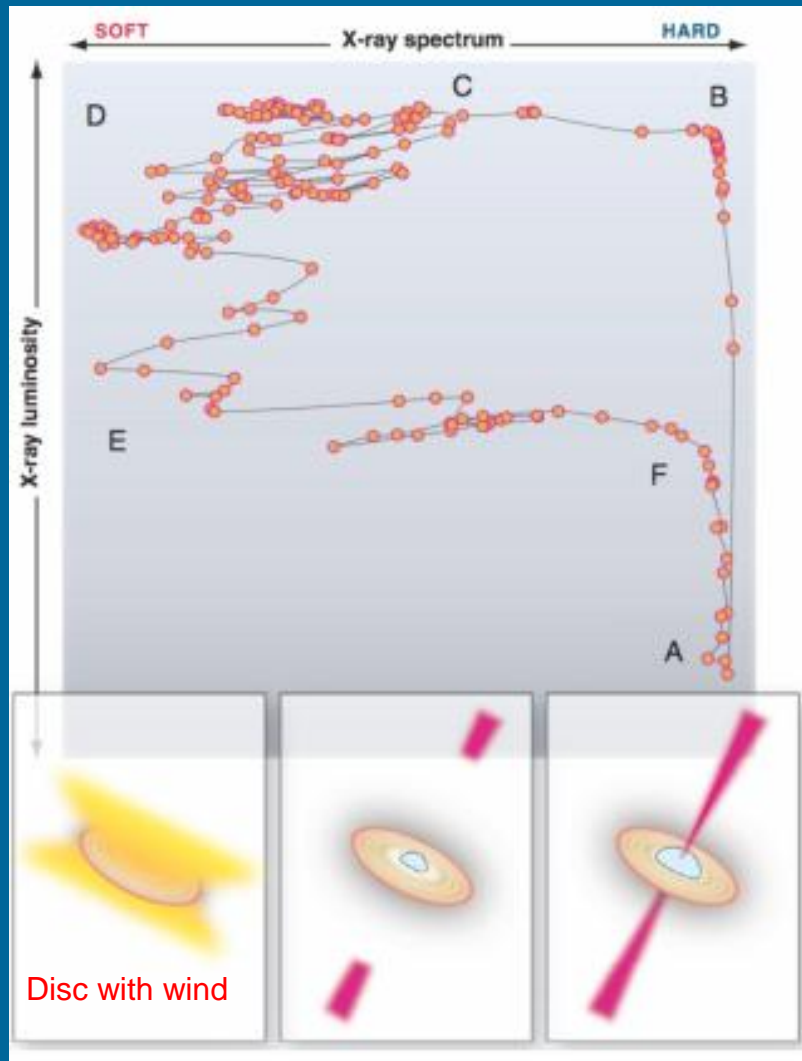


1705.09191

Blazars

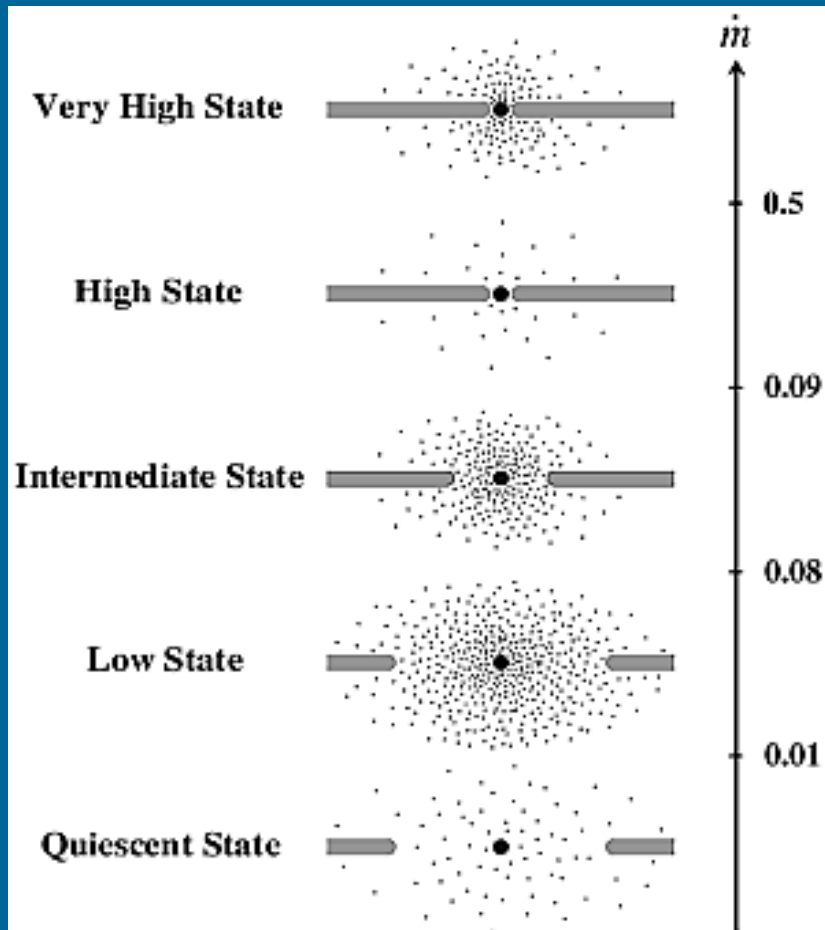
GRBs

Jets behaviour in BH binaries



A large review can be found in 1407.3674

States (luminosity+spectrum+jet+variability)



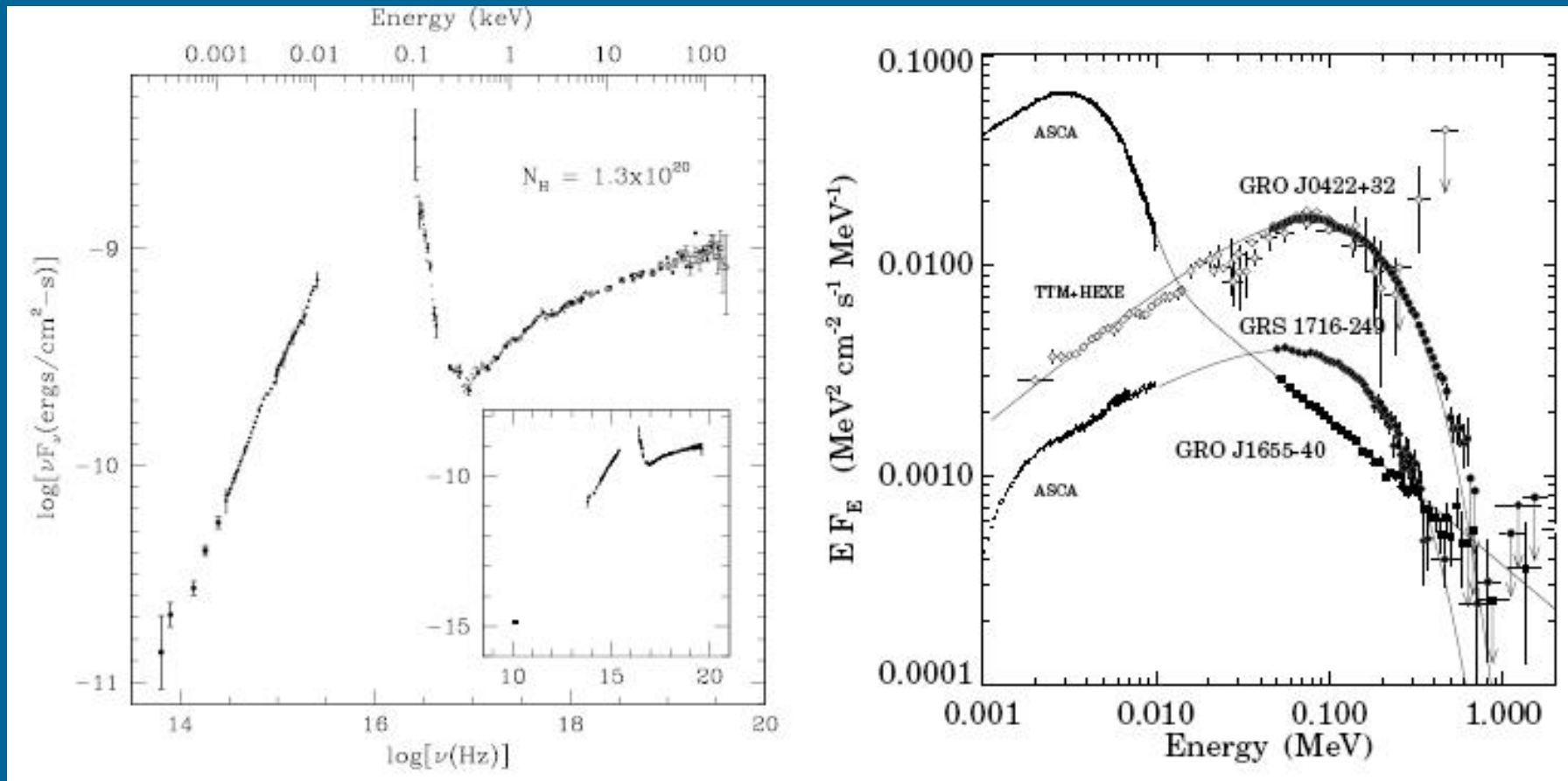
The understanding that BH binaries can pass through different “states” (characterized by luminosity, spectrum, and other features, like radio emission) appeared in 1972 when Cyg X-1 suddenly showed a drop in soft X-ray flux, rise in hard X-ray flux, and the radio source was turned on.

Now there are several classifications of states of BH binaries.

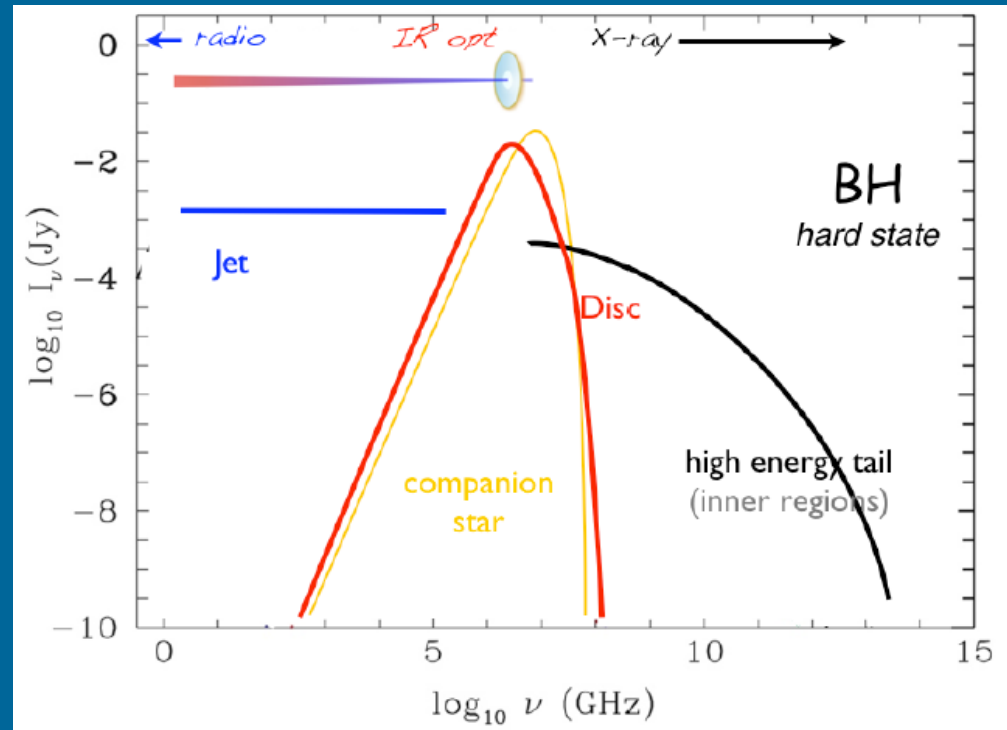
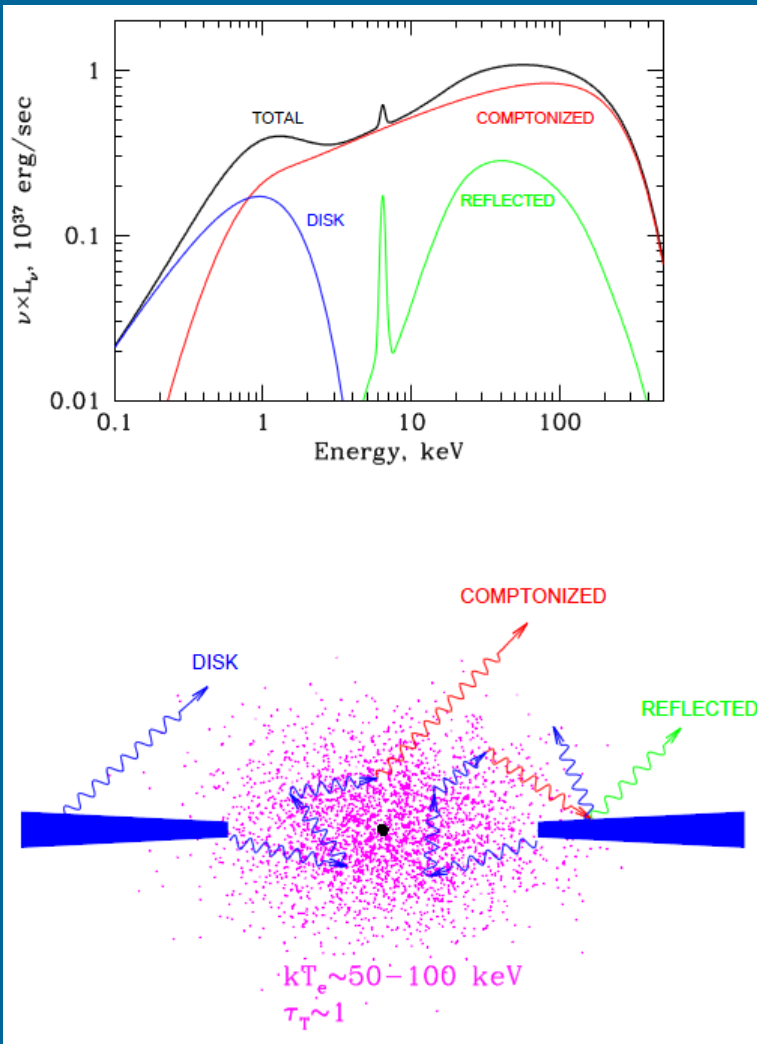
[astro-ph/0306213](https://arxiv.org/abs/astro-ph/0306213) McClintock, Remillard
Black holes on binary systems

Accretion onto BHs was reviewed in details in 1304.4879

Spectra of BH candidates



Different components of a BH spectrum



Accretion geometry
and photon paths at
the hard state

1104.0097

0909.2567

Three-state classification

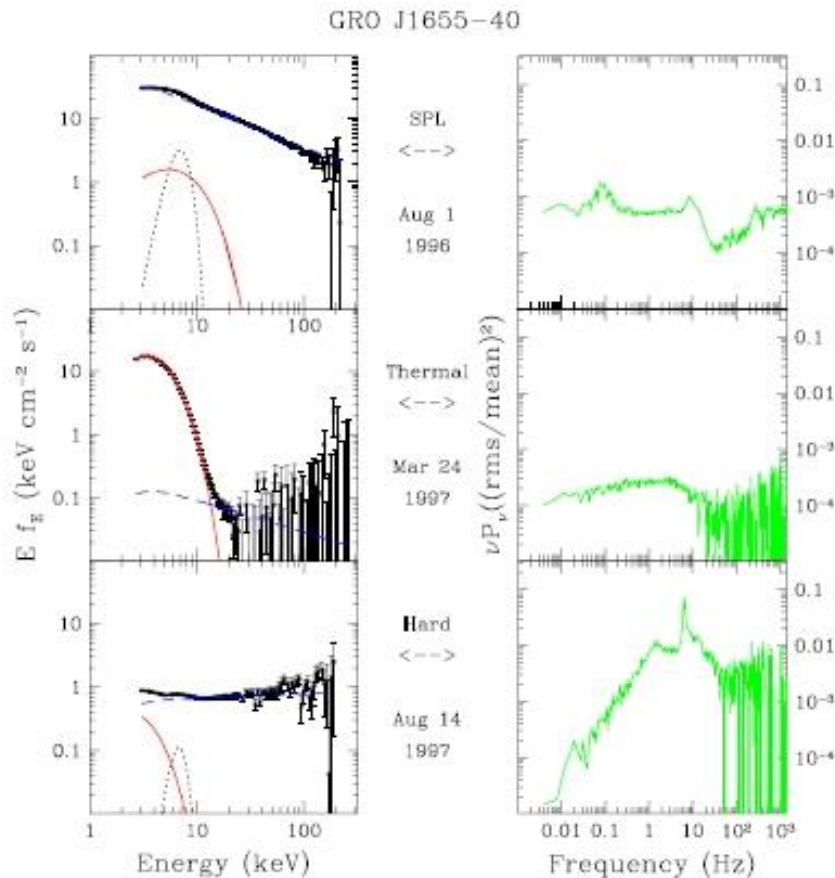
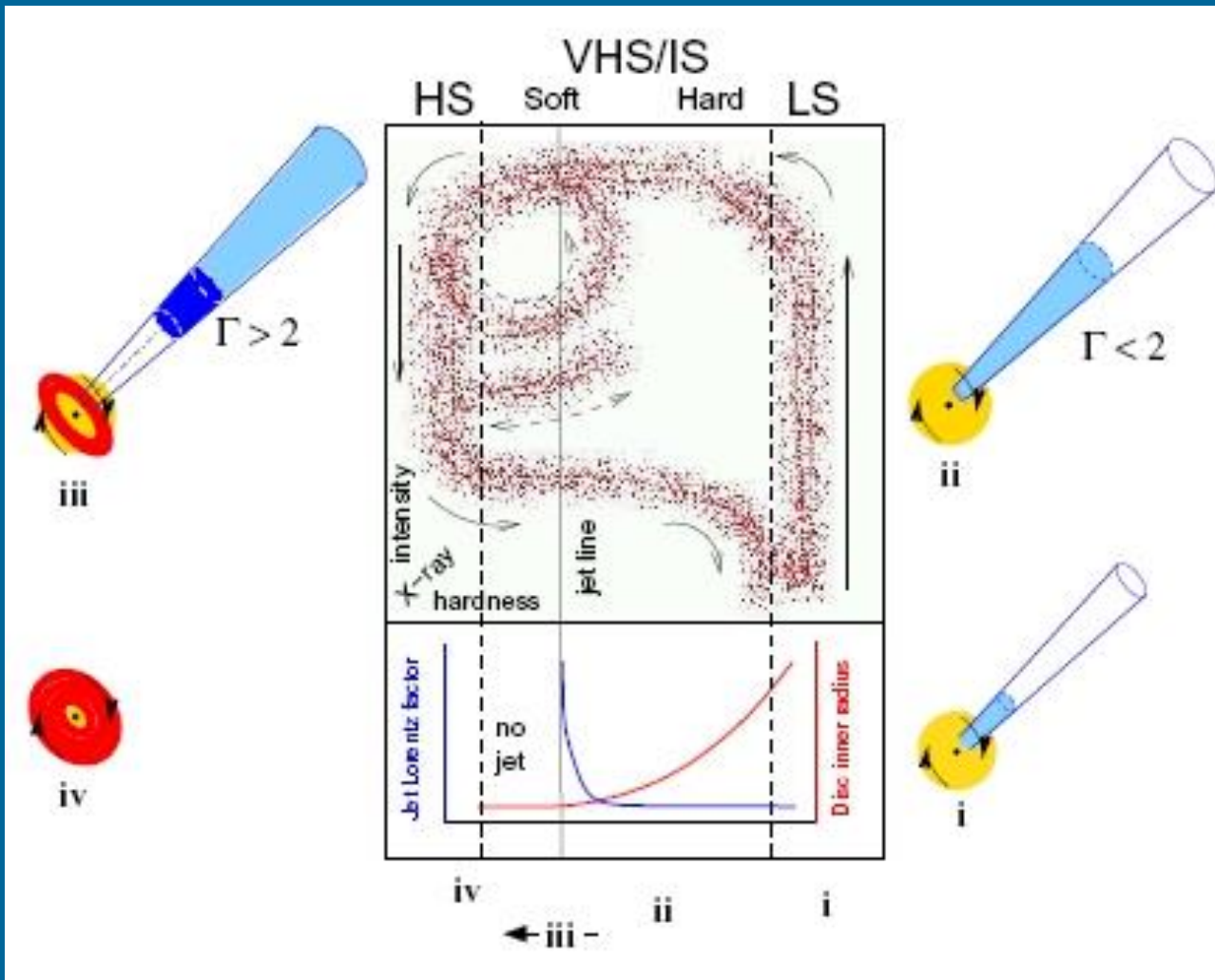


Table 2: Outburst states of black holes: nomenclature and definitions

New State Name (Old State Name)	Definition of X-ray State ^a
Thermal (High/Soft)	Disk fraction $f^b > 75\%$ QPOs absent or very weak: $a_{\text{max}}^c < 0.005$ Power continuum level $r^d < 0.075^e$
Hard (Low/Hard)	Disk fraction $f^b < 20\%$ (i.e., Power-law fraction $> 80\%$) $1.4^f < \Gamma < 2.1$ Power continuum level $r^d > 0.1$
Steep Power Law (SPL) (Very high)	Presence of power-law component with $\Gamma > 2.4$ Power continuum level $r^d < 0.15$ <i>Either</i> $f^b < 0.8$ and 0.1–30 Hz QPOs present with $a^c > 0.01$ <i>or</i> disk fraction $f^b < 50\%$ with no QPOs

In this classification the luminosity is not used as one of parameters.

Discs and jets

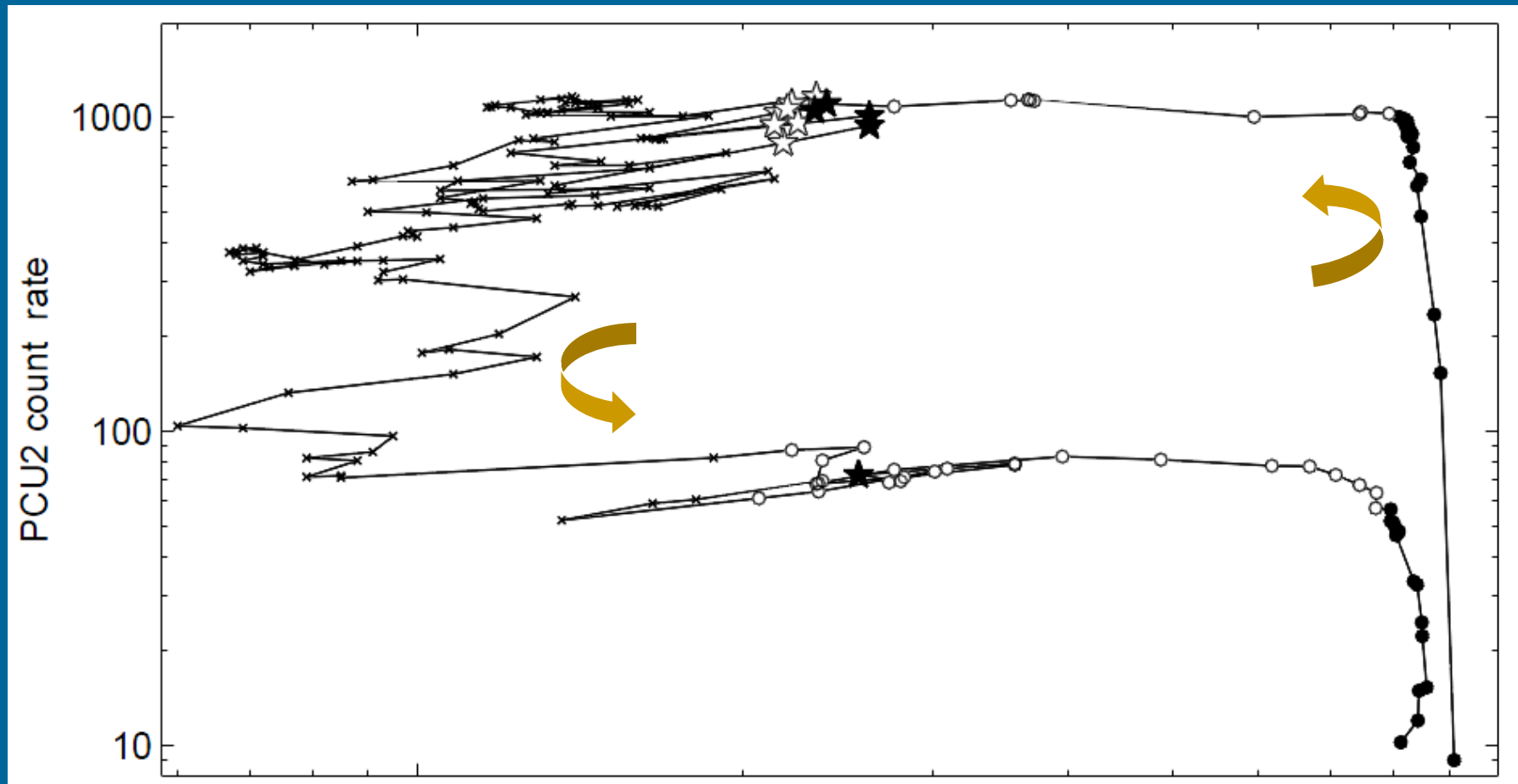


The model for systems with radio jets

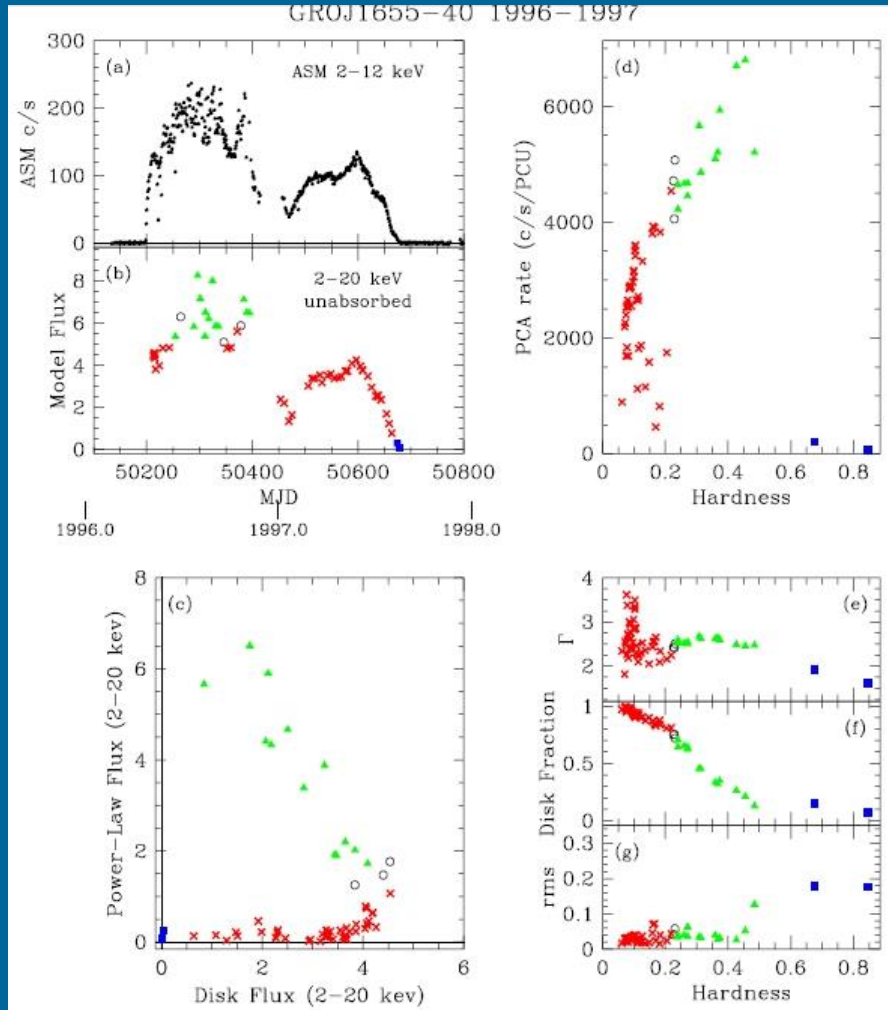
LS – low/hard state
HS – high/soft state
VHS/IS – very high and intermediate states

The shown data are for the source GX 339-4.

Hardness vs. flux: state evolution

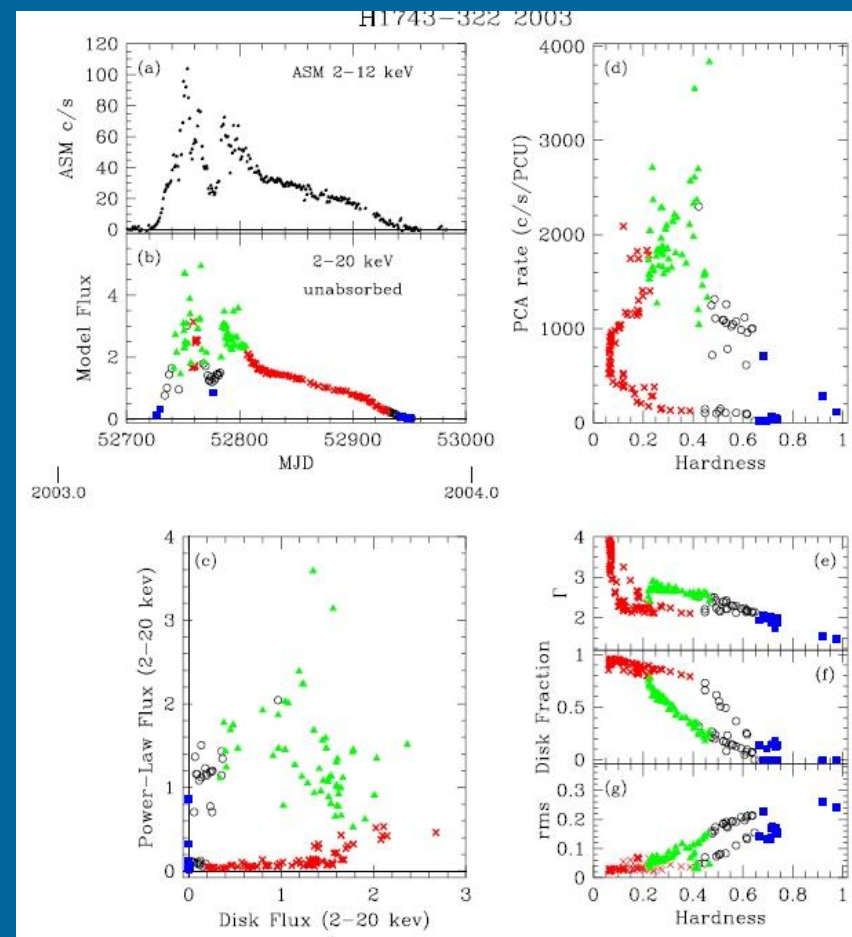
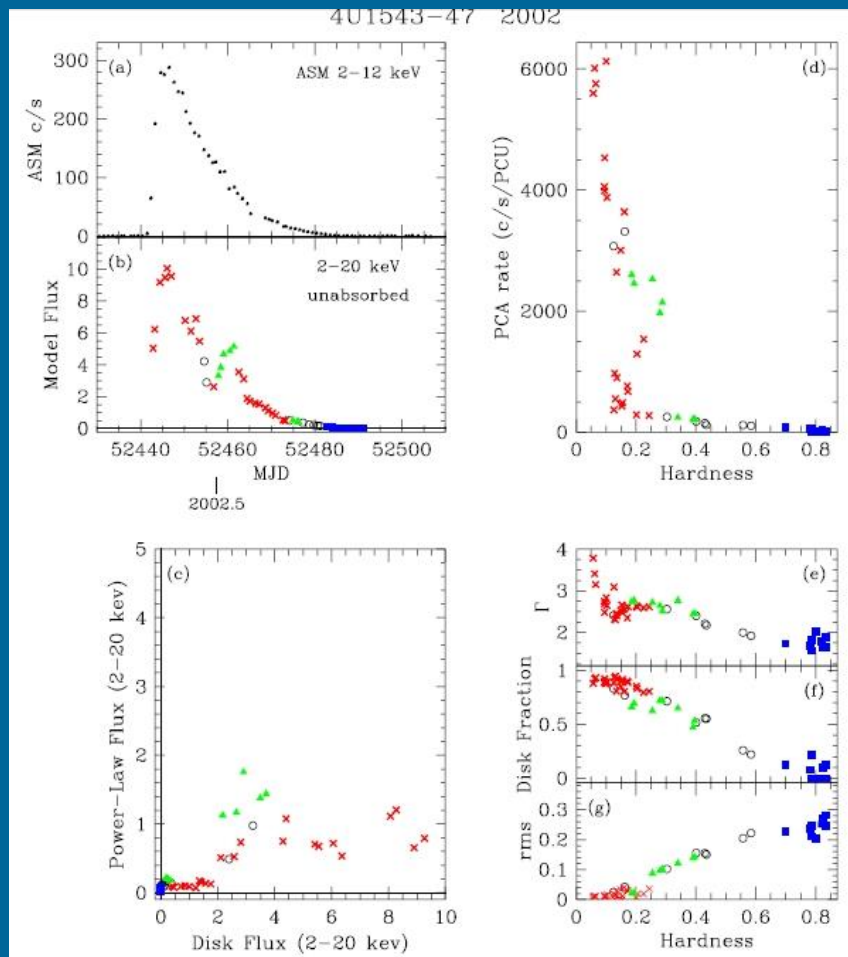


GRO J1655-40 during a burst



Red crosses – thermal state,
Green triangles – steep power-law (SPL),
Blue squares – hard state.

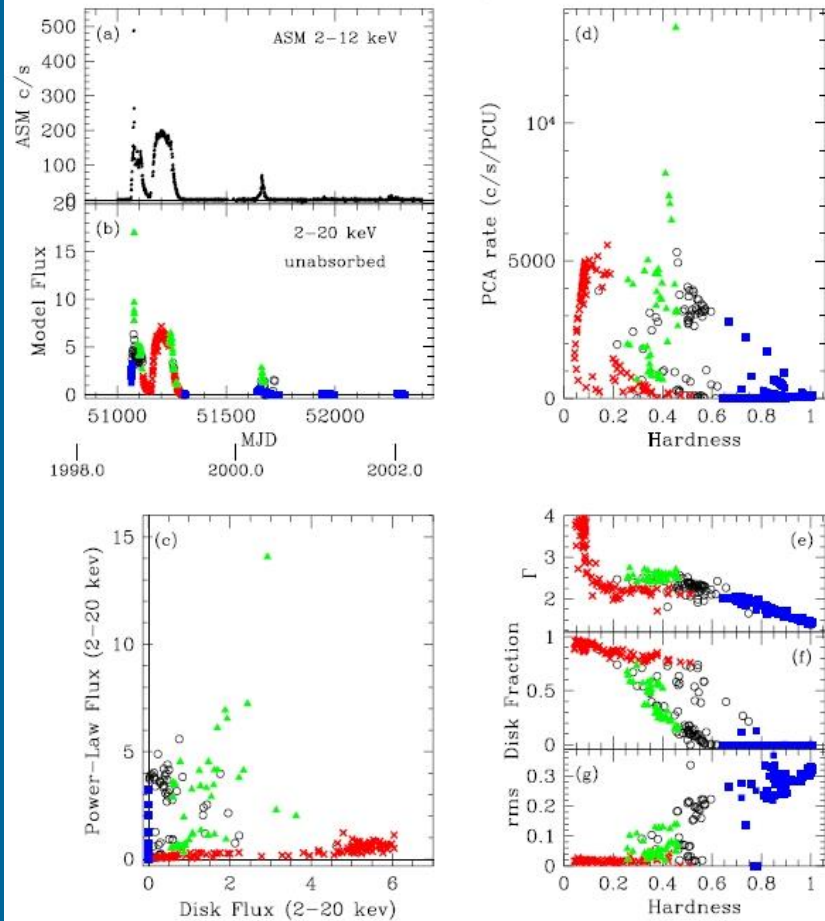
4U 1543-47 and H1743-322



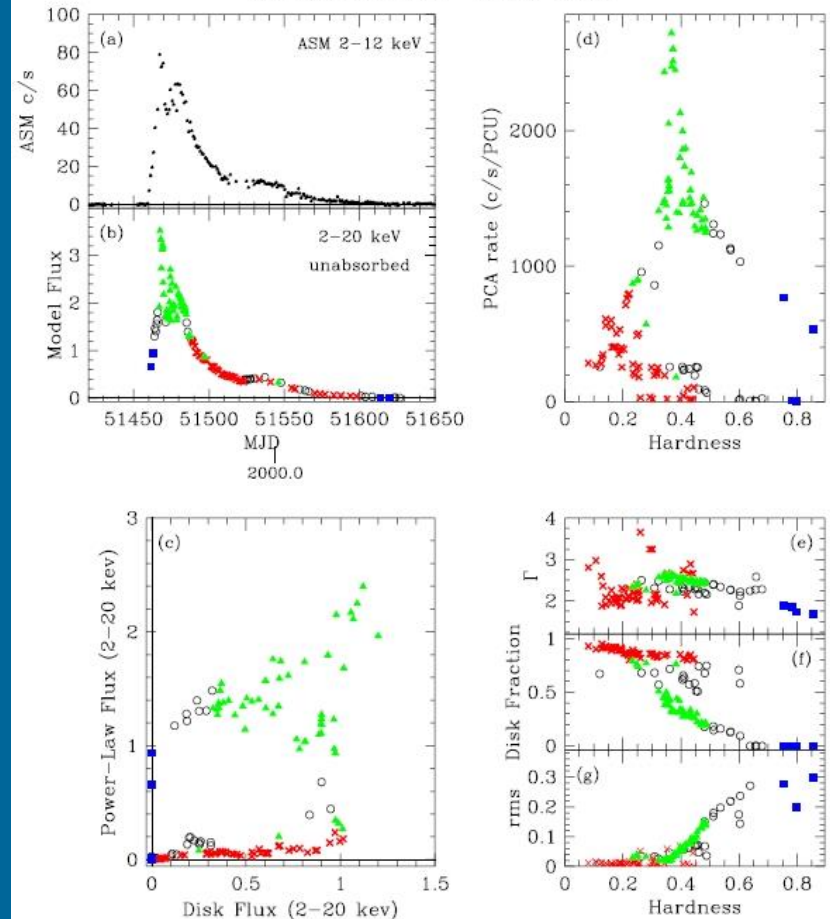
(Remillard, McClintock [astro-ph/0606352](https://arxiv.org/abs/astro-ph/0606352))

XTE J1550-564 and XTE J1859-226

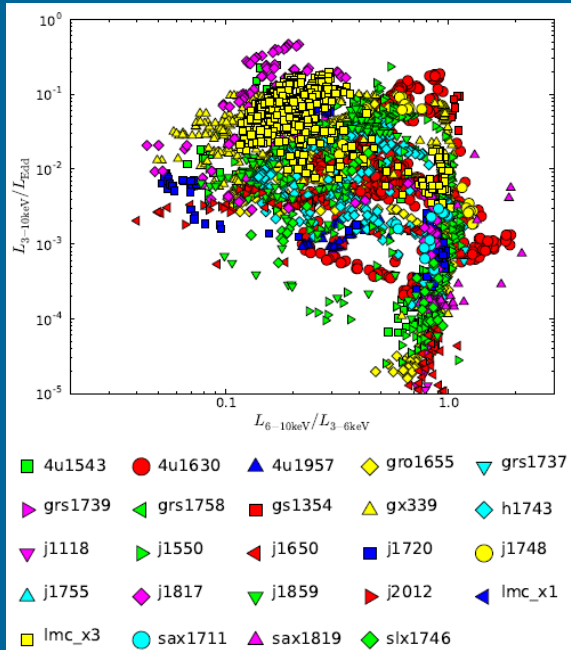
XTE J1550-564 1998-1999; 2000; 2001; 2002



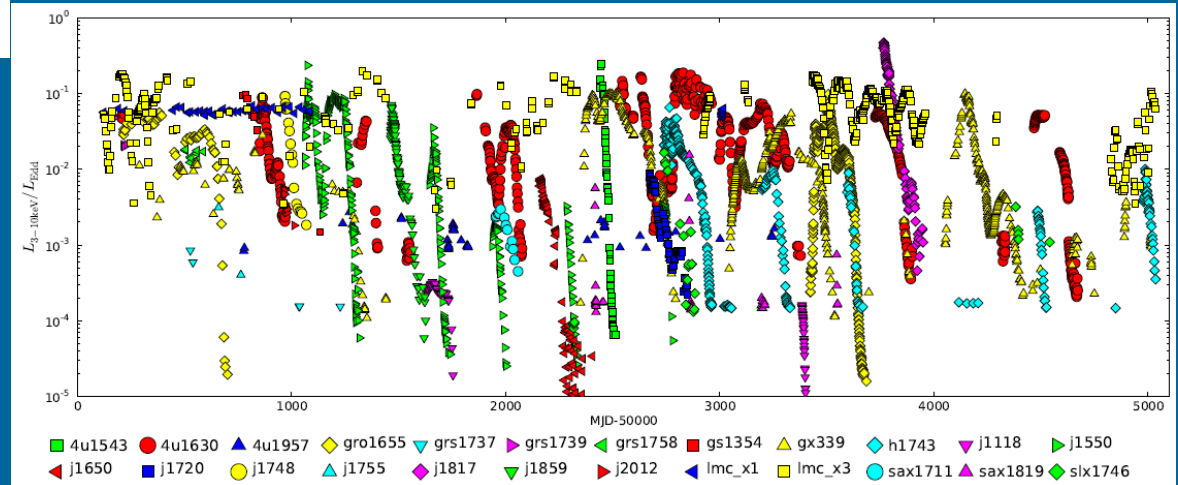
XTE J1859+226 1999-2000



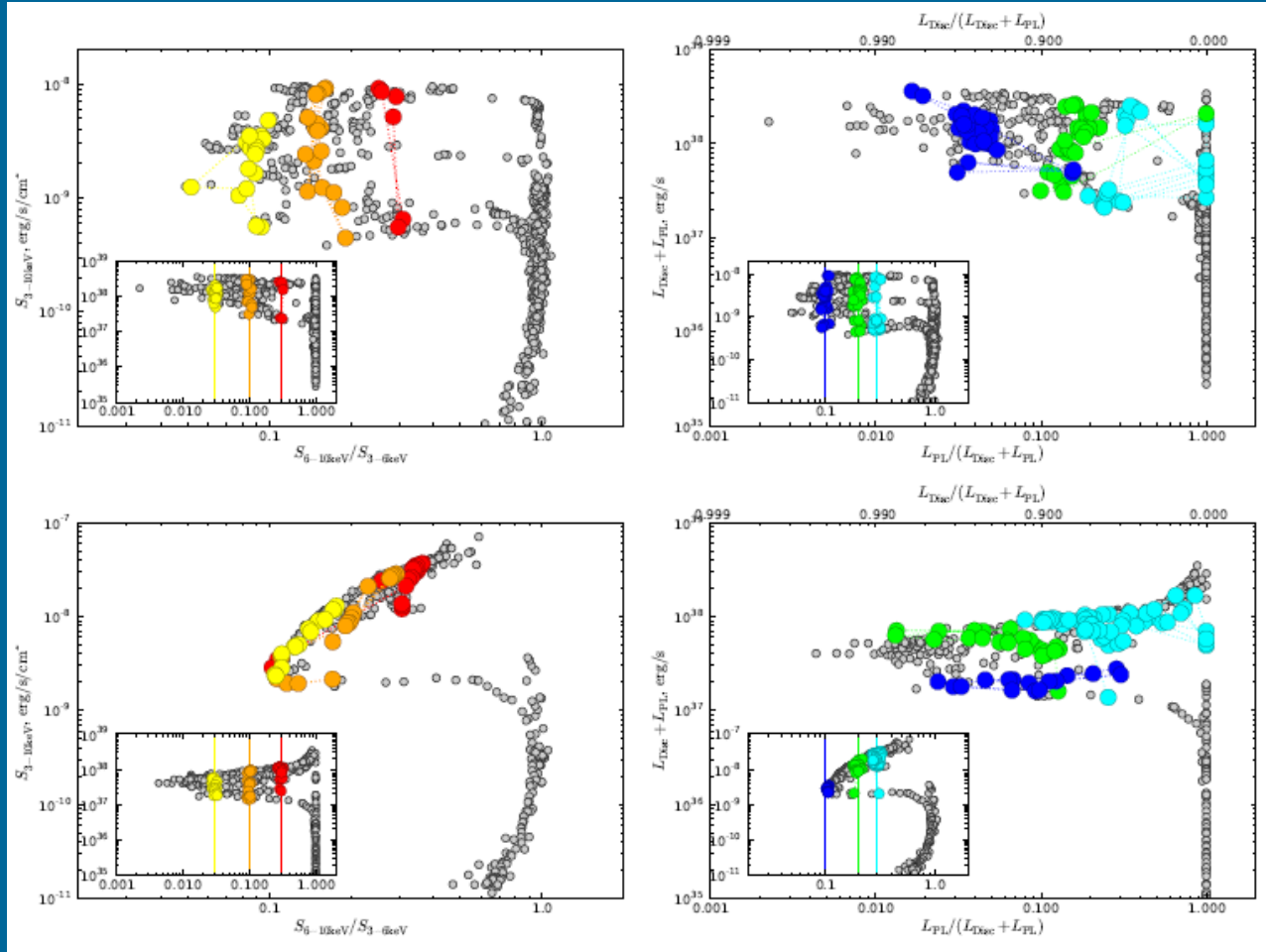
Recent large set of data



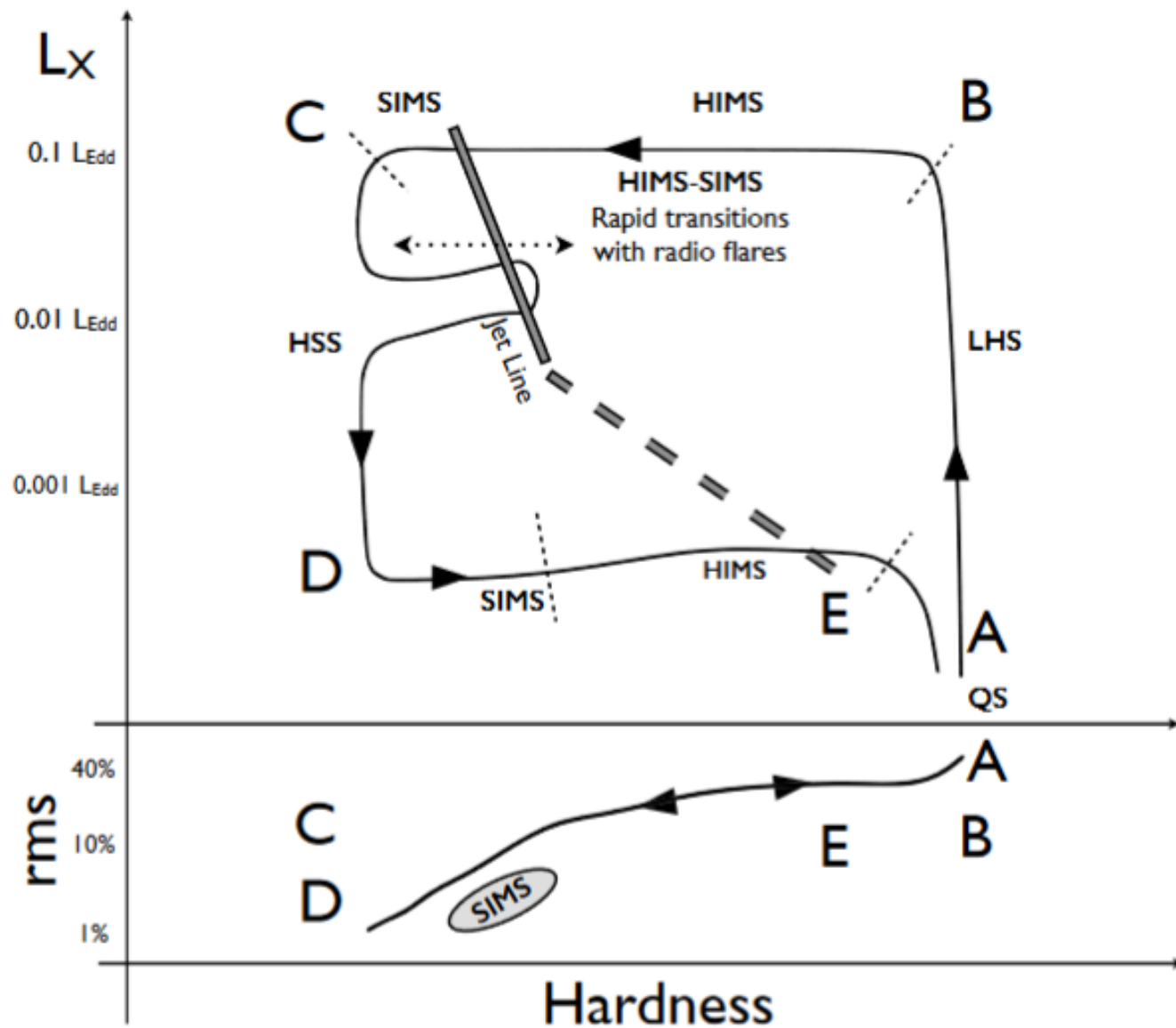
RXTE data
25 LMXBs



Hardness Intensity Diagram (HID) and Disc Fraction Luminosity Diagram (DFLD)

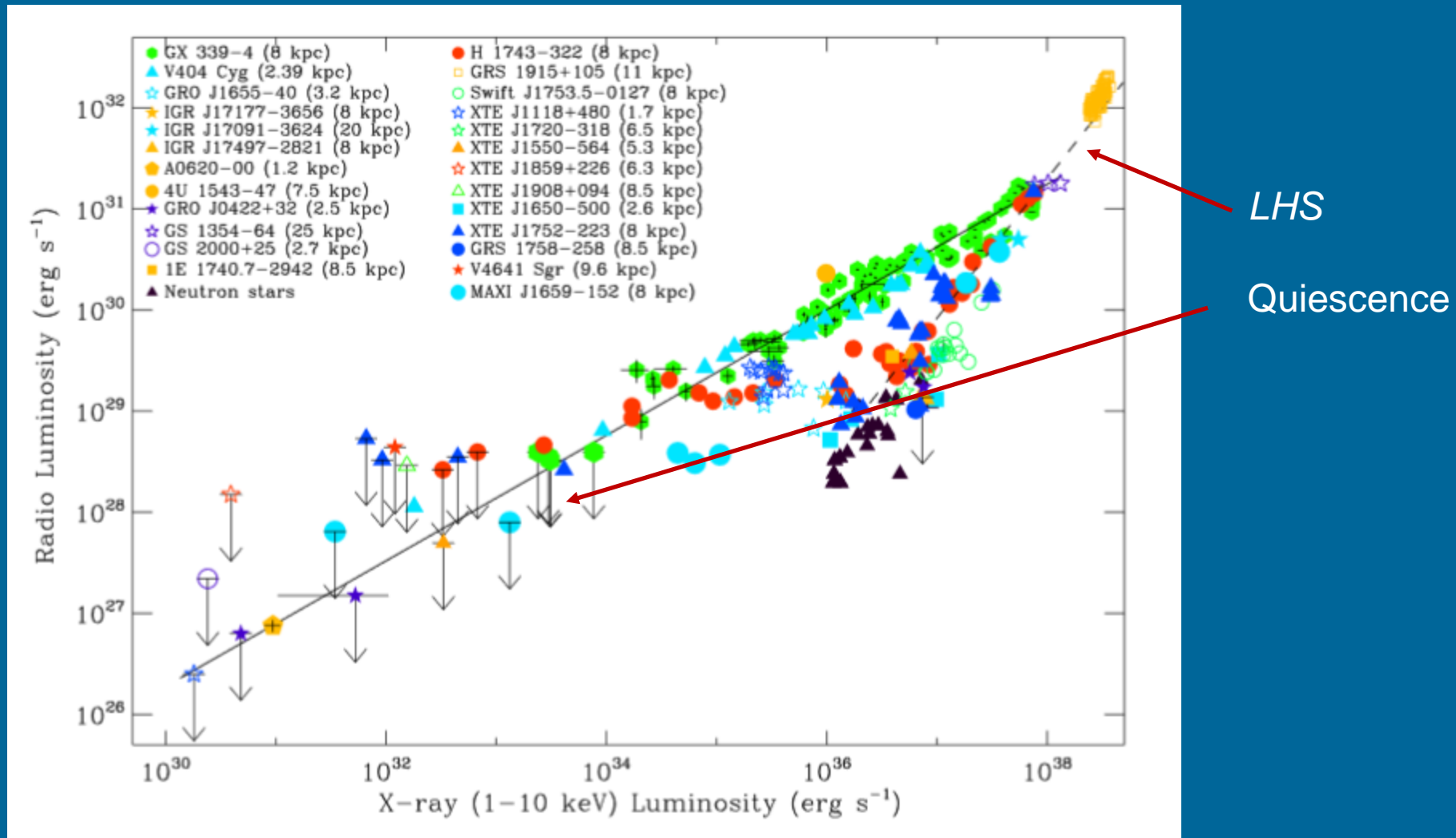


LEFT: HID with specific disc fractions highlighted
 RIGHT: DFLD with specific X-ray colours highlighted.
 The highlighted disc fractions are red 0.3, orange 0.1, yellow 0.03; and the highlighted X-ray colours are cyan 0.3, green 0.2, blue 0.1.
 TOP: GX 339-4,
 DOWN: GRO 1655-40



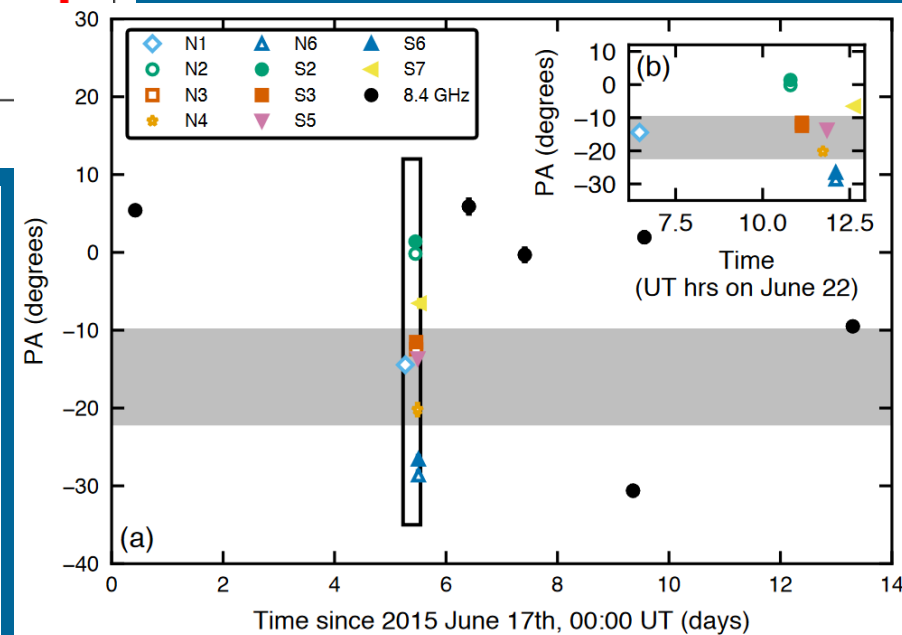
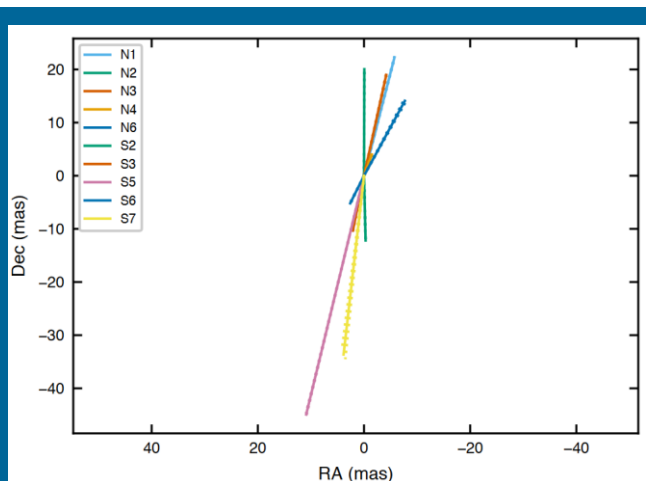
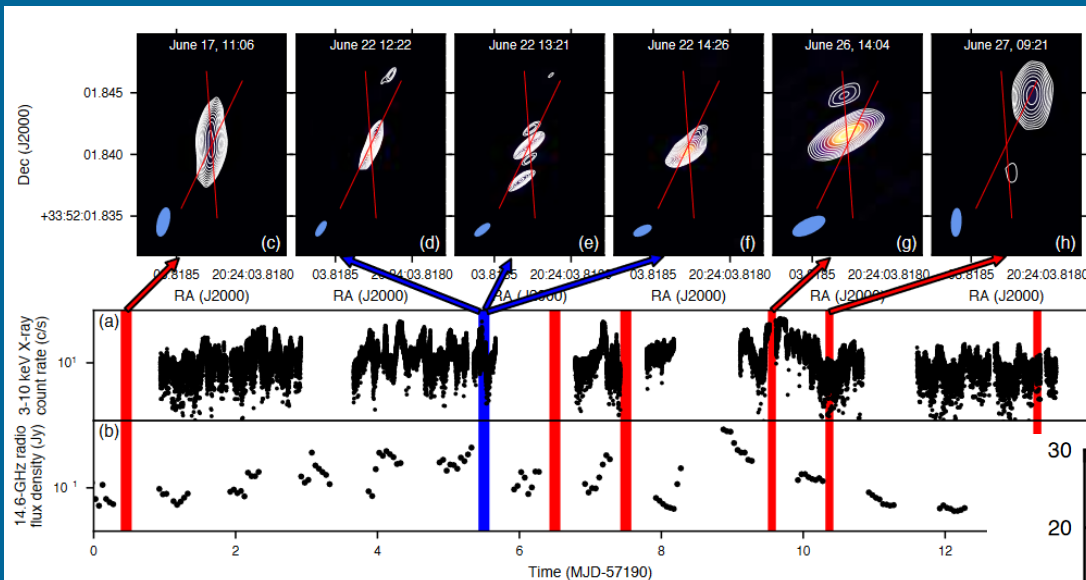
See p.17-19 for a very clear description.

X-ray – radio correlation



Jet variation in Cyg V404 during outburst

Rapid jet direction variability during an outburst can be due to Lense-Thirring precession of the inner disc.



Summary of states with jets in BH binaries

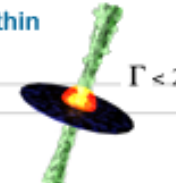
JET LINE AREA:

- 2 - 50% L_{Edd} .
- High-frequency QPOs (after).
- Type A & B QPOs (after).
- See radio ejecta (fast) each "crossing" of jet line.
- RMS drop ("The Zone") associated with ~ 0.2 Hz lowest frequency Lorentzian, close to ejecta time.



HIMS:

- Disk starts near ISCO.
- Transition starts around 2 - 50% L_{Edd} .
- Type C QPOs.
- IR drops.
- Radio starts going optically thin and variable (new ejecta?).

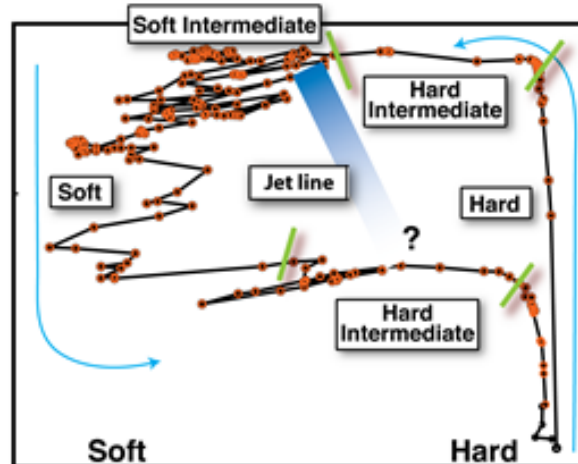


SOFT STATE:

- Optically nuclear thin jet radio emission observed initially, but quenched by at least 20-50x by full transition. Detected radio flux not nuclear?
- Type C QPOs.
- Non-thermal power law extending to \sim MeV.
- Thin disk ~ 0.1 - $1.0 L_{\text{Edd}}$ at ISCO.



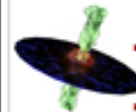
X-ray Luminosity



Spectral Hardness
(spectral slope, soft=steep, hard=flat)

HARD STATE:

- Disk moves in to \sim few R_g by 10% L_{Edd} .
- Lorentzian/broad noise components.
- High RMS variability.
 - Flat spectrum jet up to IR/opt.
 - Compact jet sometimes resolved.
 - Radio/IR/X-ray correlations.
 - Reflection "bump".



T. Belloni
A. Celotti
S. Corbel
R. Fender
E. Gallo
M. Hanke
E. Kalemci

D. Maitra
S. Markoff
I. McHardy
M. Nowak
P.-O. Petrucci
K. Pottschmidt
J. Wilms

HIMS:

- Same as upper branch but:
 - No optically thin radio flare.
 - Radio recovers close to hard state.
 - Lower flux level (hysteresis).

QUIESCENCE:

- Thin disk recessed to $> 10^2 R_g$.
- BB component seen in UV/Optical.
- Disk 10-100x more luminous than LX. By $\sim 10^{-4} L_{\text{Edd}}$.
- No iron lines?



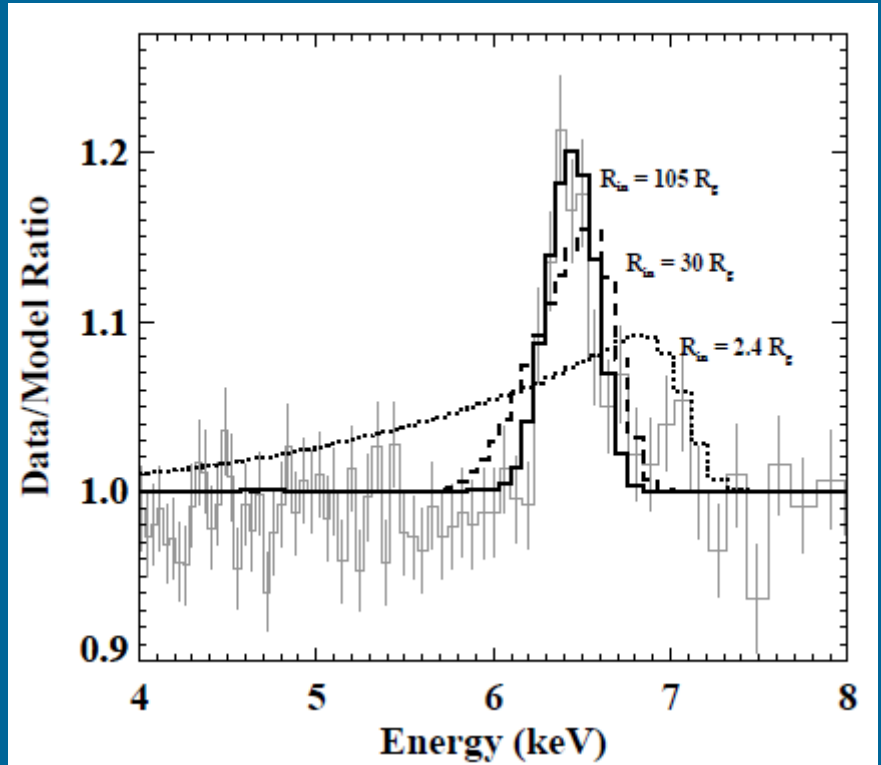
Probing the Accretion/Outflow Connection in
X-Ray Binaries and Active Galactic Nuclei

Inner disk boundary

In BH binaries there are different spectral and luminosity states. It was suggested that the inner disk boundary moves significantly from stage to stage.

For the first time the effect was measured thanks to the iron line data.

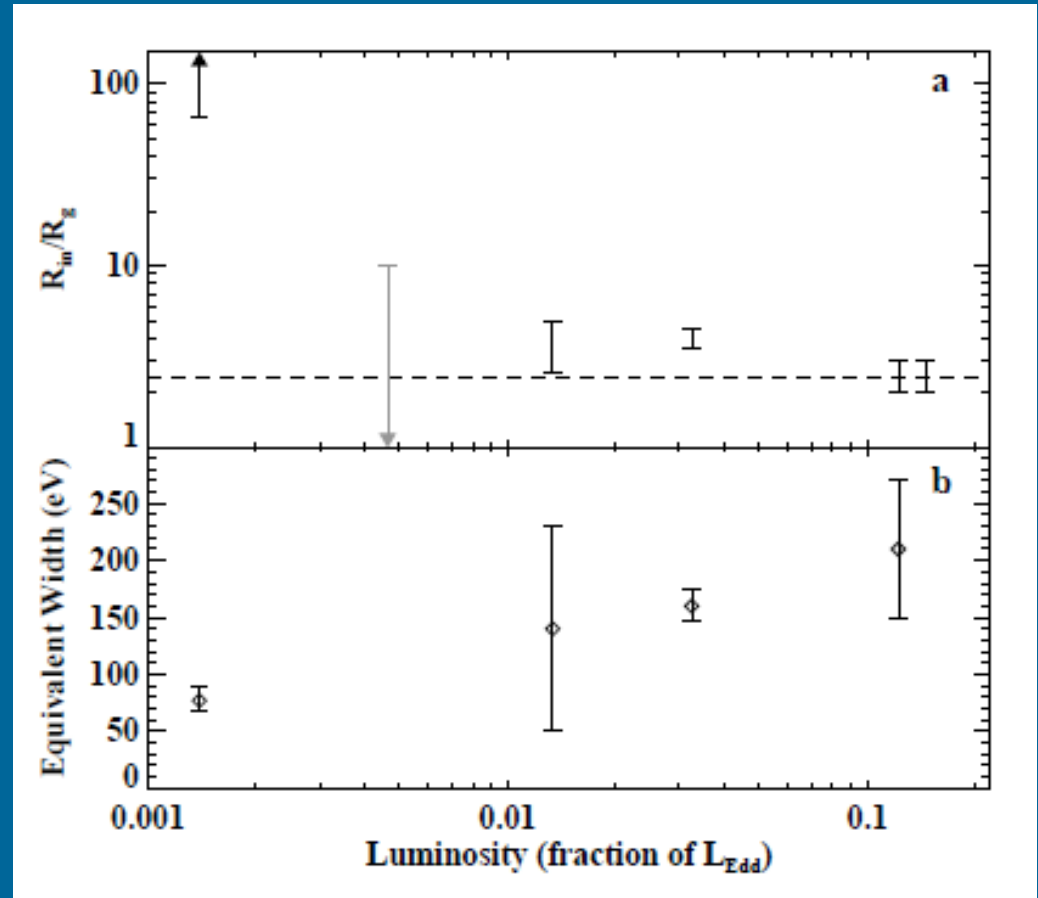
At low luminosity the inner disk boundary is far from the BH.



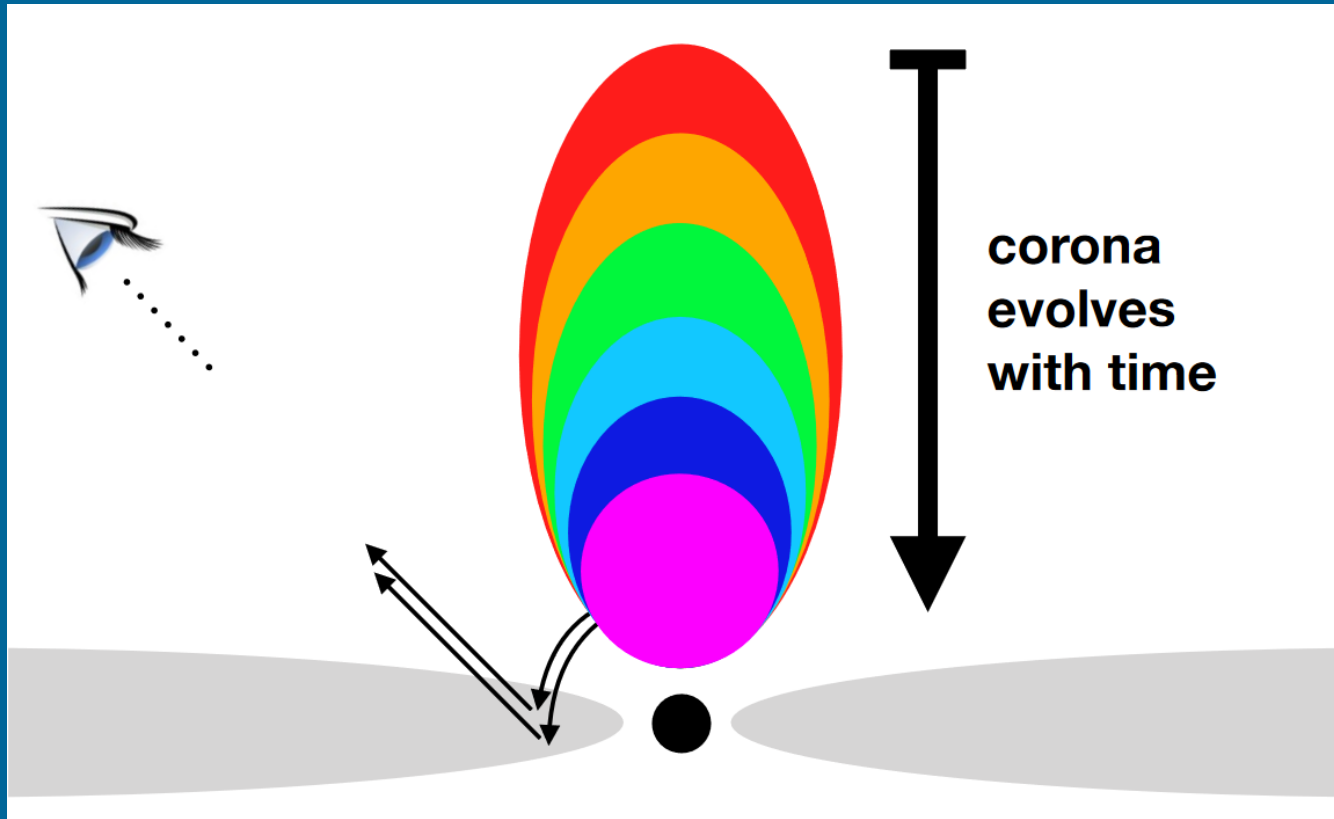
Inner disc boundary

Position of the inner disc boundary is clearly different at different luminosities: from 0.1 to 0.001 L_{Edd} .

In a separate paper another group of scientists put constraints on the spin rate of the BH in this system.



Disc truncation or corona expansion?

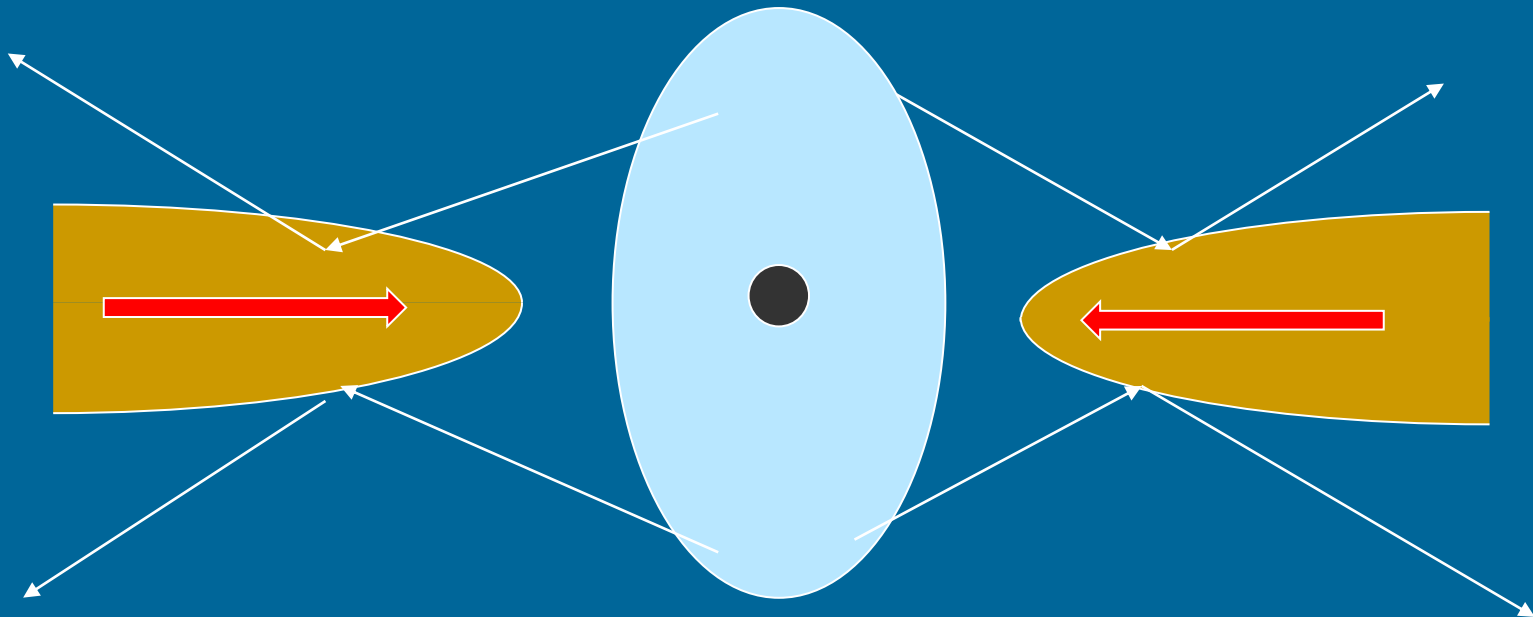


In the case of MAXI J1820+070 observations suggest that changes are mostly not due to modification of the inner disc radius, but due to changes in the hot corona size.

The result is based on time lags between corona and disc emission.

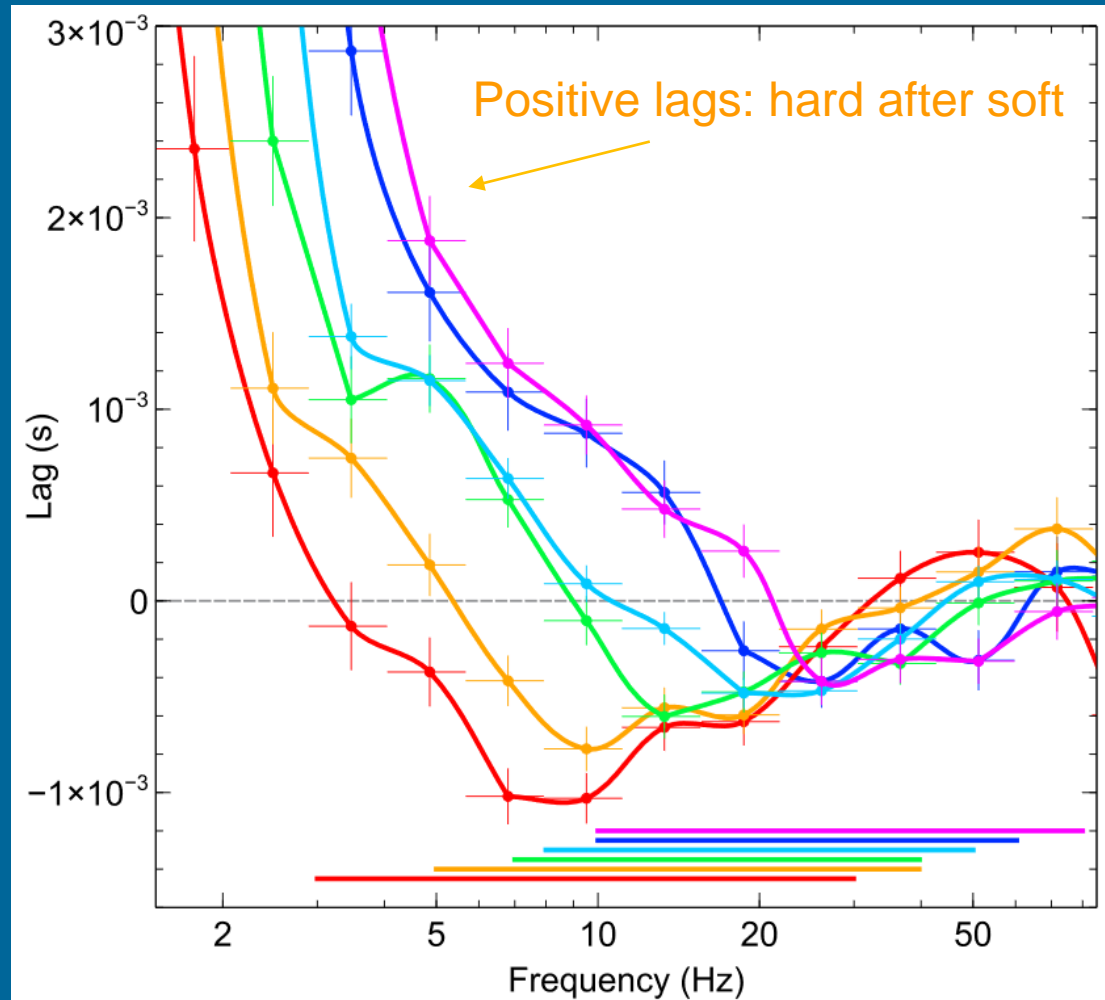
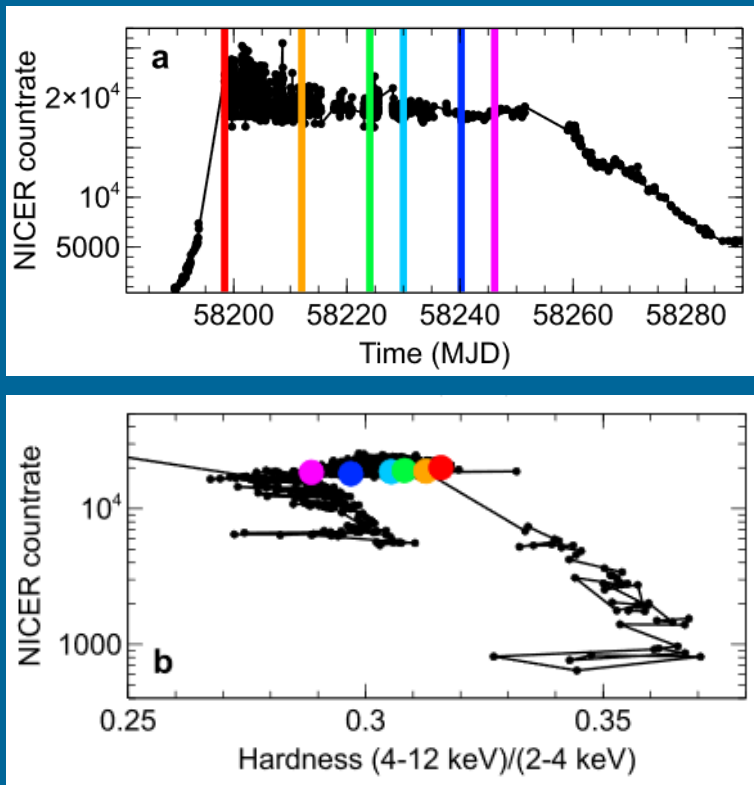
Scheme of time lags

Low-frequency hard lags (soft before hard)
is due to propagation of disturbances in the disc

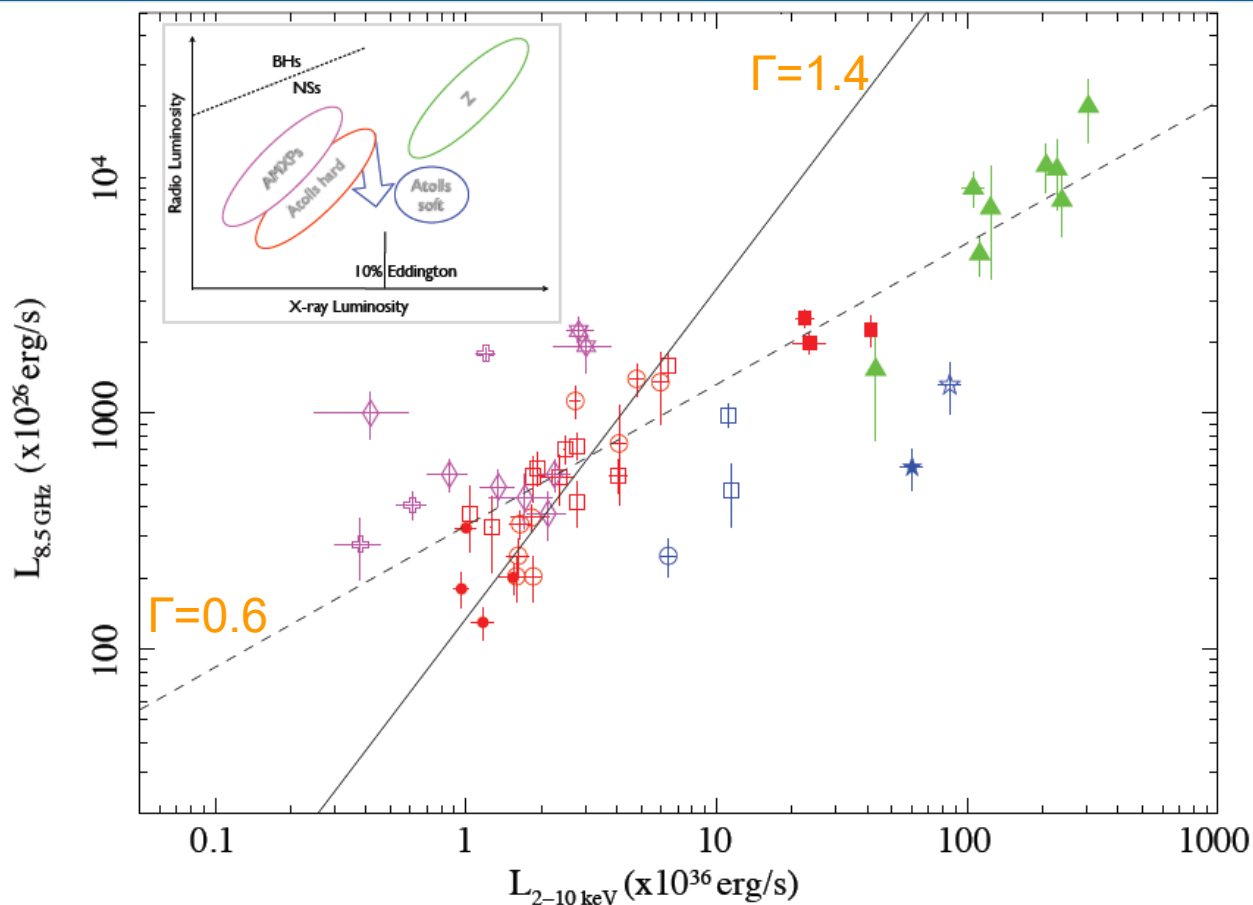


High-frequency soft lag (hard before soft) is due to irradiation of the disc by corona

Hard lags and soft lags

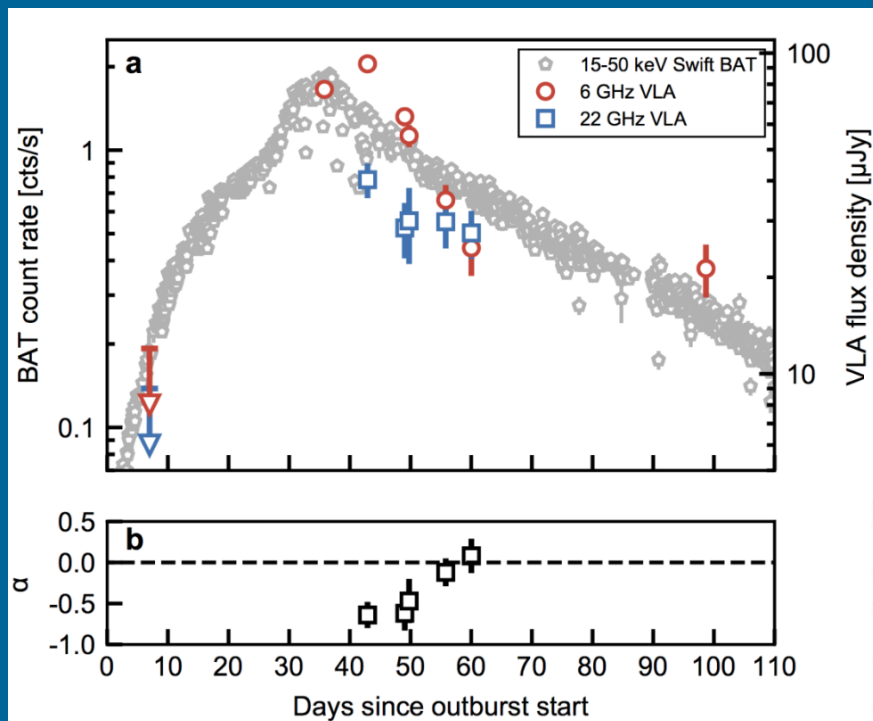


NS jets



open circles, 4U 1728-34;
 filled squares, MXB 1730-335;
 open squares, Aql X-1;
 filled circles, 4U 0614+091;
 Open star, Ser X-1;
 filled star, 4U 1820-30;
 filled triangles are Z sources;
 open diamonds, SAX J1808.4-3658;
 open crosses are IGR J00291+5934;
 stars of David, XTE J0929-314.
 Colors:
 red, atolls in hard state or
 in outburst, up to the peak;
 blue, atolls in steady soft state;
 green, Zsources; magenta, AMXPs.

A jet from normally magnetized NS



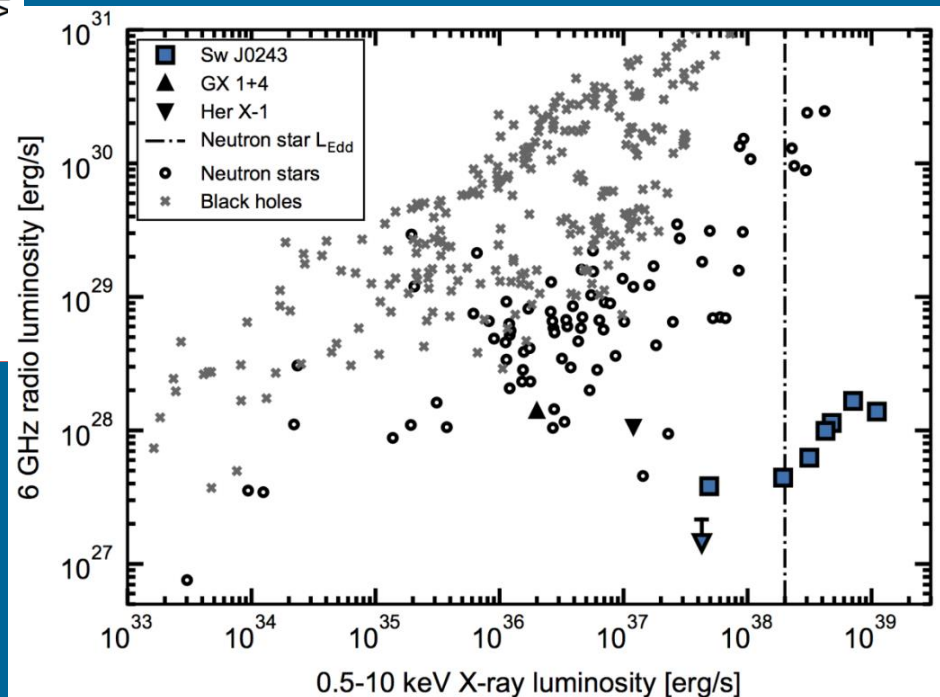
$$L_R \propto L_X^{0.54 \pm 0.16}$$

VLA detection of emission from Swift J0243.6+6124.

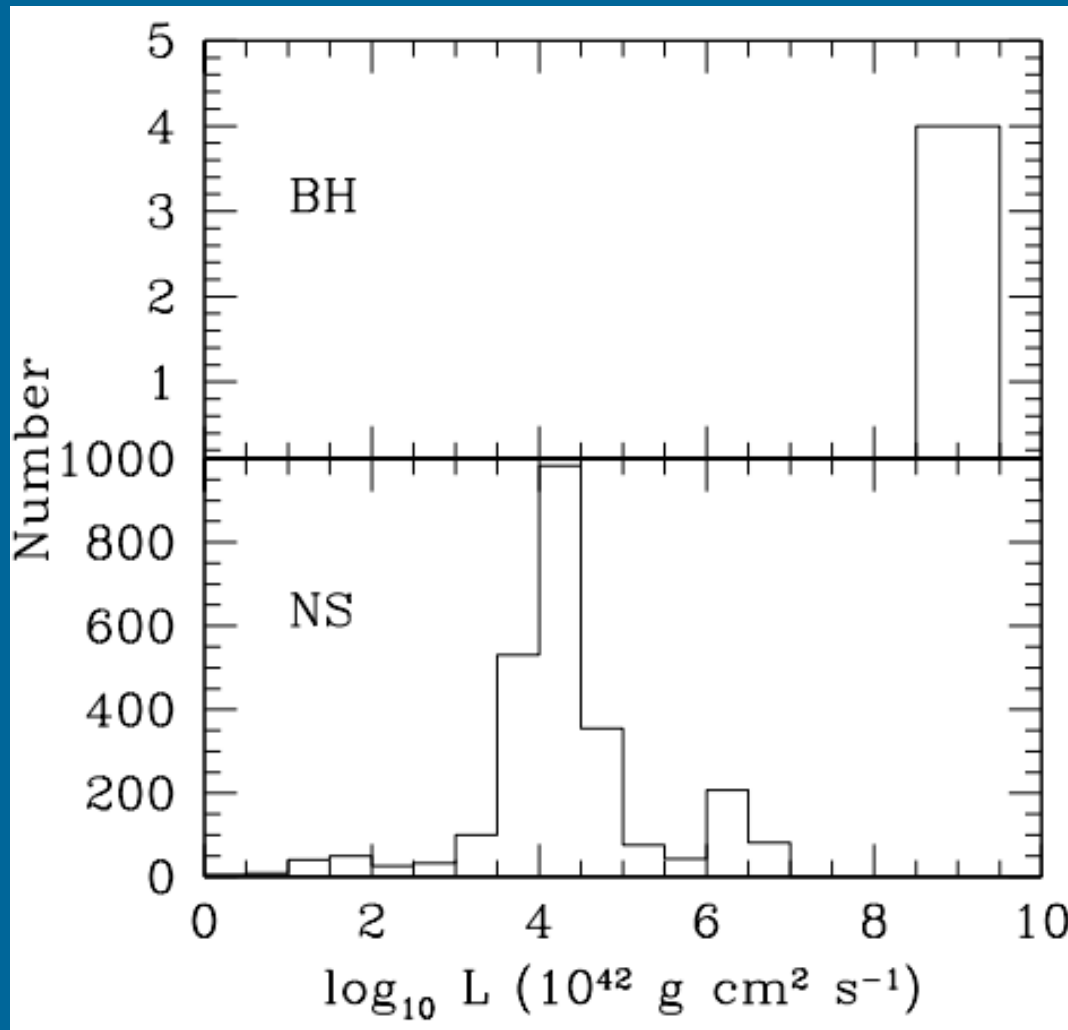
Spin period ~ 10 sec.

Before jets have been detected from rapidly spinning NSs.

Blandford-Znajek, not Blandford-Payne.



Spins: NSs vs. BHs



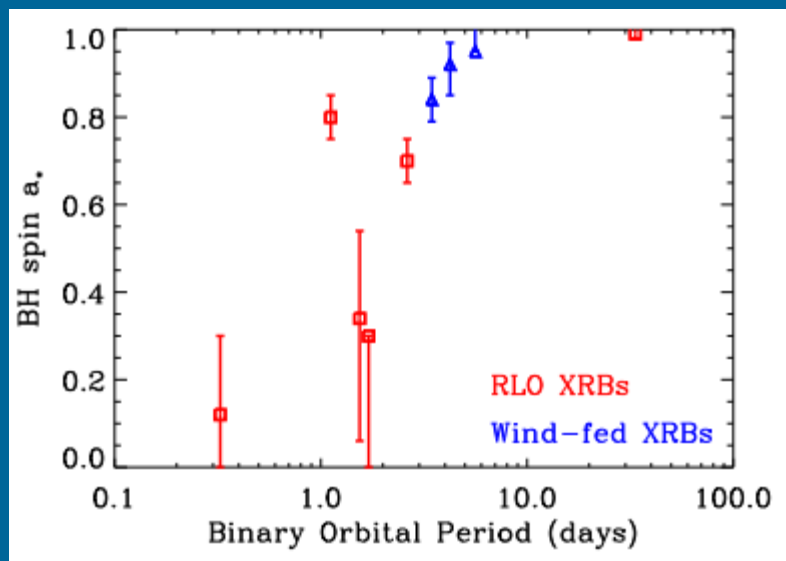
BHs win!!!!

They nearly do not lose angular momentum.

1408.4145

Mass and spin determinations are reviewed in 1408.4145 and spin in 1507.06153

Origin of BH spin



Spin is due to accretion.

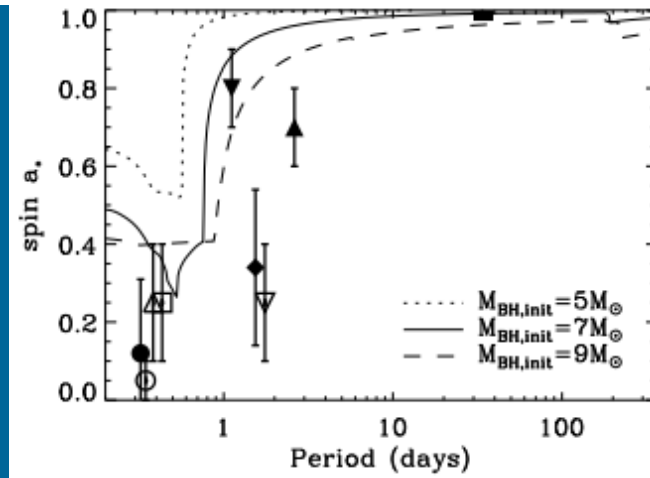
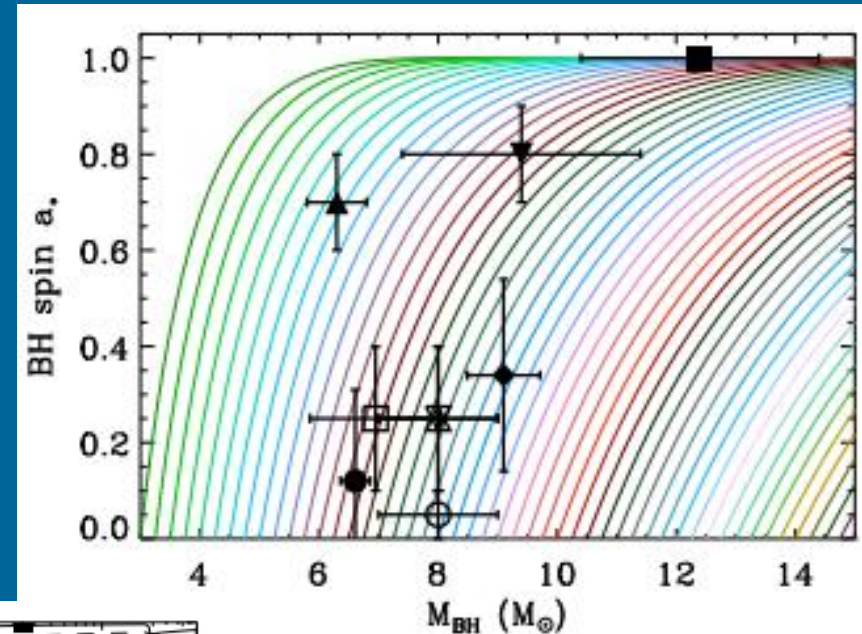
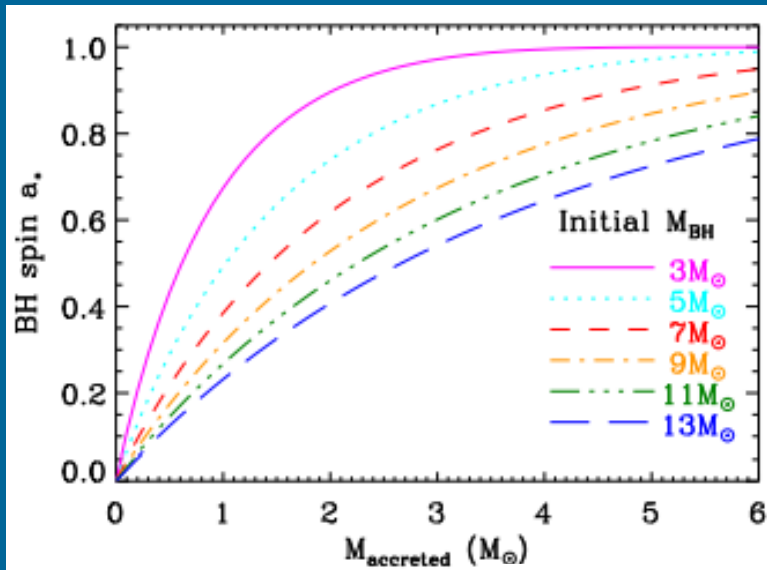
BHs accrete (on average)
~1.5 solar mass

Source	MT Type ^b	P_{orb} (days) ^b	Spin a_*	Reference
GRS 1915+105	RLO	33.5	> 0.98	McClintock et al. (2006)
Cyg X-1	Wind	5.6	> 0.95	Gou et al. (2011)
LMC X-1	Wind	4.23	$0.92^{+0.05}_{-0.07}$	Gou et al. (2009)
M33 X-7	Wind	3.45	0.84 ± 0.05	Liu et al. (2008, 2010)
4U 1543-47	RLO	1.15	0.80 ± 0.05	Shafee et al. (2006)
GRO J1655-40	RLO	2.62	0.70 ± 0.05	Shafee et al. (2006)
XTE J1550-564	RLO	1.54	$0.34^{+0.20}_{-0.28}$	Steiner et al. (2011)
LMC X-3	RLO	1.7	$< 0.3^c$	Davis et al. (2006)
A0620-00	RLO	0.33	0.12 ± 0.18	Gou et al. (2010)

1408.2661

New measurements for 4U1543 are consistent with the value above: 2002.11922

Spin (and mass) growth due to accretion



The hypothesis is that spin is gained due to accretion (at birth $a=0$).

QPO

BH candidates demonstrate two main types of QPOs:
Low-frequency (0.1-30 Hz) and high-frequency (40-450 Hz).

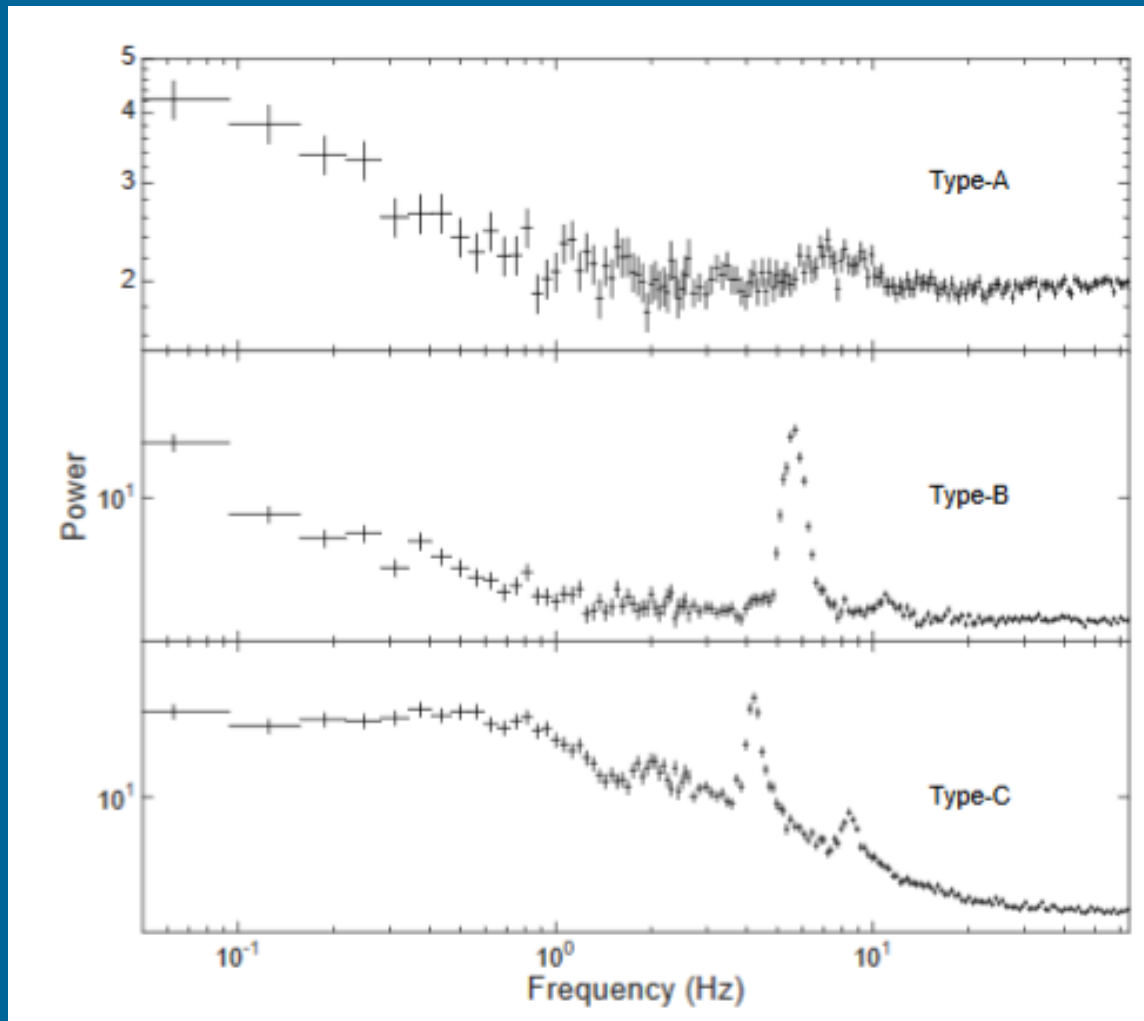
Low-frequency QPOs are found in 14 out of 18 objects.
They are observed during different states of sources.
Probably, in different states different mechanisms of QPO are working.

High-frequency QPOs are known in a smaller number of sources.
It is supposed that frequencies of these QPOs correspond to the ISCO.

Recent reviews: Ingram, Motta 2001.08758

Different types of variability in BH sources are also discussed in
1407.7373 and 1603.07872.

Low-frequency QPO

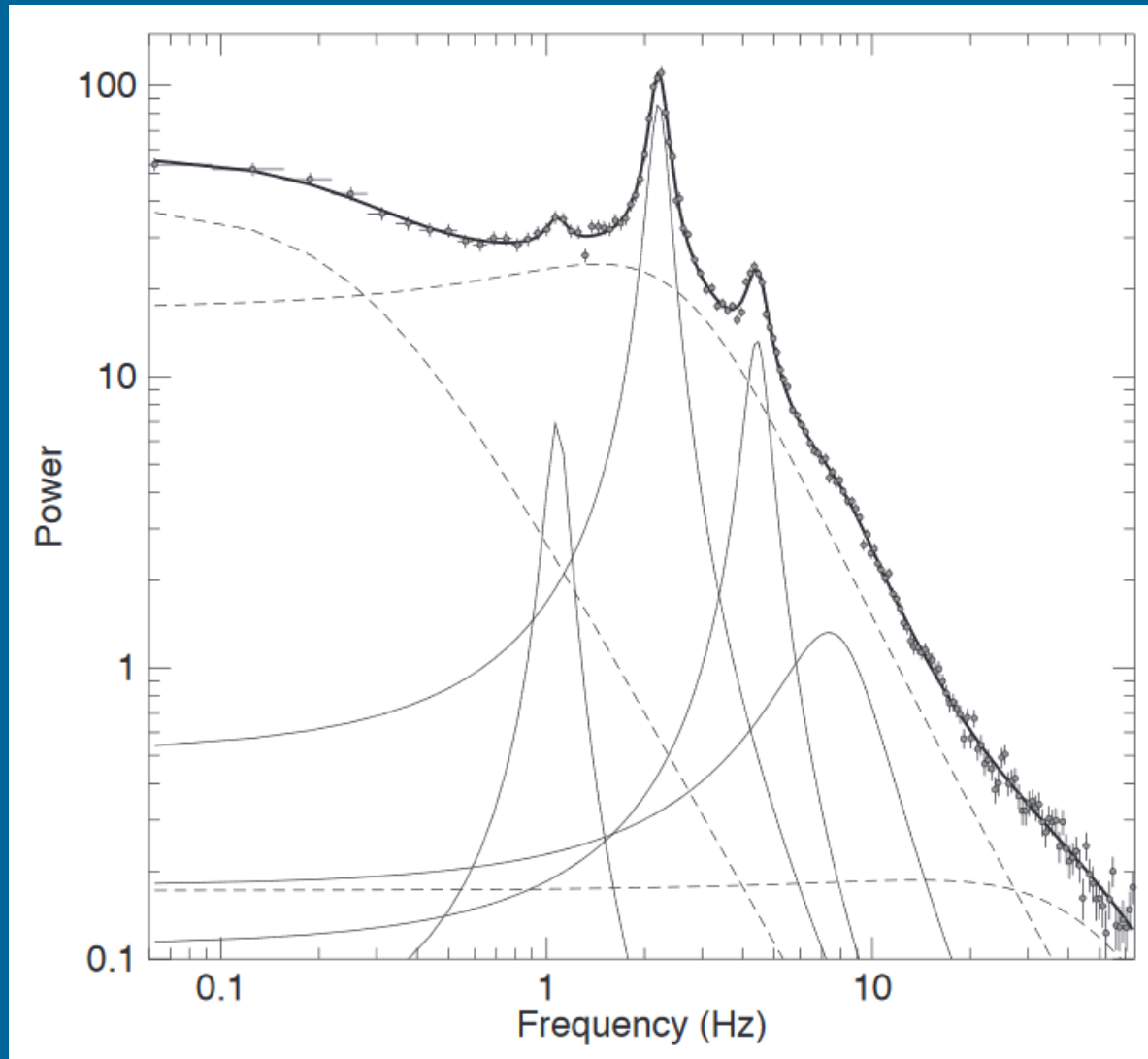


Disc instabilities ?

Jets?

Disc instabilities ?

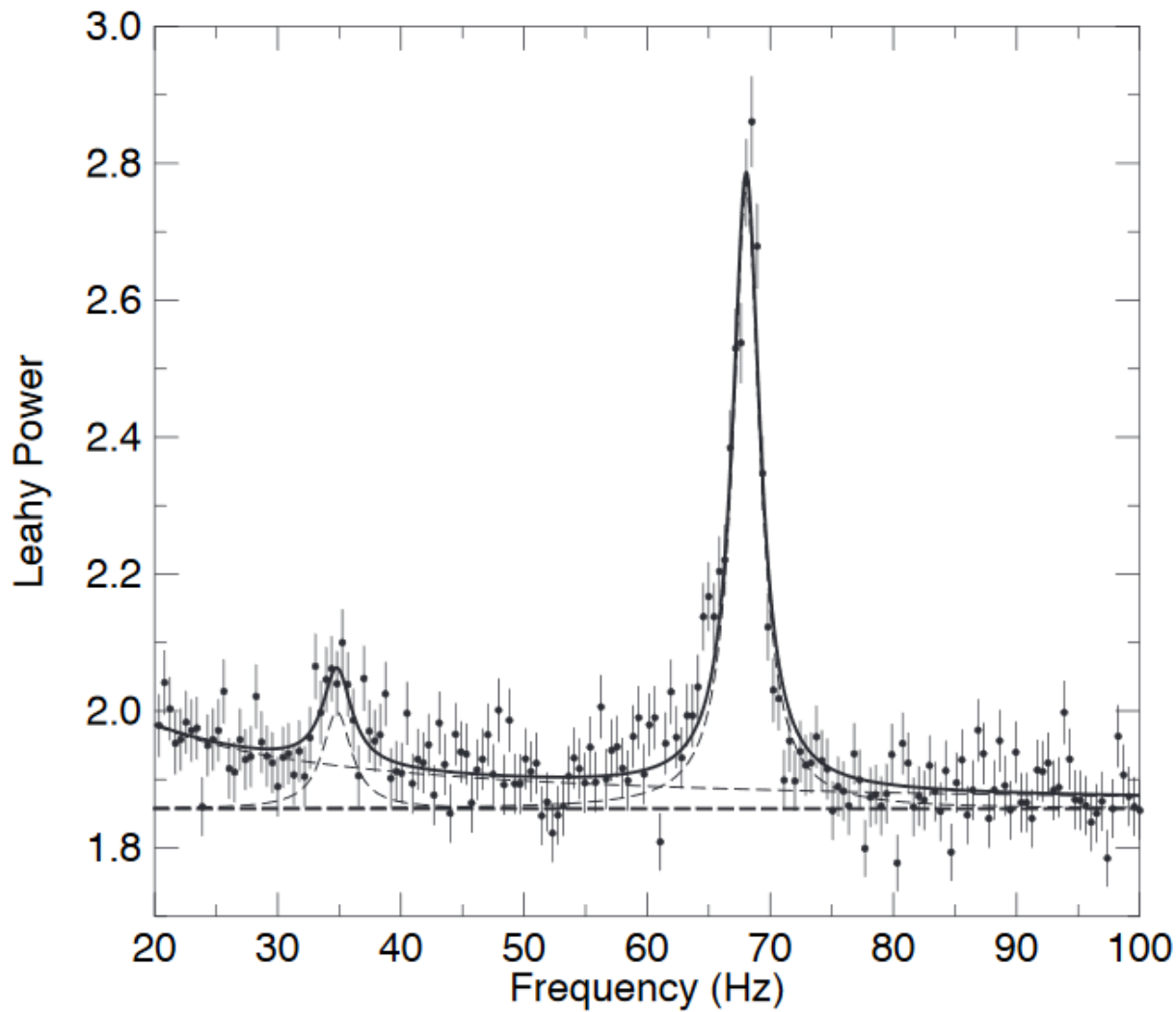
GRS 1915+105



Low-frequency QPO

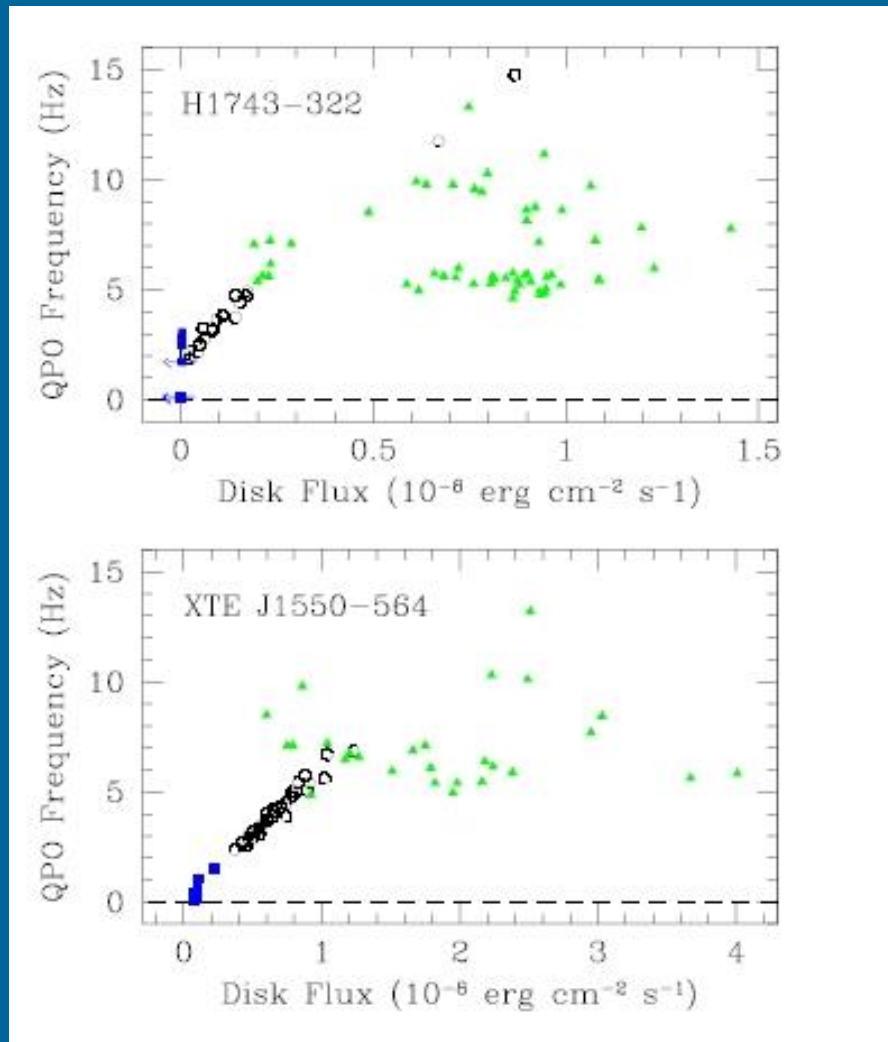
1902.06586

GRS 1915+105



High-frequency QPO

QPO and flux from a disc

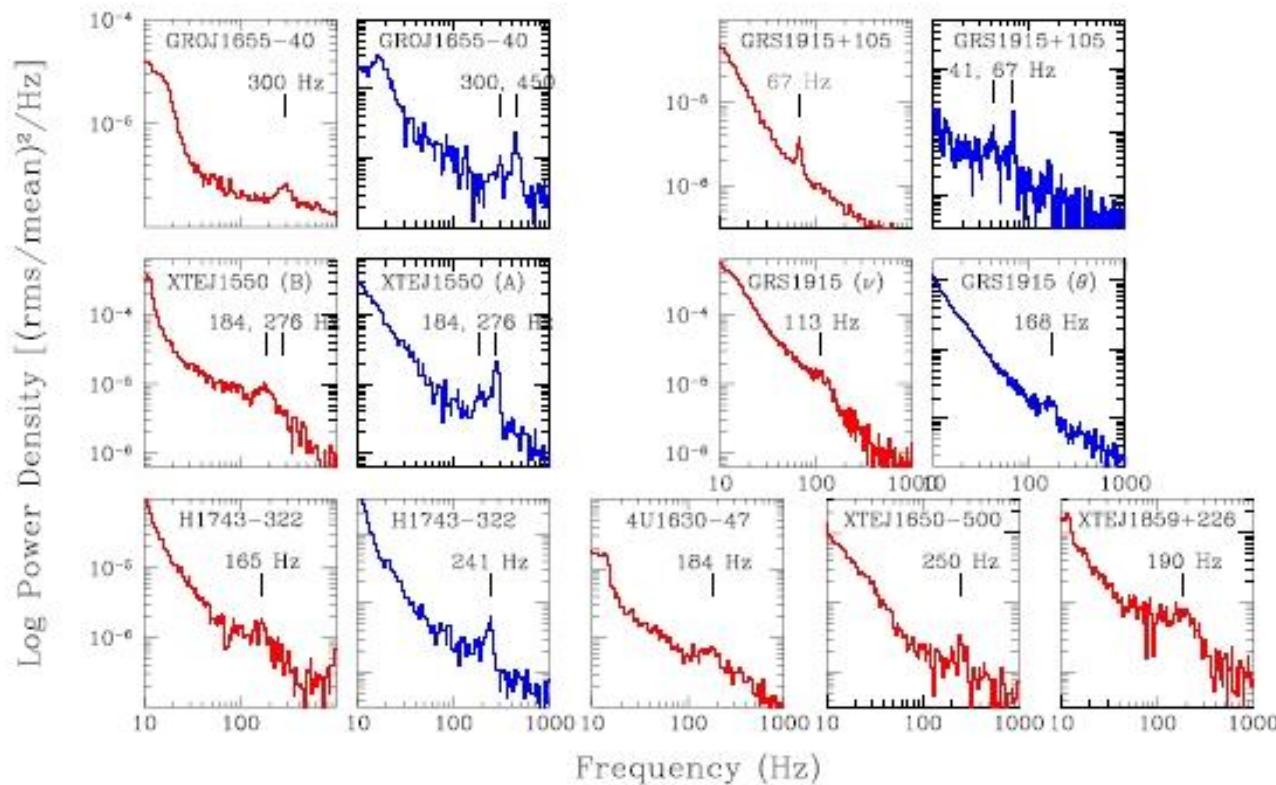


SPL – green triangles
Hard – blue squares
Intermediate states – black circles

Low-frequency QPOs
(their frequency and amplitude)
correlate with spectral parameters.

Probably, QPO mechanisms
in the hard state
and in the SPL state are different.

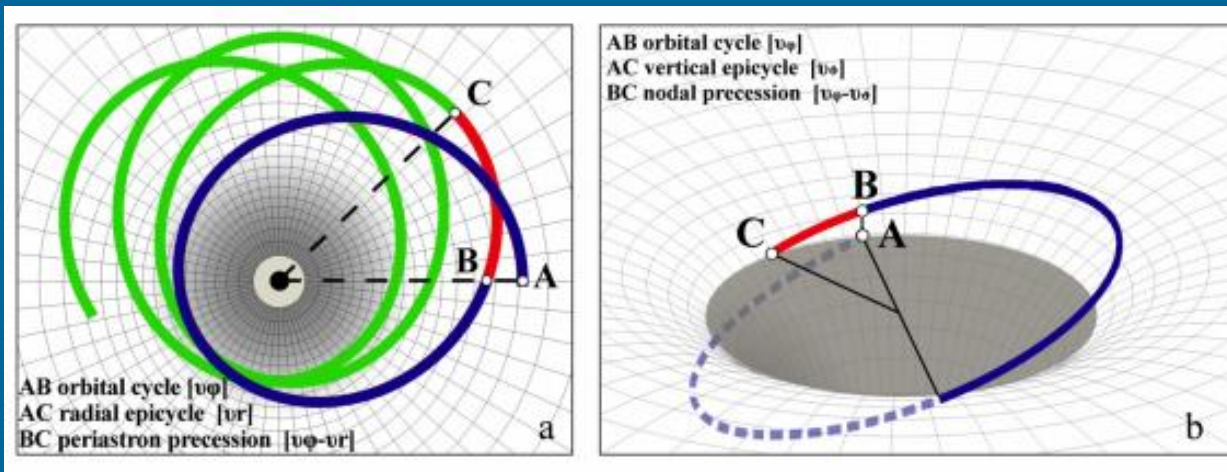
QPO at high (for BHs) frequency



All QPO at >100 Hz are observed only in the SPL state.

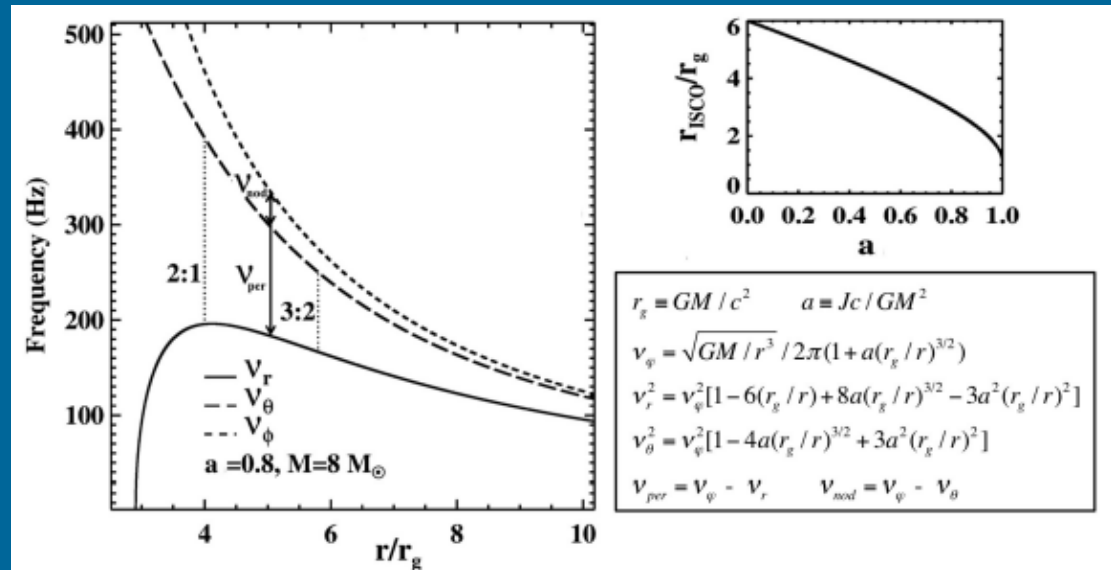
Blue curves: for the range 13-30 keV.
Red curves: for a wider range (towards lower energies).

Possible interpretations



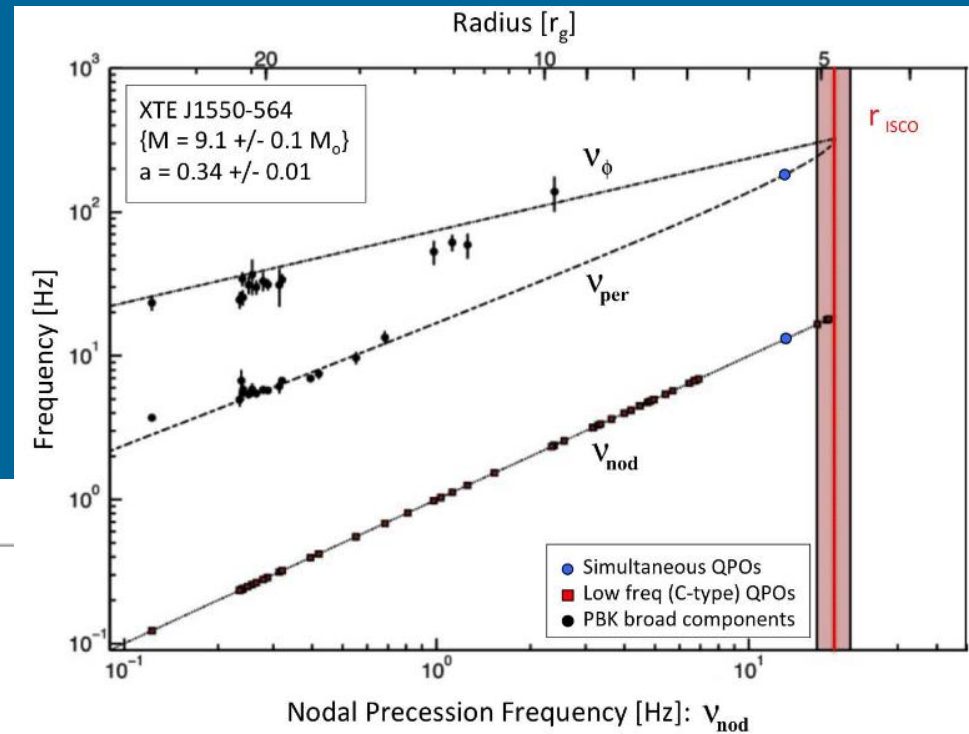
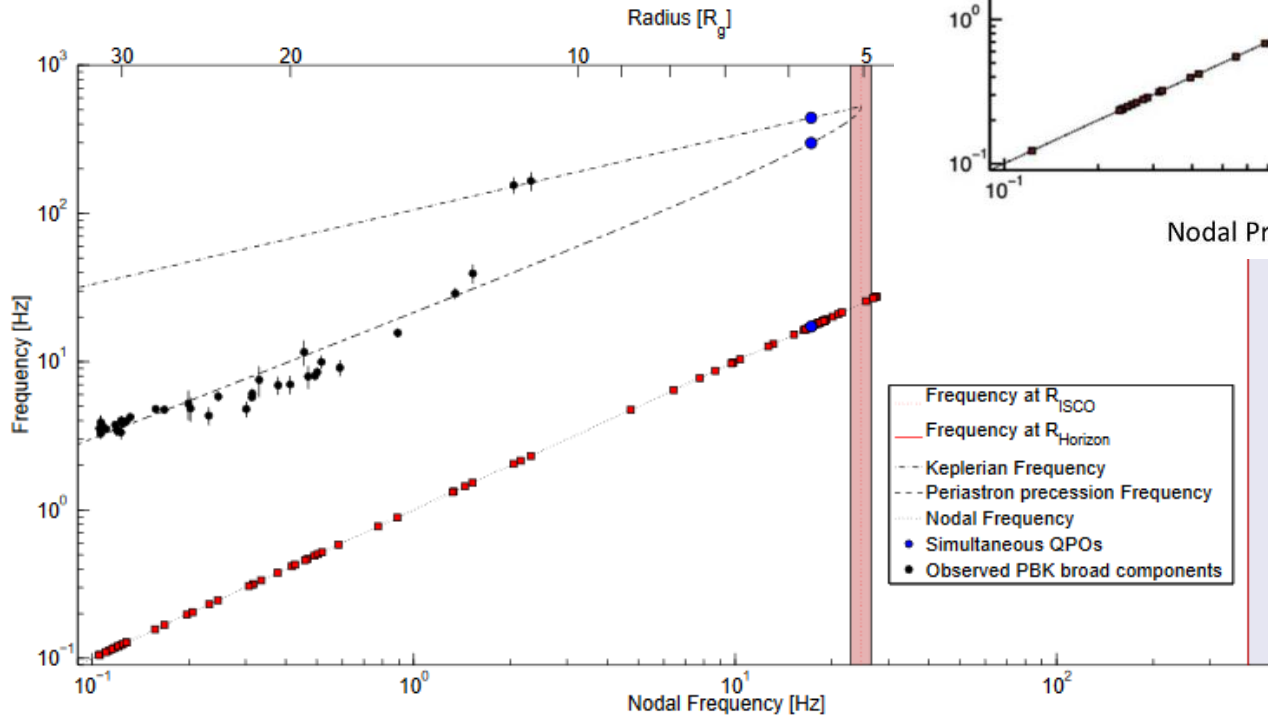
v_ϕ – Keplerian frequency
 v_r – radial epicyclic
 v_θ – vertical epicyclic

periastron precession
 frequency $v_\phi - v_r$
 nodal precession
 frequency $v_\phi - v_\theta$



Correlations

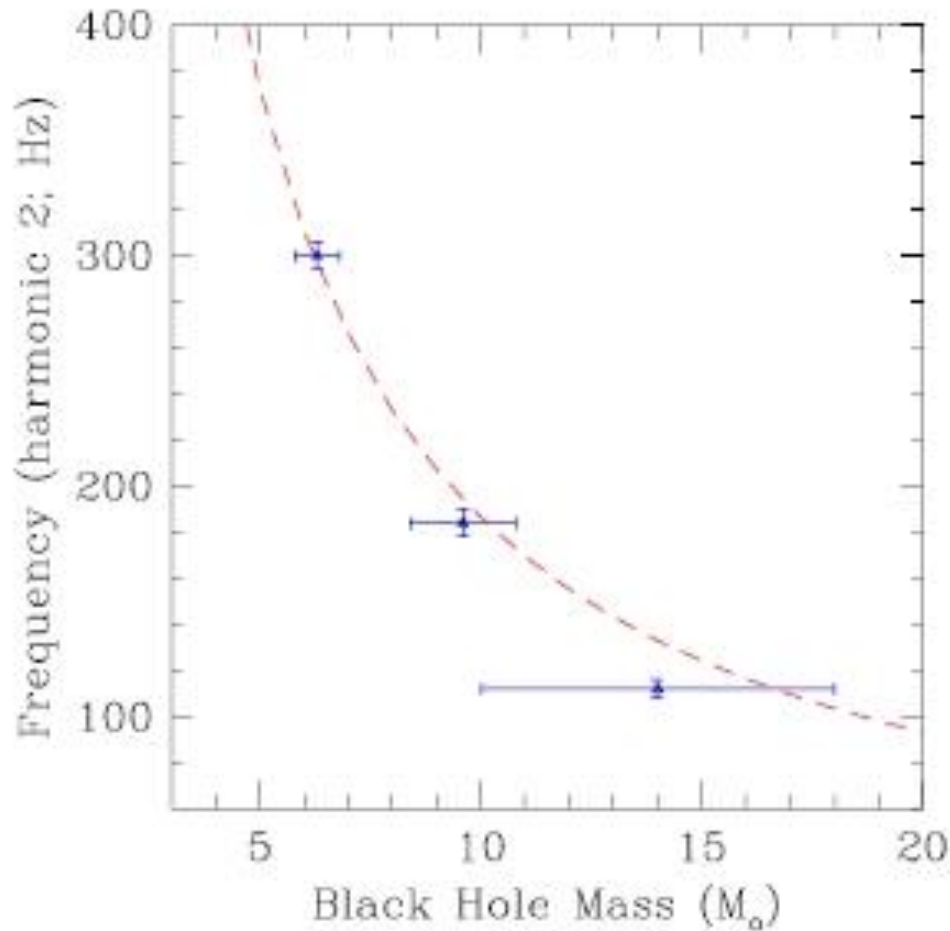
GRO J1655-40



GRO J1550-40

1902.06586

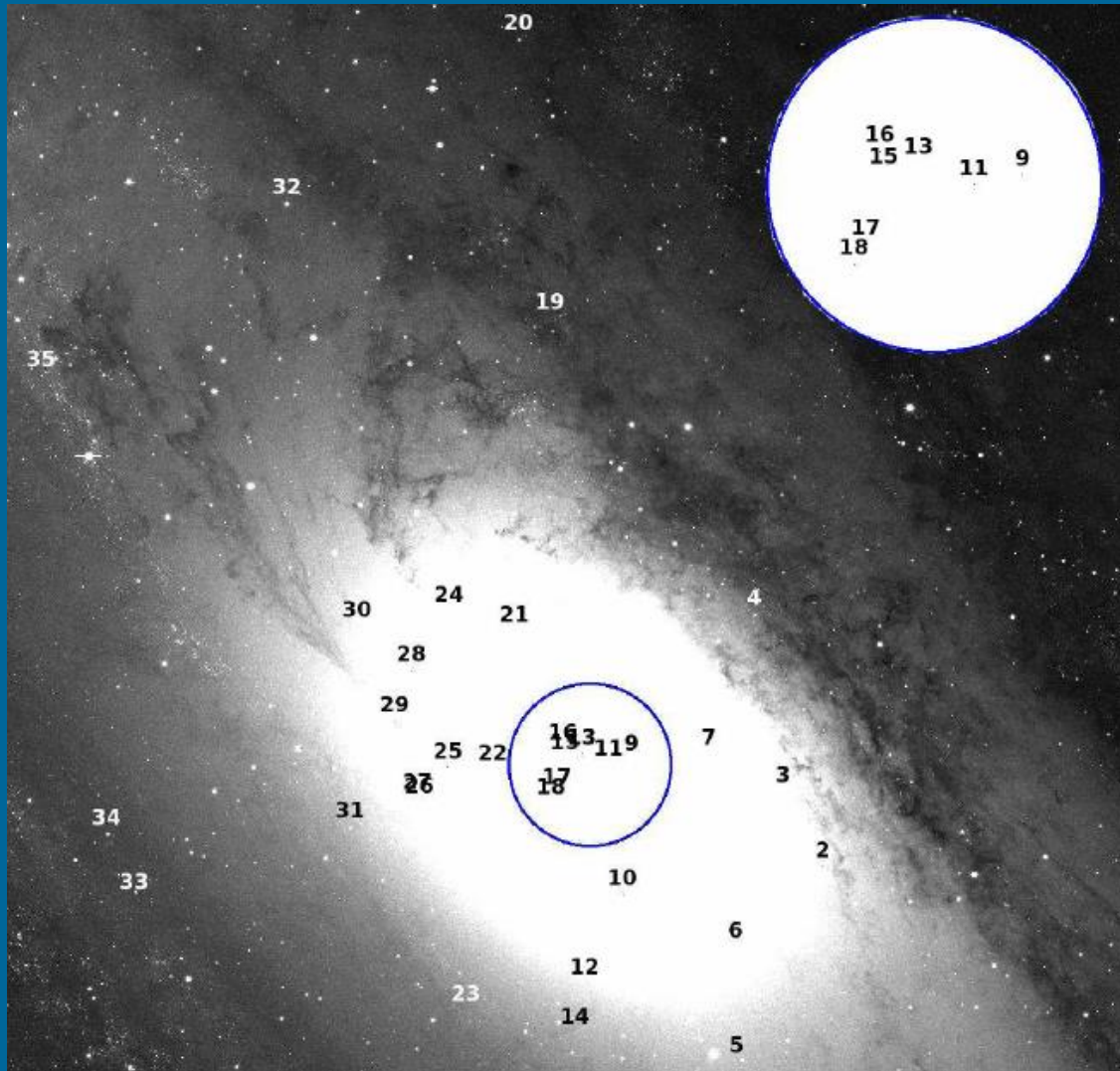
QPOs and BH masses



XTE J1550-564,
GRO J1655-40,
GRS 1915+105

Dashed line is plotted
for the relation
 $v_0 = 931 \text{ Hz } (M/M_o)^{-1}$
The ordinate shows $2v_0$

Extragalactic BHs: the case of M31



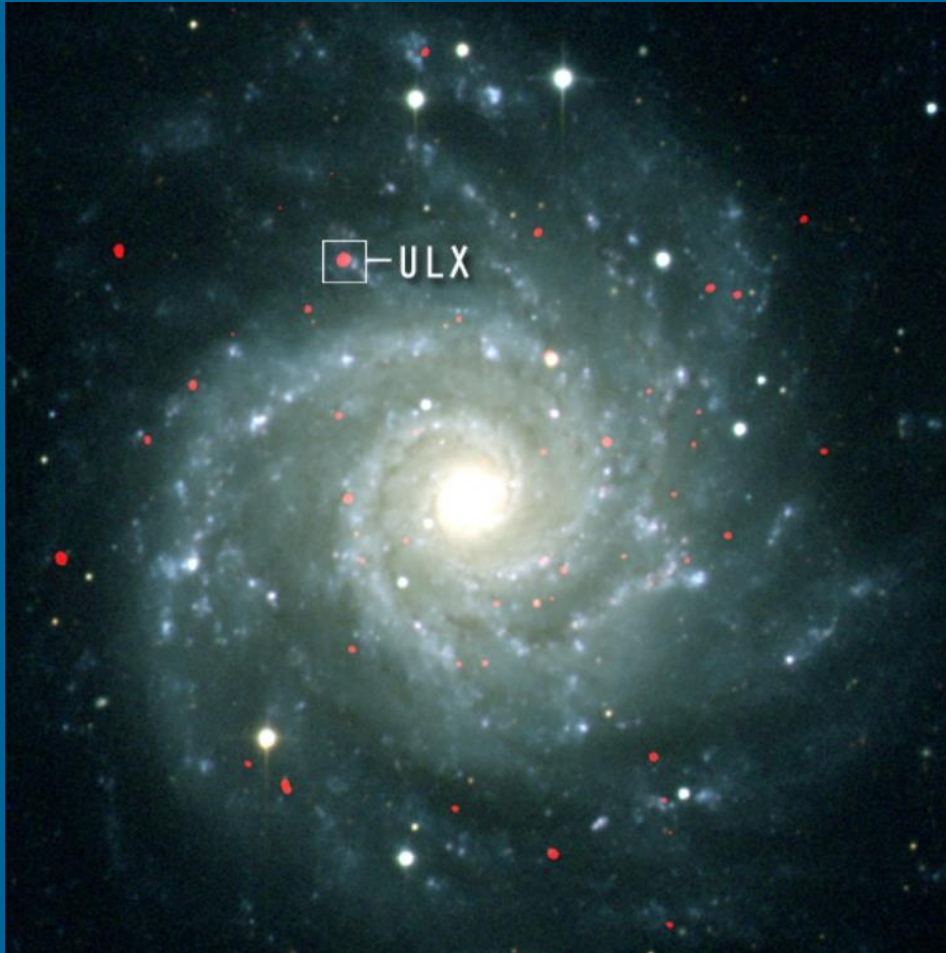
Chandra identification of 26 new black hole candidates in the central region of M31

50 BHCs in M31

Classification is mainly based on spectral properties.

Src	ID	$D_{M31}/''$	$L_{\text{Max}}^{\text{H}}$	Γ_{Max}	$L_{\text{Min}}^{\text{H}}$	Γ_{Min}	N_{O}	DC 1	DC 2	$\chi^2_{\text{con}}/\text{dof}$
S109	BH1	15.85	37 (5)	1.5 (3)	14.1 (17)	1.4 (3) ^a	P			230/76
S111	T1	6.24	18.3 (17)	2.0 (4)	<0.06	1.9 (5) ^a	2	0.04	0.06	234/79
S117	T2	5.11	53 (3)	4.9 (6)	<0.04	1.7	1	0.05	0.05	3957/99
S122	BH2	5.28	15 (2)	1.47 (7) ^a	1.73 (15)	1.47 (7) ^a	P			1527/164
S151	BH3	4.06	31 (2)	2.5 (5)	4.31 (17)	1.552 (15) ^a	P			28720/166
S159	BH4	4.63	5.5 (5)	1.89 (7) ^a	0.39 (0.10)	1.89 (7) ^a	P			3999/167
S167	BH5	6.85	7.9 (1.6)	1.5 (1) ^a	1.7 (2)	1.5 (1) ^a	P			568/157
S168	BH6	4.83	19.0 (18)	1.58 (3) ^a	0.6(2)	1.58 (3) ^a	P			5639/162
S179	BH7	2.49	21 (2)	2.7 (5)	4.9(13)	1.69 (3) ^a	P			669/168
S199	BH8	19	19 (3)	1.8 (4)	<0.4	1.37 (15) ^a	Many	0.33	0.33	664/26
S214	BH9	0.9	8.5 (4)	2.36 (16) ^a	0.05	2.36 (16) ^a	3	0.08	0.09	3482/94
S223	BH10	2.78	4.5(4)	1.64 (5) ^a	0.55(7)	1.64 (5) ^a	P			4983/167
S233	T5	0.66	9.8(13)	2.0 (5)	<0.04	1.7	2	0.02	0.06	317/100
S236	BH11	0.41	23(2)	1.41 (7) ^a	<0.05	1.41 (7) ^a	1 (turn off)	0.16	0.12	2319/95
S251	U2	9.2	320 (8)	3.9 (5)	<0.4	1.7	1	0.11	0.08	61651/69
S265	BH12	4.52	9.0(18)	2.5 (9)	1.5(2)	2.08 (4)	P			3701/167
S269	BH13	0.26	4.9(3)	1.78 (5) ^a	0.76(8)	1.78 (5) ^a	P			3625/170
S276	BH14	5.55	14 (2)	2.9 (7)	<0.05	2.6 (3) ^a	1	0.30	0.17	8381/98
S286	BH15	0.5	7.9 (9)	1.61 (4) ^a	1.2 (2)	1.61 (4) ^a	P			3472/170
S287		2.1	20.5 (5)	3.67 (13)	0.07(2)	1.7	1	0.05	0.03	82/92
S289	BH16	0.62	26.3 (6)	1.58 (3) ^a	0.6 (2)	1.58 (3) ^a	P			16817/164
S293	B128	4.96	5.9 (5)	1.64 (10) ^a	<0.03	1.64 (10) ^a	2	0.14	0.13	2348/87
S297	BH17	0.89	8.0 (3)	1.91 (4) ^a	0.73 (14)	1.91 (4) ^a	P			4602/170
S299	BH18	1.12	20 (2)	1.50 (2) ²	6.8 (8)	1.8 (3)	P			842/170
S300	BH19	9.26	21 (3)	1.9 (6)	0.75(18)	1.84 (5) ^a	P			9096/127
S322		1.62	13 (2)	2.5 (6)	<0.04	1.7	1	0.02	0.04	227/72
S327	BH20	15.1	62 (3)	1.14 (14)	30 (2)	1.89 (2) ^a	P			587/73
S330	T8	8.4	2.7 (4)	2.10 (17) ^a	<0.06	2.10 (17) ^a	1 (turn on)	0.73	0.79	2941/158
S331	T13	1.6	6.1 (6)	4.02 (17)	<0.0016	1.7	1	0.018	0.05	171/45
S335	BH21	3.2	20.6(17)	1.9 (4)	5.6 (4)	1.7	P			441/108
S339	T9 / U1	2.4	394 (2)	?	<0.025	1.74 (2) ^a	1	0.06	0.04	37255/89
S345	BH22	2	23 (2)	1.70 (5) ^a	0.82 (18)	1.7	P			5782/108
S353		3.5	5.8 (15)	1.6 (3) ^a	<0.05	1.70 (5) ^a	5	0.20	0.21	1984/112
S358	BH23	5.7	8.9(13)	2.5 (6)	<0.18	1.6 (3) ^a	P			651/167
S365		2.8	14(2)	2.9 (9)	<0.009	1.78 (4)	1	0.06	0.04	503/60
S372	BH24	4.3	7.2(13)	1.8 (4)	2.8(3)	2.37 (19) ^a	P			801/168
S373	BH25	2.9	7.2 (11)	1.9 (6)	3.1(9)	1.78 (8)	P			406/107
S386	BH26	3.6	8.2 (13)	1.84 (5) ^a	1.3 (2)	1.4 (3)	P			5245/170
S389	BH27	3.6	13.0 (18)	2.01 (5) ^a	0.37 (9)	1.84 (5) ^a	P			14549/170
S391	BH28	4.2	7.7 (3)	1.69 (4) ^a	1.8 (2)	2.1 (5)	P			2885/169
S396	BH29	4.1	46.8 (5)	1.46 (8) ^a	<0.07	1.69 (4) ^a	1	0.05	0.05	20445/99
S411	BH30	5.6	12 (2)	1.9 (6)	<0.16	1.46 (8) ^a	Many	0.26	0.42	2667/145
S415	BH31	5.1	20 (3)	1.6 (3)	7.5 (14)	1.9 (2) ^a	P			511/102
S438	BH32	13.2	14.2 (12)	1.6 (2)	<0.007	1.47 (2) ^a	3	0.70	0.13	3195/76
S448		6.9	97 (6)	3.8 (4)	<0.04	1.58 (2) ^a	2	0.06	0.10	3198/89
S484	BH33	9.8	10 (3)	1.94 (6) ^a	1.4 (2)	1.7	P			1450/111
S487	BH34	10.1	10.2 (13)	1.9 (5)	3.3 (11)	1.94 (6) ^a	P			100/39
S497	BH35	13.9	12.8 (15)	1.7 (4)	1.07 (16)	1.49 (5) ^a	P			2578/78

Ultraluminous X-ray sources



ULXs are sources with fluxes which correspond to an isotropic luminosity larger than the Eddington limit for a 10 solar mass object.

Now many sources of this type are known. Their nature is unclear. Probably, the population contains both: stellar mass BHs with anisotropic emission and intermediate mass BHs.

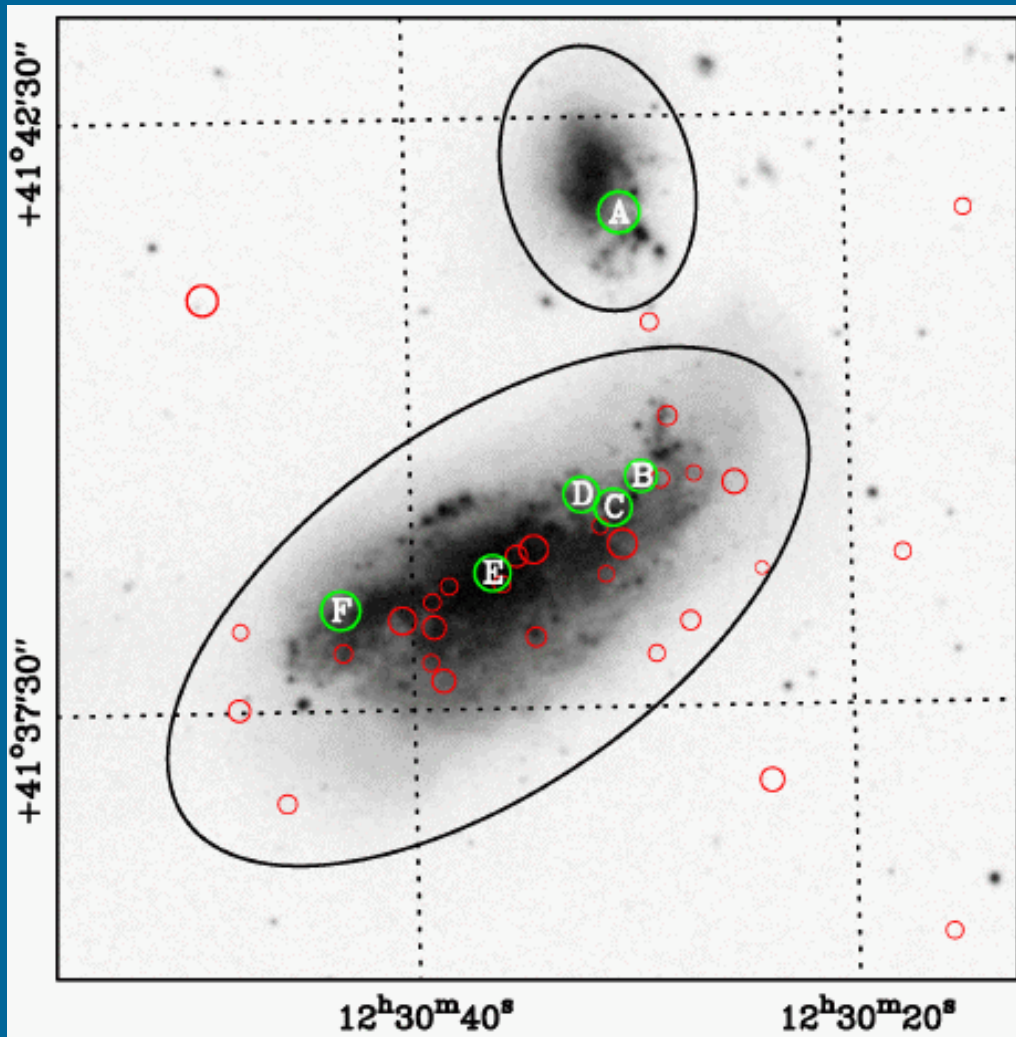
Recent reviews:

1702.05508 - short

1703.10728 – long

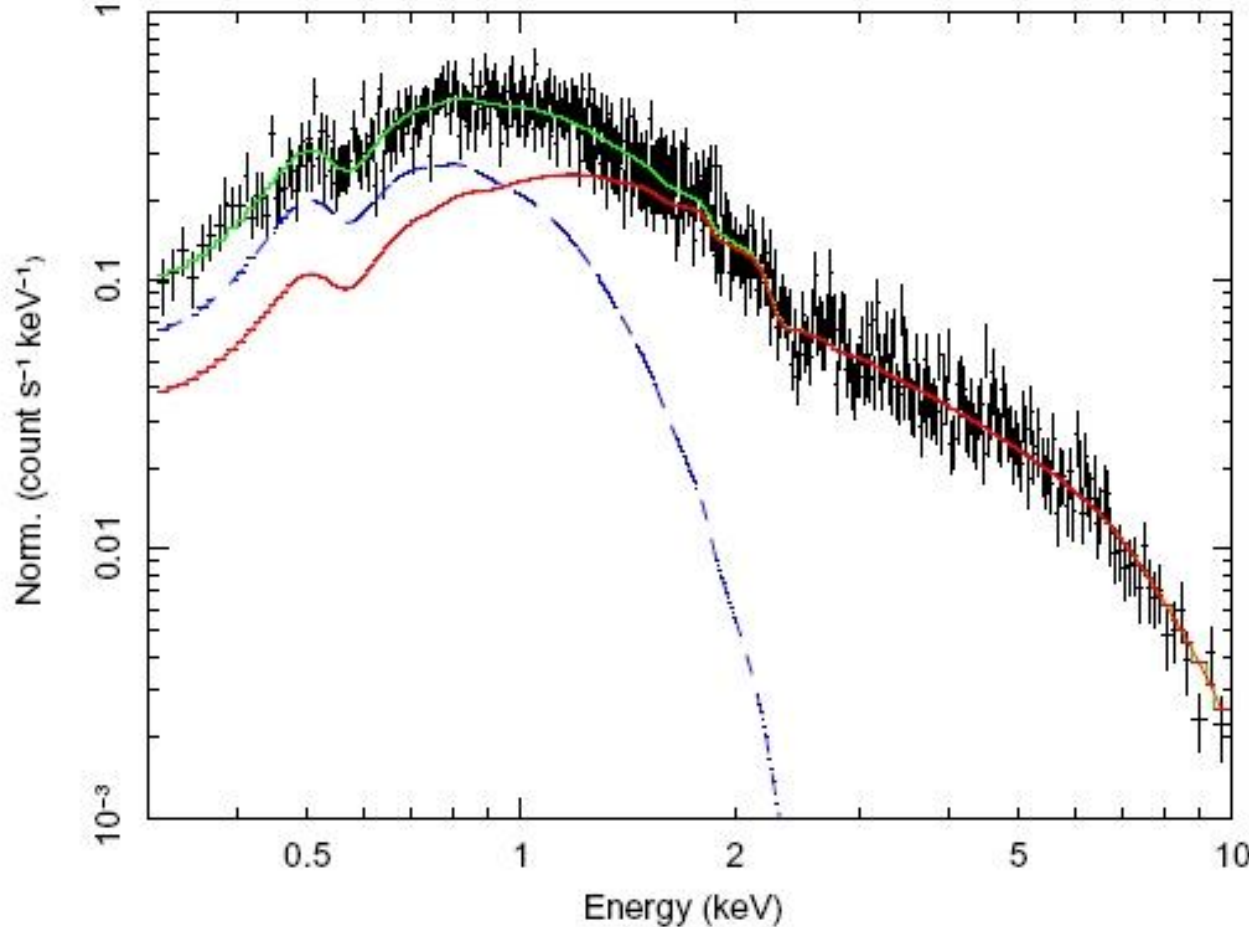
1907.08213 – catalogue of candidates

ULXs in NGC 4490 and 4485



Six marked sources are ULXs

Spectrum of the ULX in NGC 1313



NGC 1313 X-1

Green line –
the IMBH model.

Red – power-law.

Blue – multi-color disc.

ULX in galaxies of different types

In the following two slides there are images of several galaxies from the SDSS in which positions of ULXs are marked.

Crosses (x) mark sources with luminosities $>10^{39}$ erg/s.

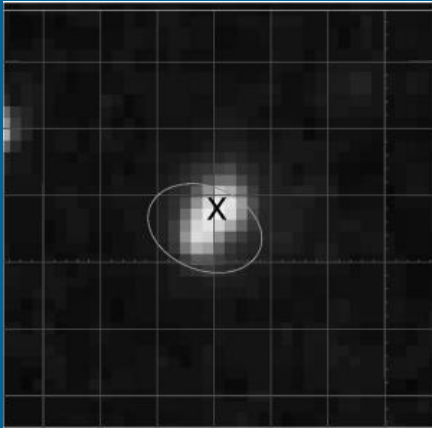
Pluses (+) mark sources with luminosities $>5 \cdot 10^{38}$ erg/s.

The size of one square element of the grid is 1.2 arcminute (except IZW 18, in which case the size is 0.24 arcminute in right ascension and 0.18 in declination).

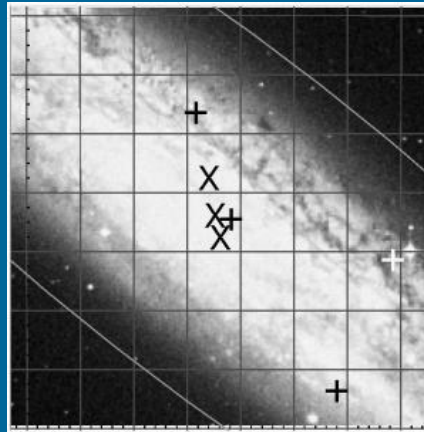
Galaxies NGC 4636, NGC 1132, NGC 4697, NGC 1399 are ellipticals, IZW 18 – irregular, the rest are spiral galaxies.

Ellipses mark the 25-th magnitude isophotes (this a typical way to mark the size of a galaxy).

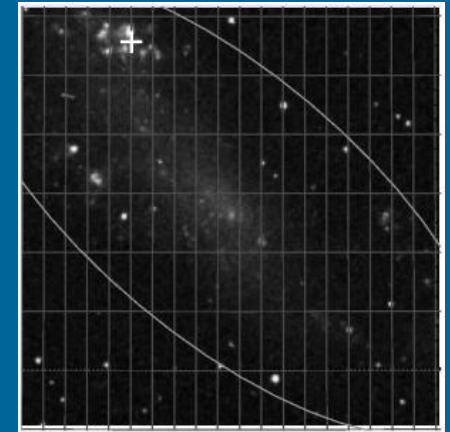
ULX in galaxies of different types



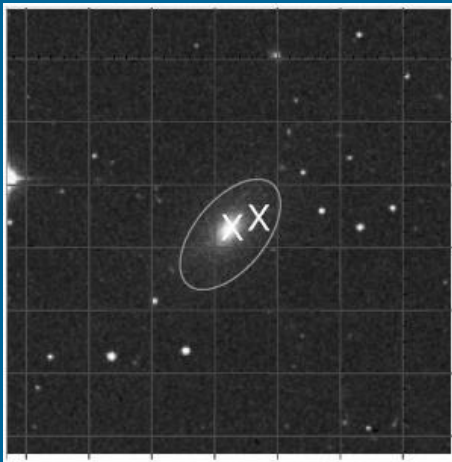
IZW 18



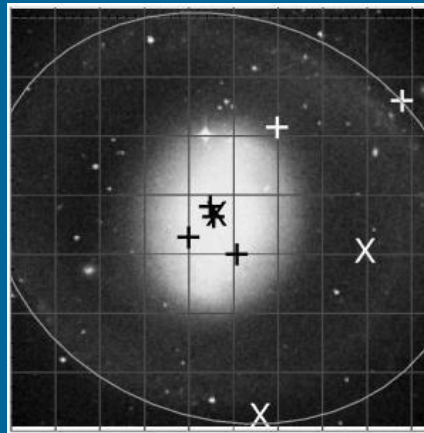
NGC 253



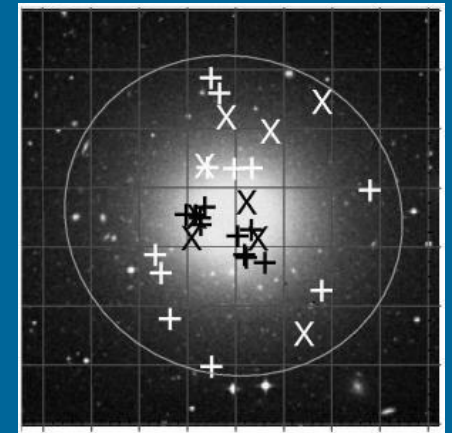
IC 2574



NGC 1132

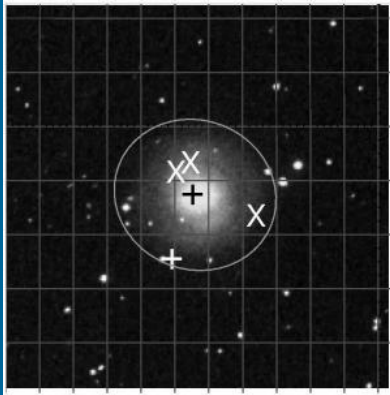


NGC 1291

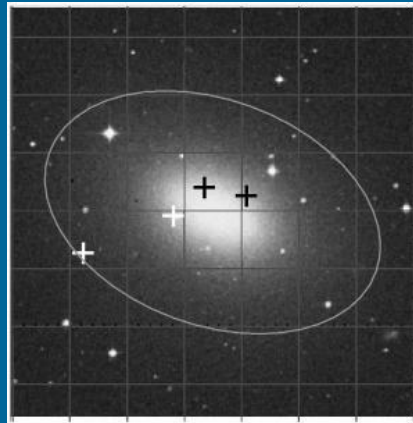


NGC 1399

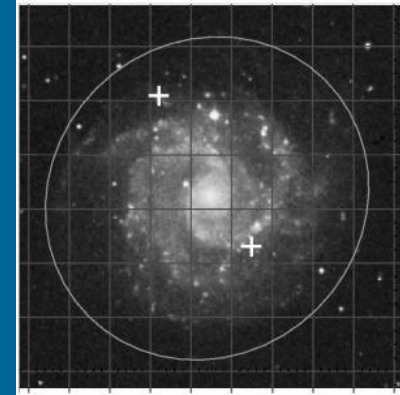
ULX in galaxies of different types



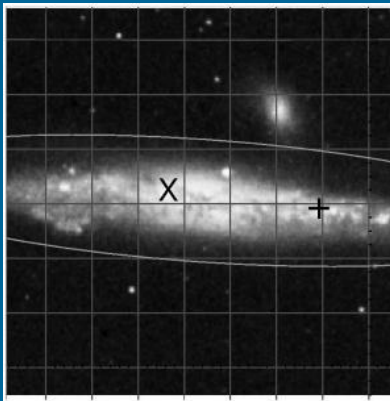
NGC 2681



NGC 4697

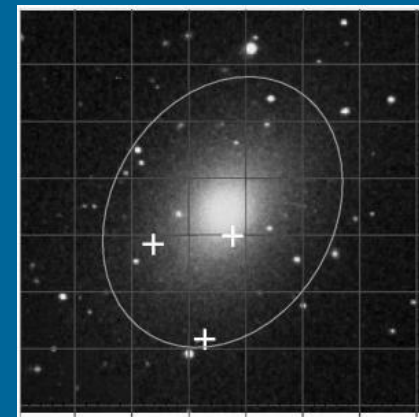


NGC 3184



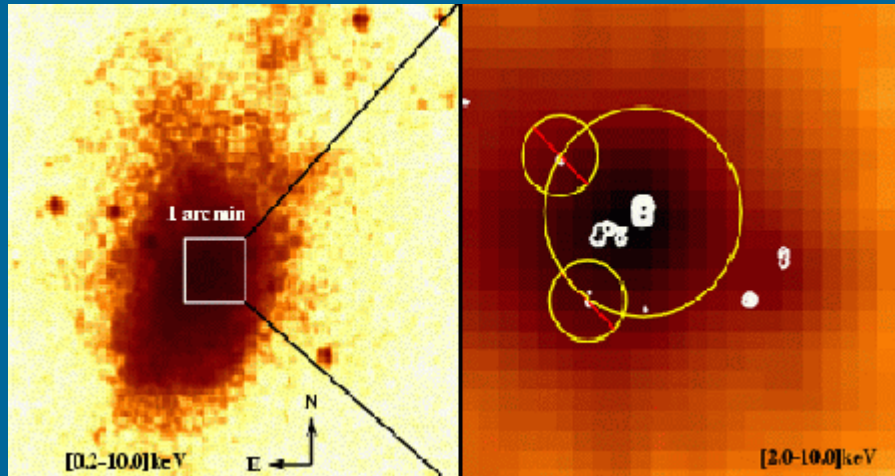
NGC 4631

Large sample of
host galaxies for ULX:
1108.1372



NGC 4636

The source X-1 in M82



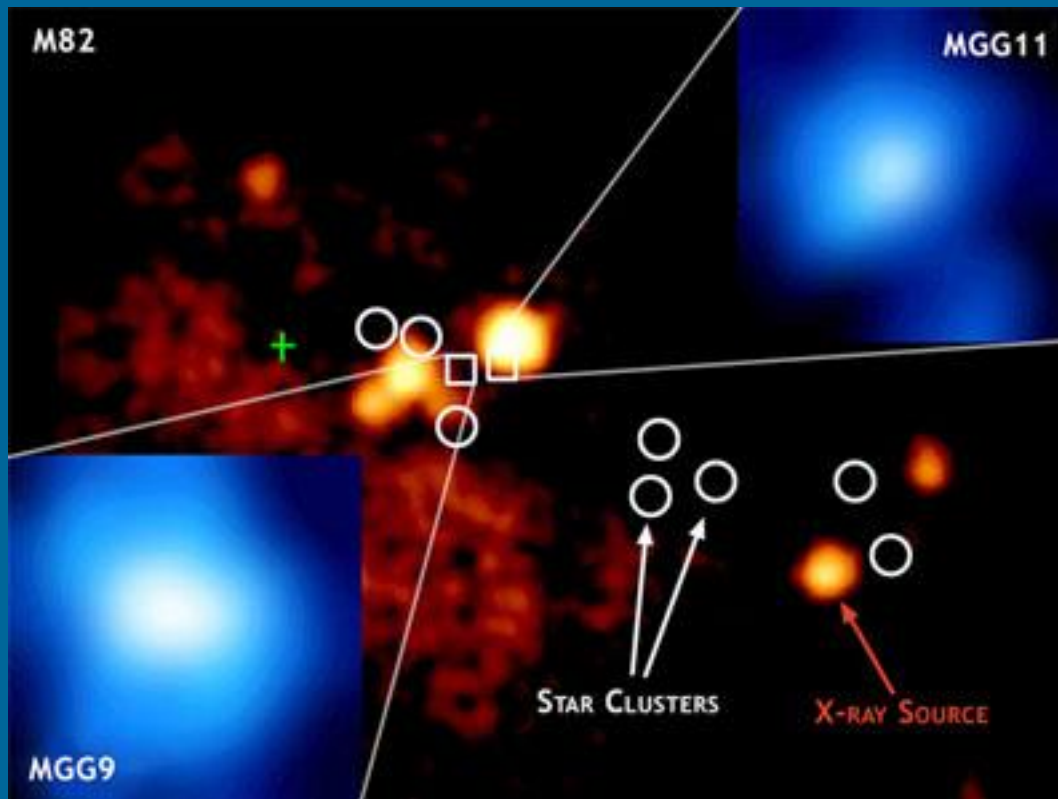
The source M82 X-1 is one of the most luminous, and so it is the best candidate to be an intermediate mass BH.

QPOs are observed in this source. Their properties support the hypothesis of an intermediate mass BH.

QPO was recently detected (1309.6101).
Scaling points to masses 10^4 - 10^5 solar masses.

Pasham et al. (2014) estimated the mass to be 400 Msolar
Nature **513**, 74–76 (04 September 2014)

M82, stellar clusters and ULXs



Intermediate mass BHs can be formed in dense stellar clusters.

See, however, 0710.1181 where the authors show that for solar metallicity even very massive stars most probably cannot produce BHs massive enough.

McCrady et al (2003)

<http://www.nature.com/nature/journal/v428/n6984/full/nature02448.html>

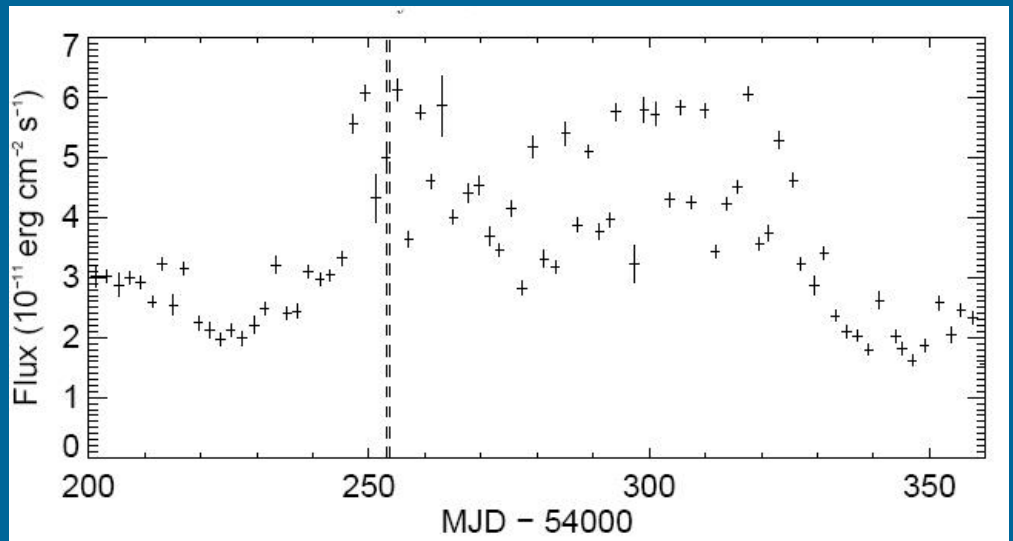
X41.4+60 in M82

79-day burst. Isotropic luminosity $\sim 5 \cdot 10^{40}$ erg/s

Hard state. Usually $L \sim 0.3 L_{\text{edd}}$, here there are indications (photon index $\Gamma = 1.6$) that it is even $\sim 0.1 L_{\text{edd}}$.

QPOs.

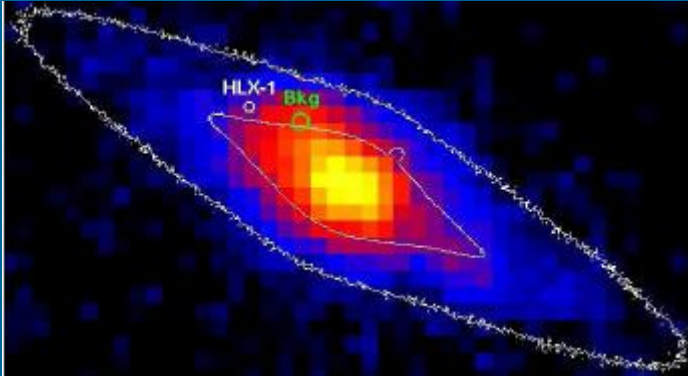
Altogether: mass \sim few 1000 Solar.



RXTE + Chandra observations

(Kaaret et al. 0810.5134)

The most luminous ULX: HLX-1 in the galaxy ESO 243-49,

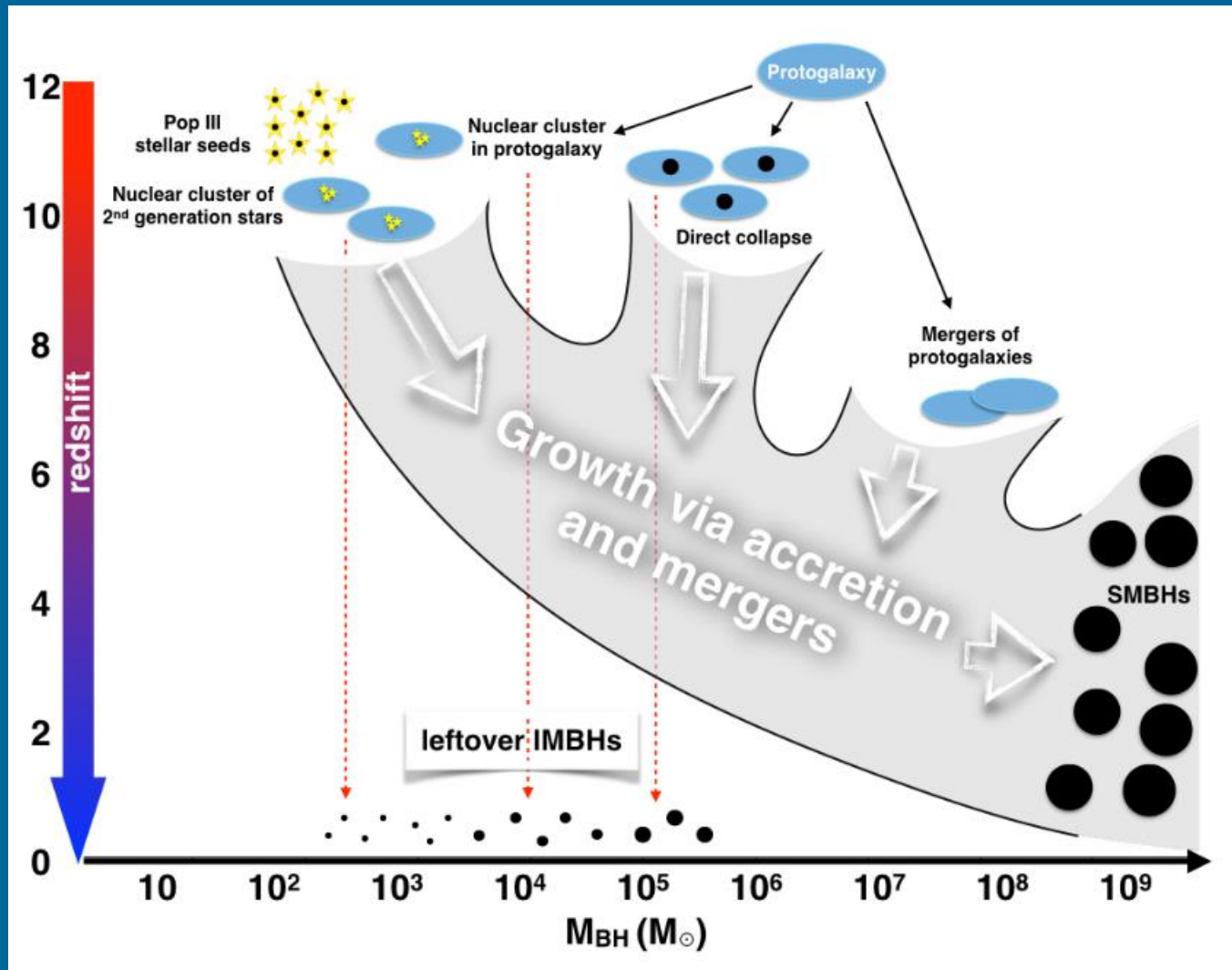


$L > 10^{42}$ erg/s
 $M \sim 500 M_{\odot}$

1011.1254, 1104.2614

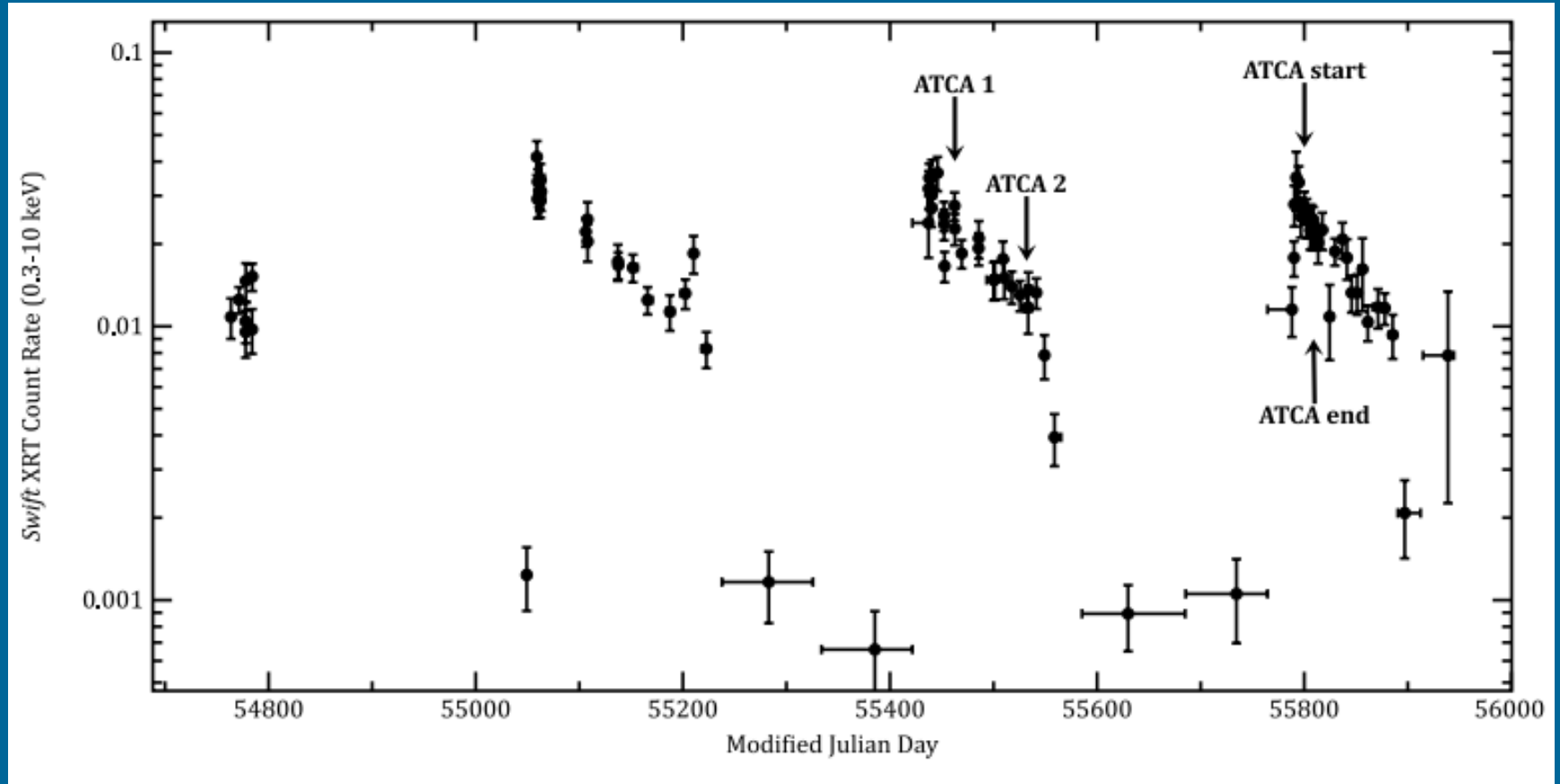
New data about this source: 1108.4405; 1203.4237; 1210.4169; 1210.4924

Origin of IMBHs



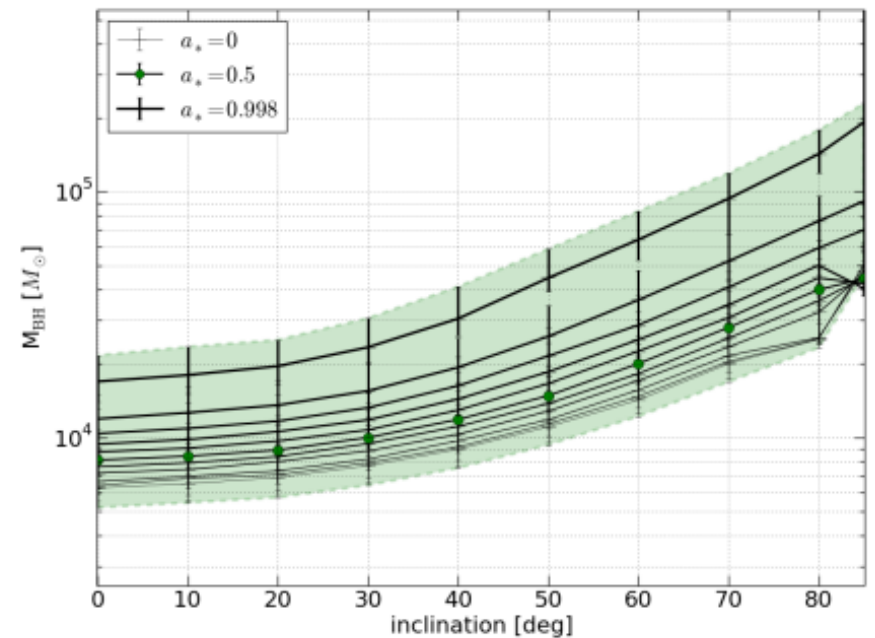
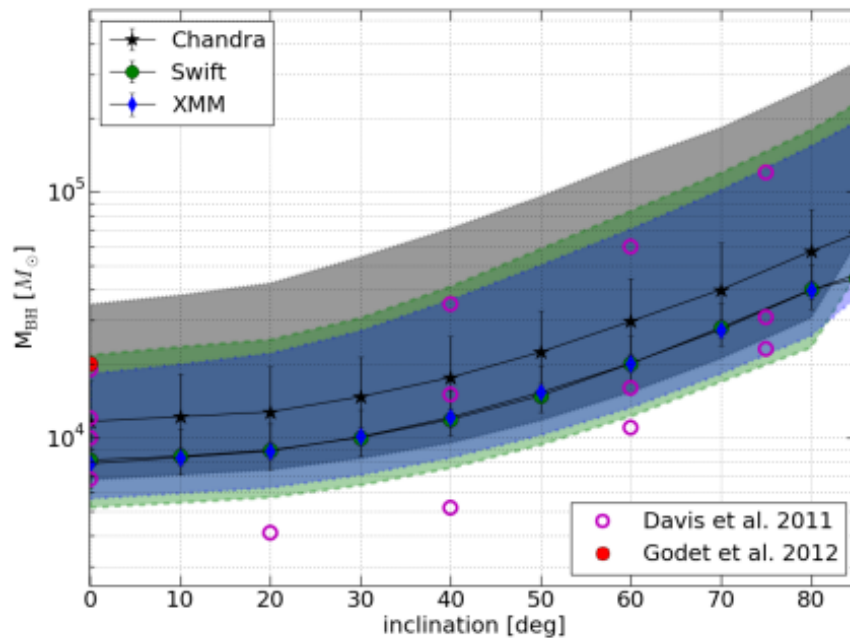
State transitions in ESO 243-49 HLX-1

Mass is estimated to be 10^4 - 10^5 Msolar



More mass estimates for HLX-1

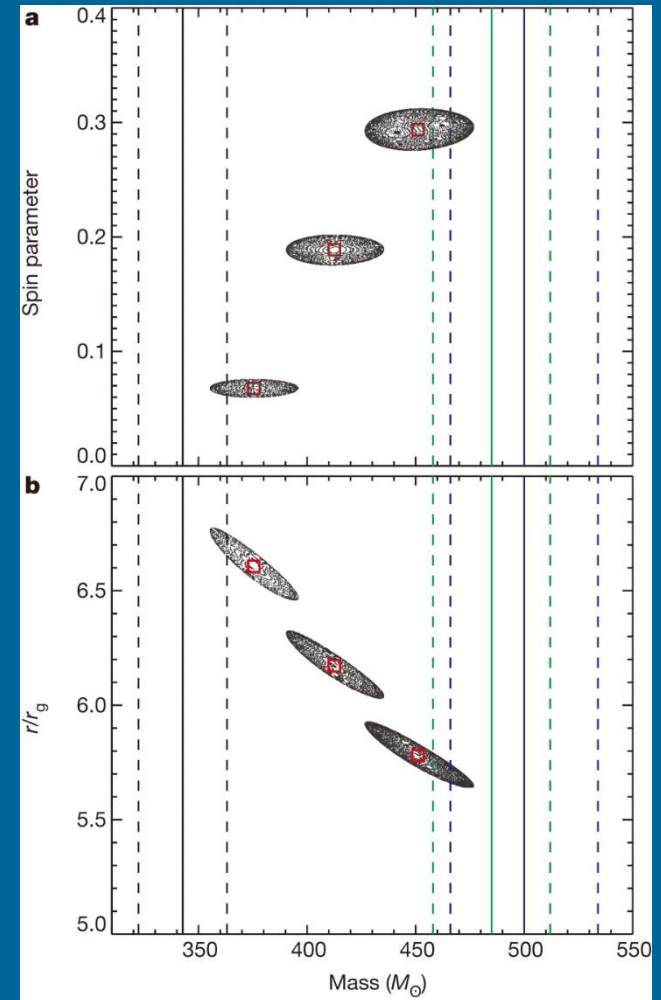
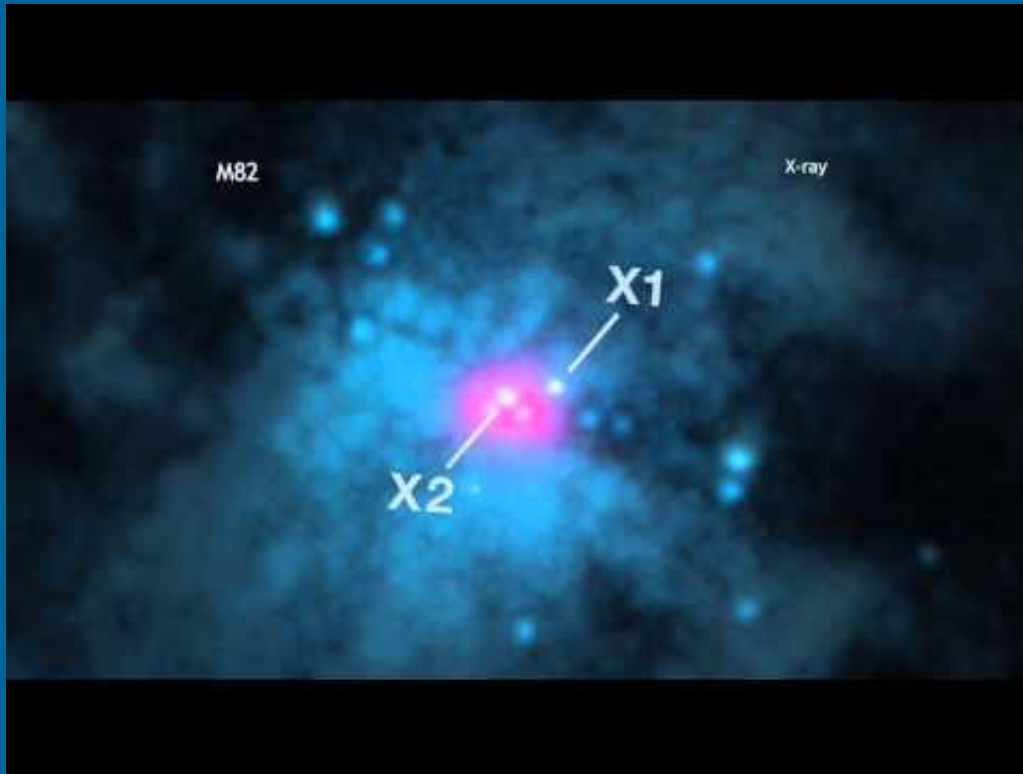
Taking into account all uncertainties the mass is still large



Accretion model for this source was presented in 1402.4863

Heavy BH in M82

Pasham et al. (Nature 2014)
дают оценку массы для X-1
около 400 масс Солнца.



IMBH in an ULXs

For the first time for one source there are both – spectral and timing – data showing evidence in favor of an IMBH.

$$M_{\text{BH}} \sim 10^3 - 10^4 M_{\text{solar}}$$

Evidence for an Intermediate Mass Black Hole in NGC 5408 X-1

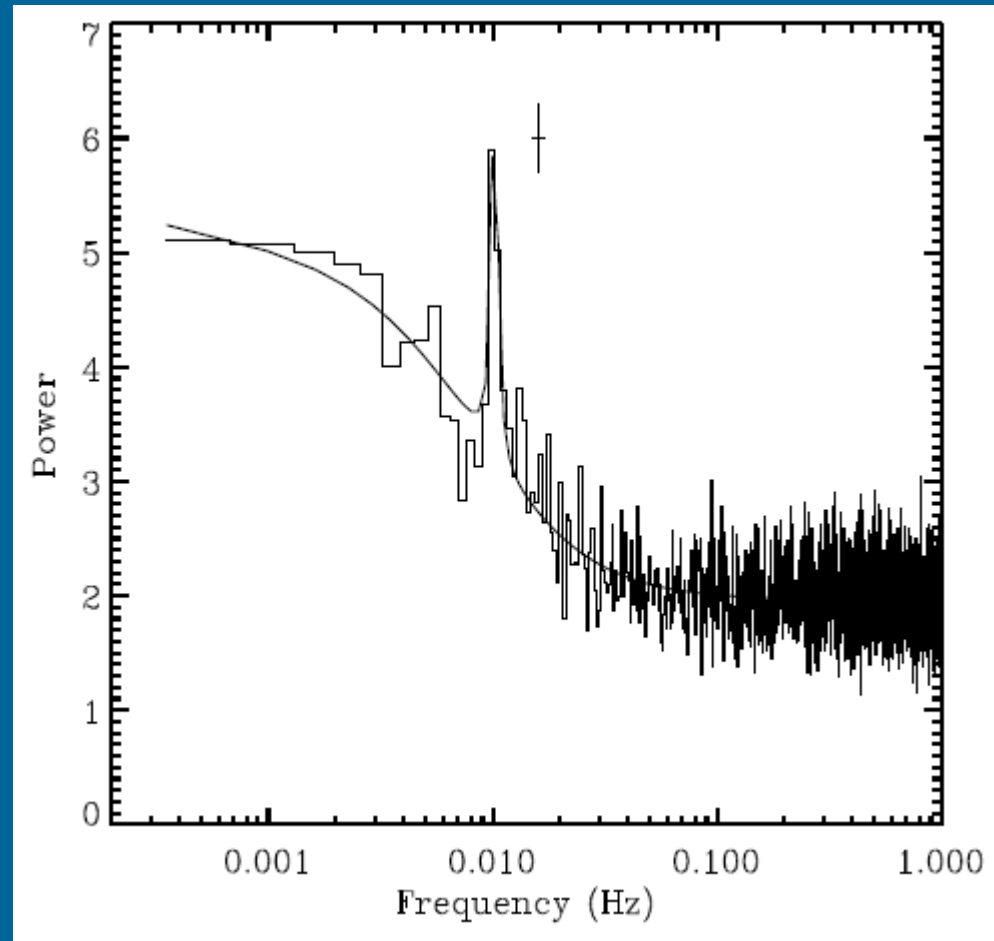
Tod E. Strohmayer¹ & Richard F. Mushotzky¹

ABSTRACT

We report the discovery with XMM-Newton of correlated spectral and timing behavior in the ultraluminous X-ray source (ULX) NGC 5408 X-1. An ≈ 100 ksec pointing with XMM/Newton obtained in January, 2008 reveals a strong 10 mHz QPO in the > 1 keV flux, as well as flat-topped, band limited noise breaking to a power law. The energy spectrum is again dominated by two components, a 0.16 keV thermal disk and a power-law with an index of ≈ 2.5 . These new measurements, combined with results from our previous January 2006 pointing in which we first detected QPOs, show for the first time in a ULX a pattern of spectral and temporal correlations strongly analogous to that seen in Galactic black hole sources, but at much higher X-ray luminosity and longer characteristic time-scales. We find that the QPO frequency is proportional to the inferred disk flux, while the QPO and broad-band noise amplitude (root mean squared, rms) are inversely proportional to the disk flux. Assuming that QPO frequency scales inversely with black hole mass at a given power-law spectral index we derive mass estimates using the observed QPO frequency - spectral index relations from five stellar-mass black hole systems with dynamical mass constraints. The results from all sources are consistent with a mass range for NGC 5408 X-1 from 1000 - 9000 M_{\odot} . We argue that these are conservative limits, and a more likely range is from 2000 - 5000 M_{\odot} . Moreover, the recent relation from Gierlinski et al. that relates black hole mass to the strength of variability at high frequencies (above the break in the power spectrum) is also indicative of such a high mass for NGC 5408 X-1. Importantly, none of the above estimates appears consistent with a black hole mass less than $\approx 1000 M_{\odot}$ for NGC 5408 X-1. We argue that these new findings strongly support the conclusion that NGC 5408 X-1 harbors an intermediate mass black hole.

Low-frequency QPO (2008 data)

NGC 5408 X-1 behaves very much like a Galactic stellar-mass BH system with the exception that its characteristic X-ray time-scales are 100 times longer, and its luminosity is greater by a roughly similar factor.

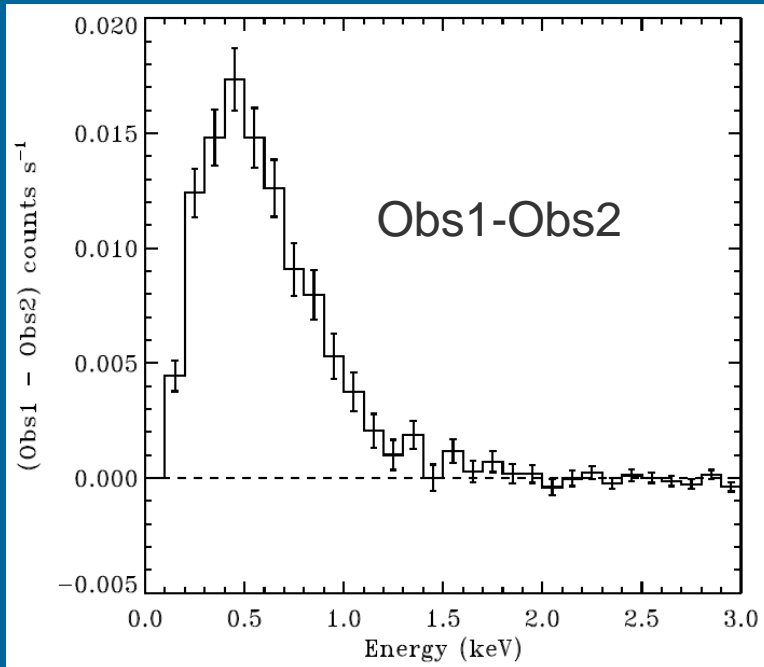


E>1 keV

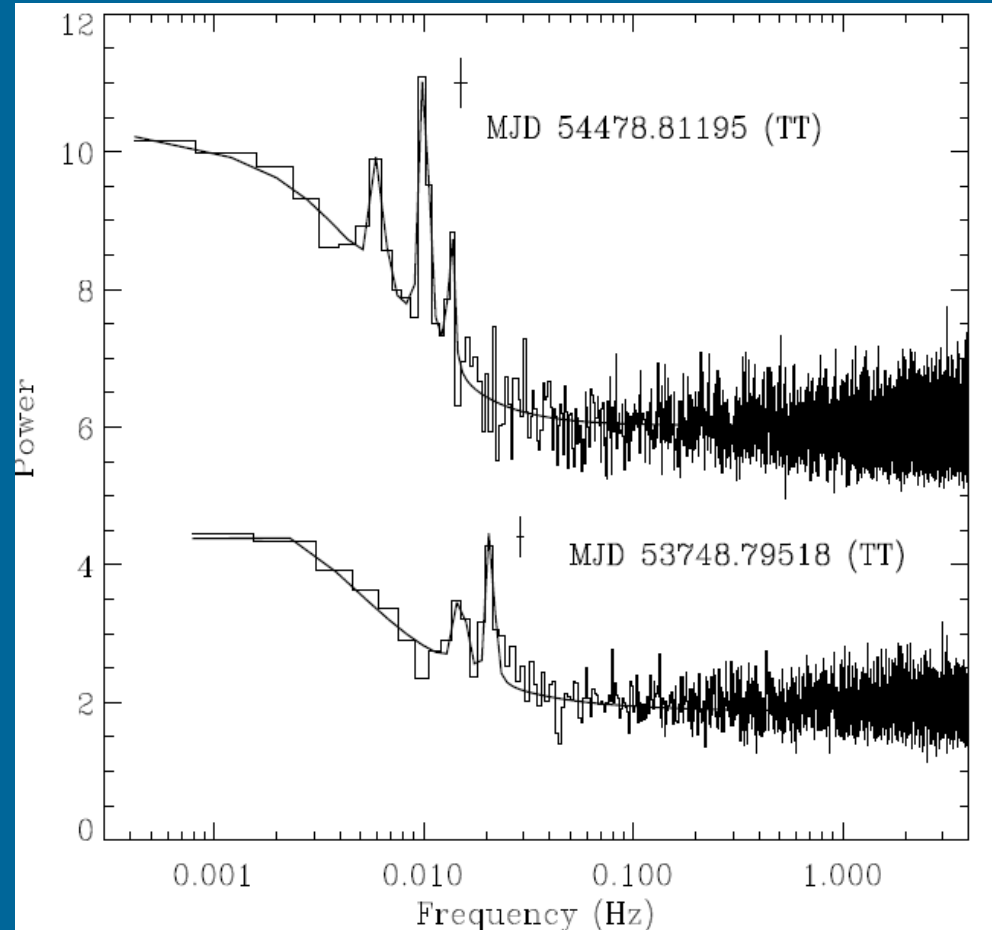
Comparison of two observations

Obs1 – 2006

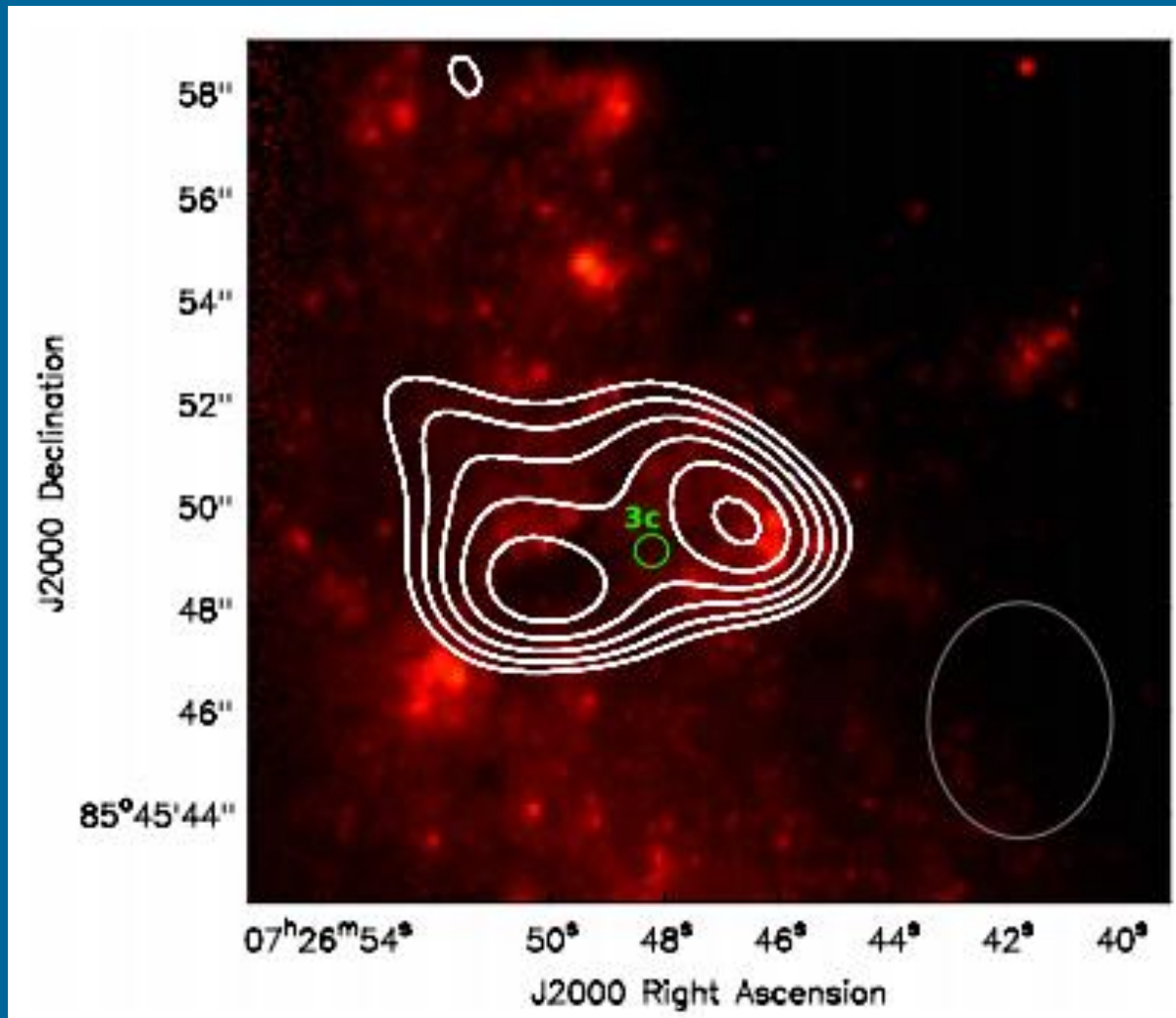
Obs2 – 2008



Obs1 was brighter, but all difference is due to soft (disc) component.

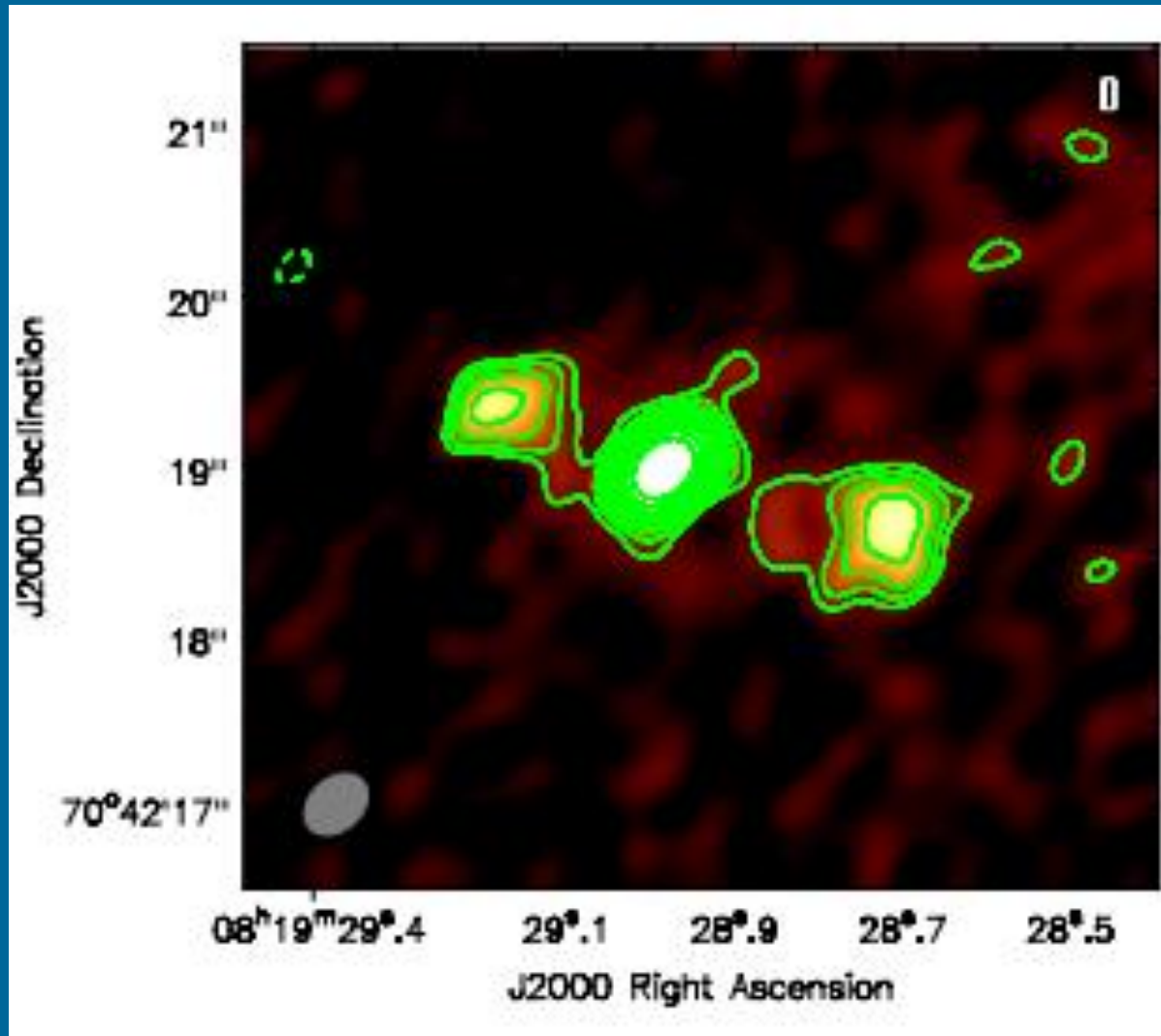


Jet from an ULX in NGC 2276



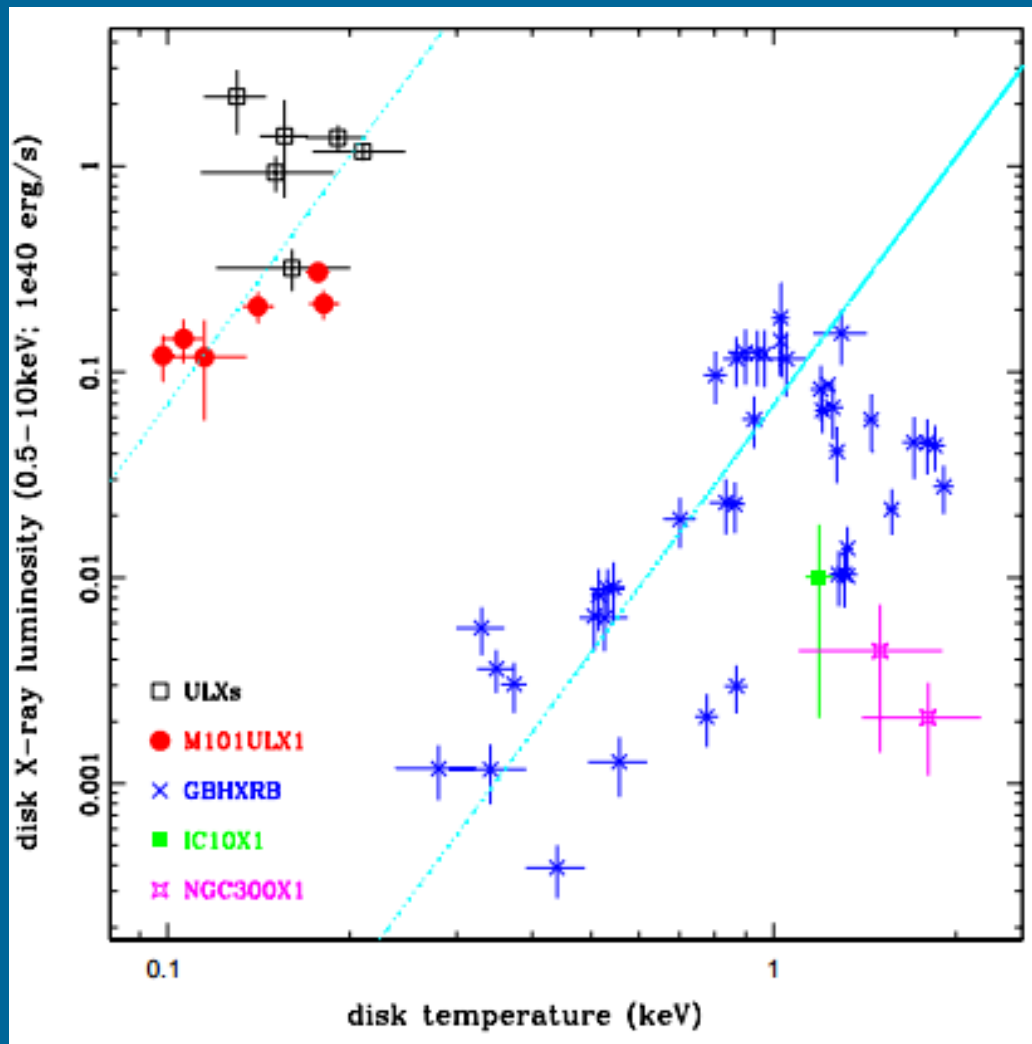
650 pc radio lobes
Scaling from usual BHs
gives the mass estimate
 $4.7 \cdot 10^3 < M < 8.5 \cdot 10^5$

Jet from ULX Holmberg II X-1



Mass limits are poor:
 $M > 25 M_{\text{solar}}$

Strange accretion in the ULX in M101



The authors determined the orbital period and determined properties of the companion.

The BH mass is estimated to be ~20-30 Msolar.

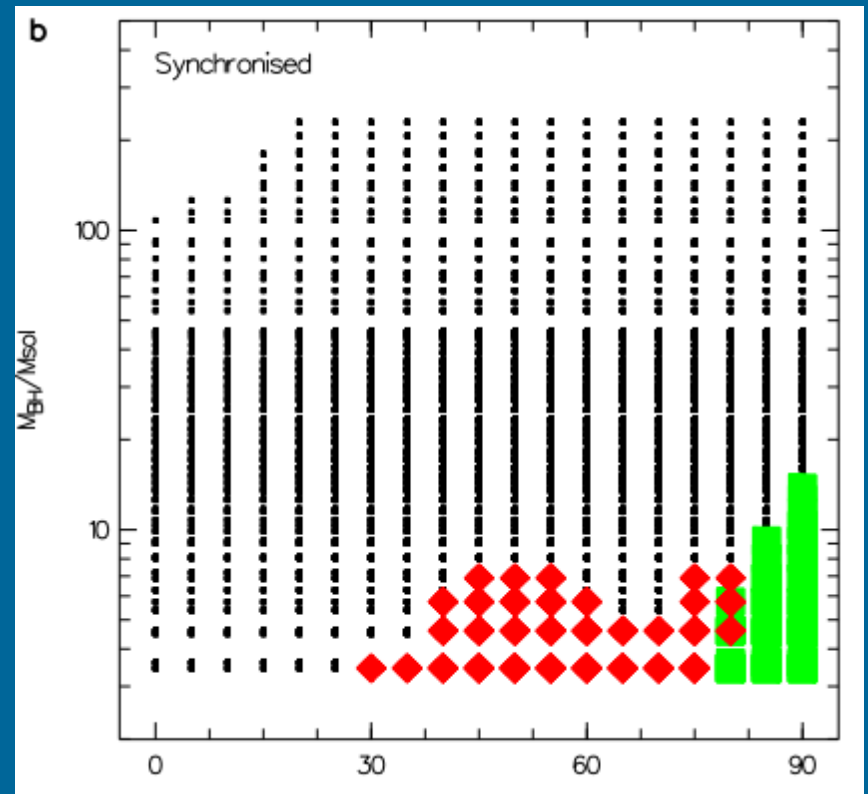
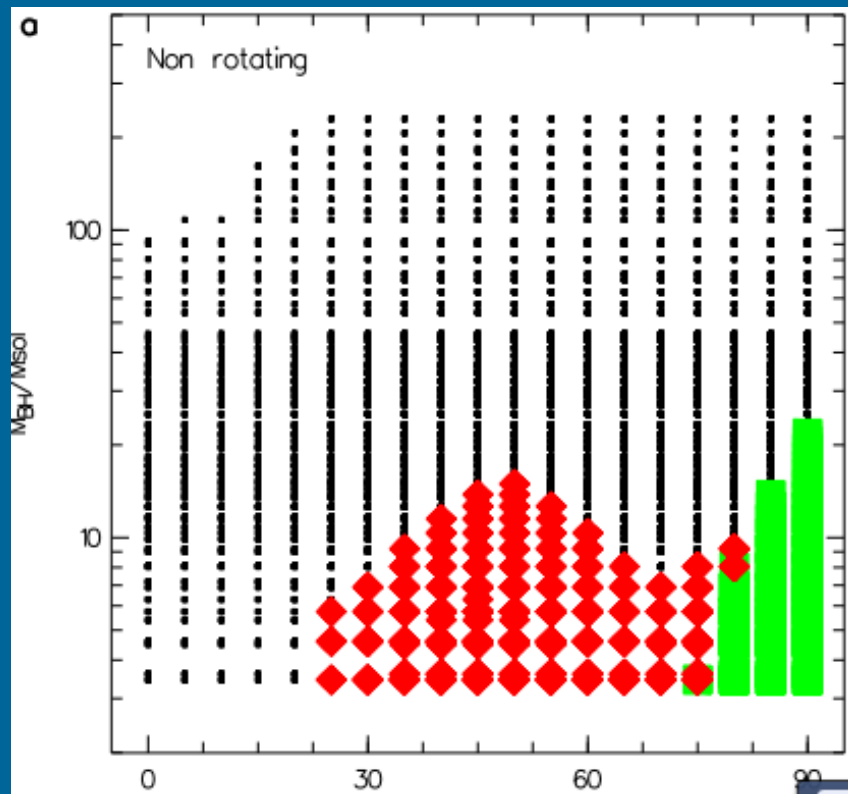
However, soft X-ray spectra is unexpected for such low mass.

Normal BH in an ULX

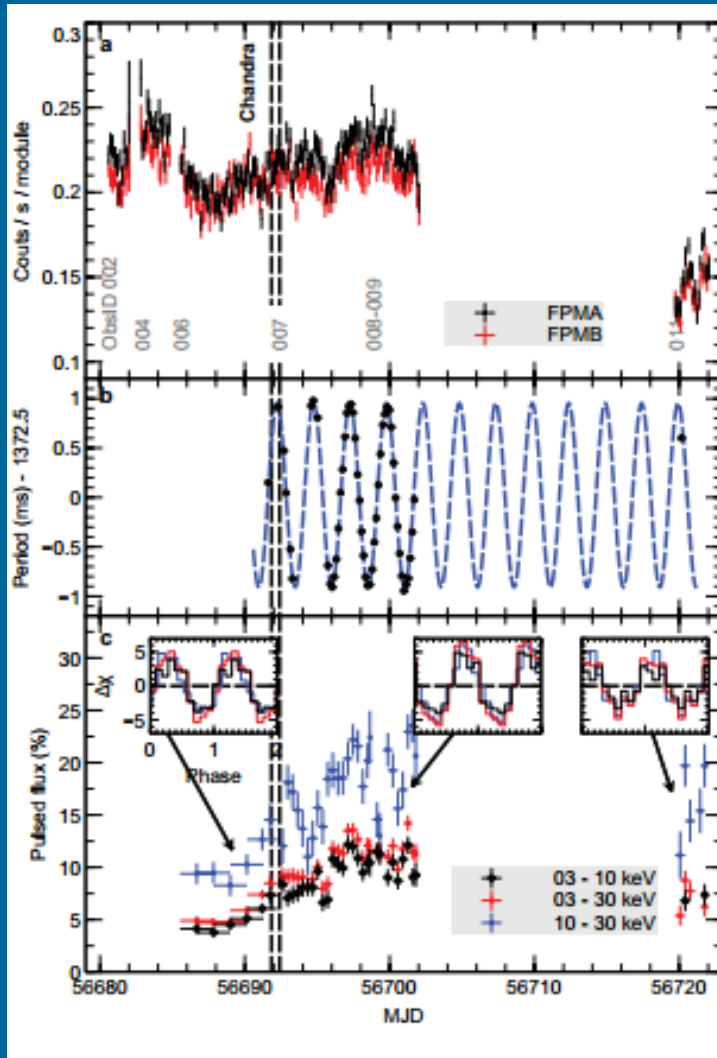
P13 in the galaxy NGC 7793

BH mass 7-15 M_{solar}

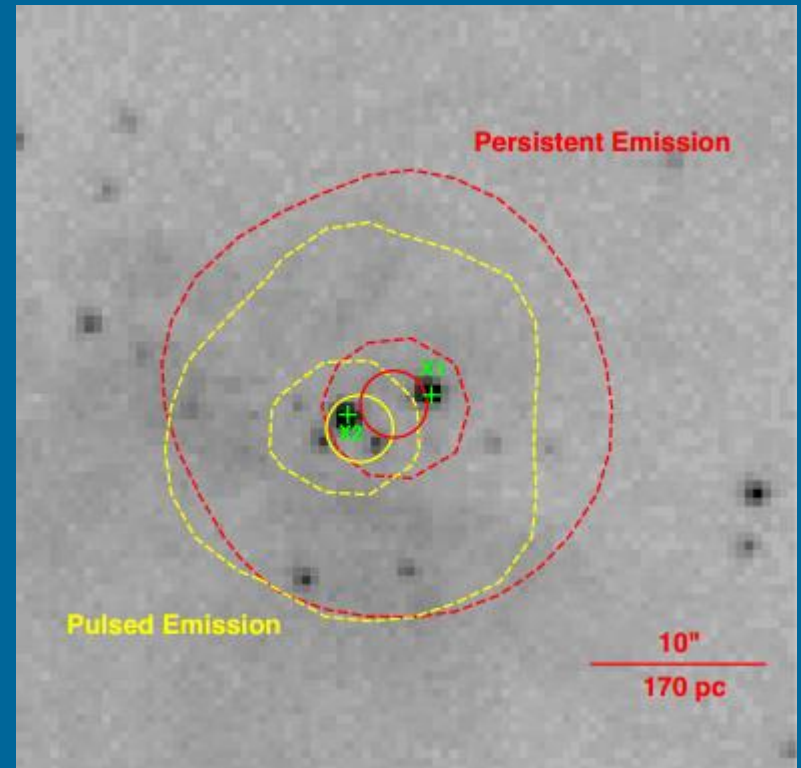
(depending on rotation)



A NS in an ULX!!!!



Pulsations with 1.37 s period found!



New search through archive data for other examples of pulsars in ULX failed to find any ([1410.7264](#))

1410.3590

Now: three NS ULXs

Recent results on NSs in ULXs

In 2020 already six ULXs with NSs are known (see the list in 1906.04791).

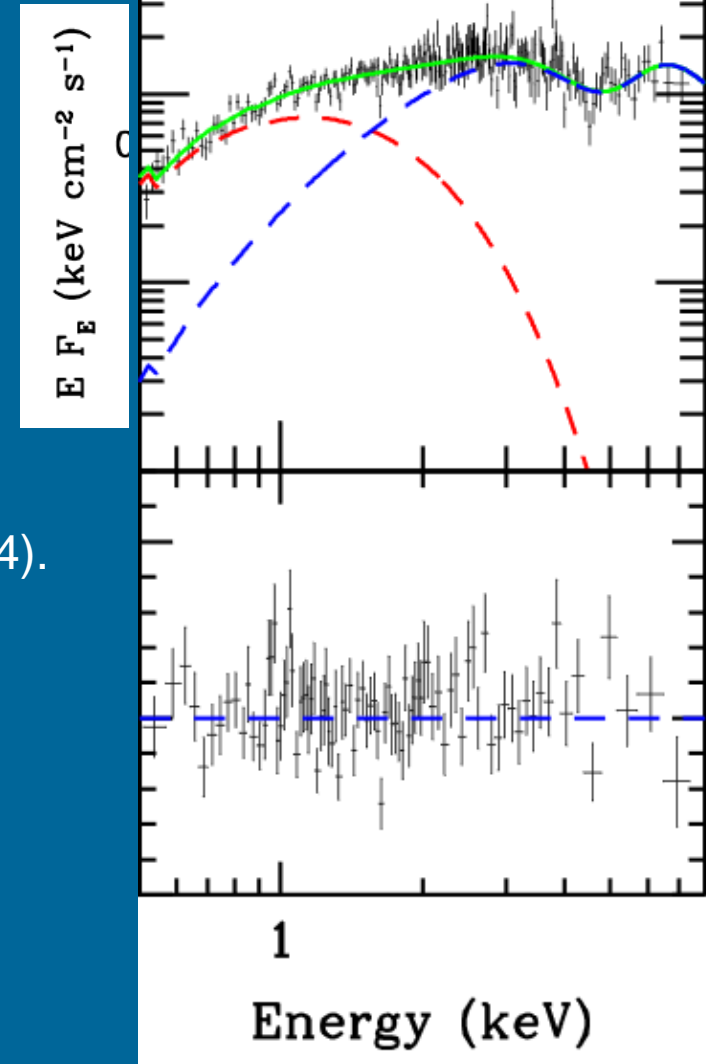
- Outflow (0.24c) in ULX NGC300. 1803.02367
- Cyclotron resonance line in ULX NGC300. 1803.07571
- Cyclotron line in ULX M51. 1803.02376
- New indirect arguments in favour of NSs in ULXs. 1803.04424
- Diffuse X-ray emission in NGC 5907 ULX-1. 1910.11876

Cyclotron line in ULX M51

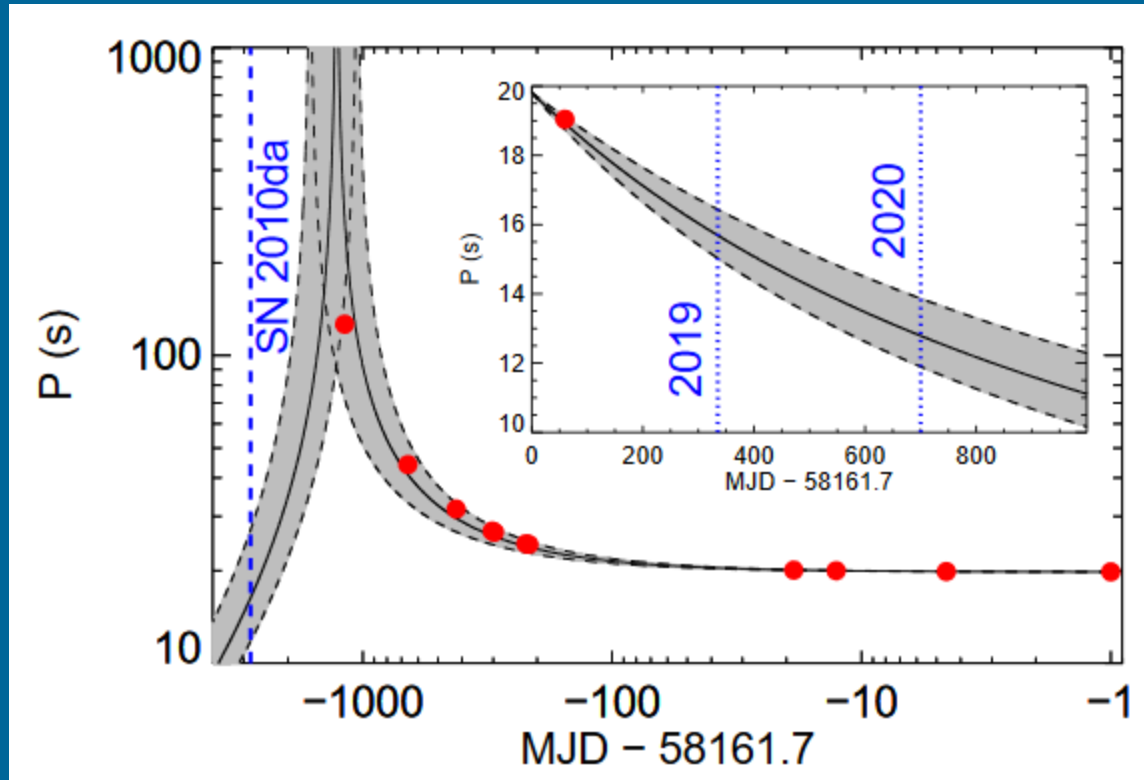
$\sim 10^{12}$ G dipolar field.
Strong dipole field is excluded,
but strong multipoles are still possible.

A big question: are there magnetars in ULX?

Recent studies suggest that – no (see 1903.03624).



Fantastic spin evolution of the ULX in NGC 300



About SN2010da see 1605.07245.
This might be not a core collapse, but an eruption on a massive evolved star.

Donor star discovered (1909.02171)!
It is a red supergiant.

Torque reversal in 2014?

The population of ULXs

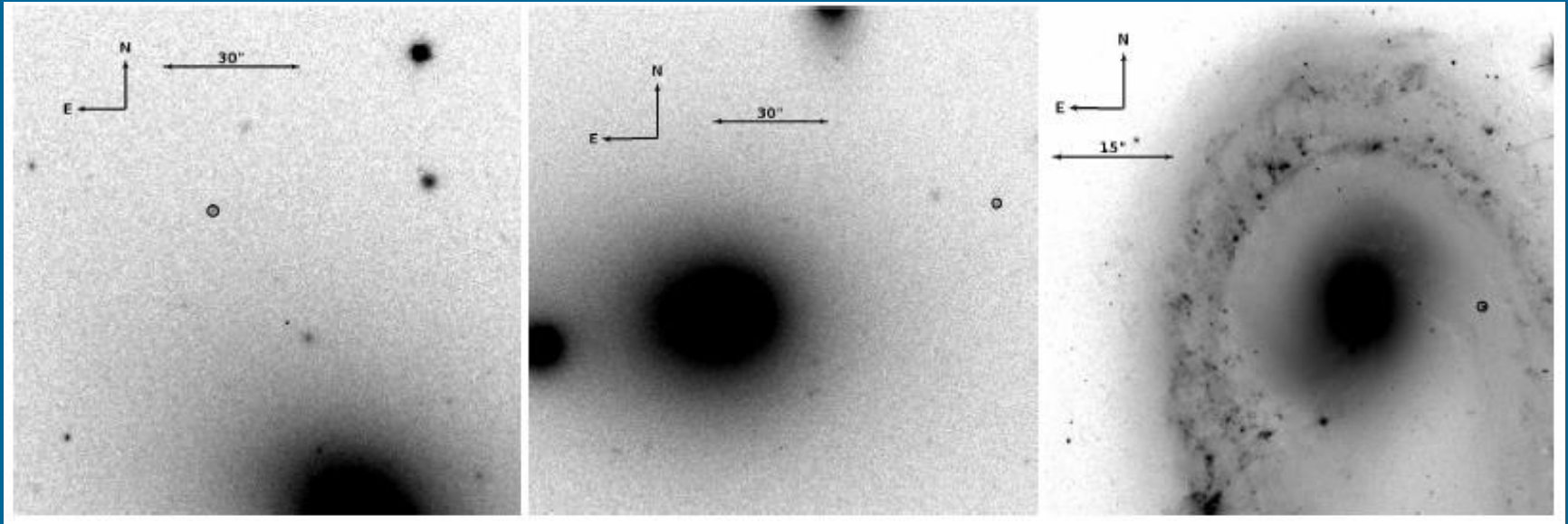
Most probably, the population of ULXs is not uniform.

1. Intermediate mass BHs
2. Collimated emission from normal stellar mass BHs
3. Accreting neutron stars
4. Different types of sources (pulsars, SNR, contamination)
5. Background sources.

The population can grow significantly (~500-600 new candidates) due to new surveys, like 2XMM slew survey (arXiv: 1011.0398), and some other projects (arXiv: 1002.4299).

Mass estimates for BHs (including IMBHs) are well reviewed recently in 1311.5118

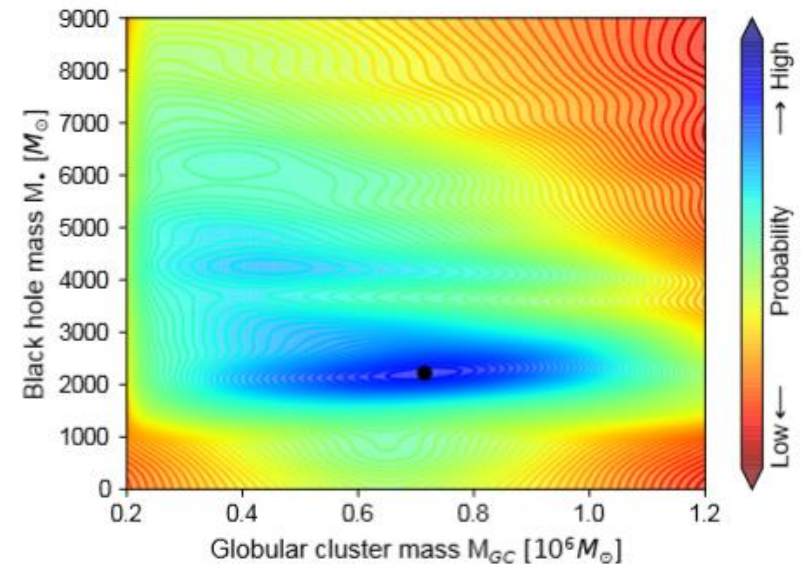
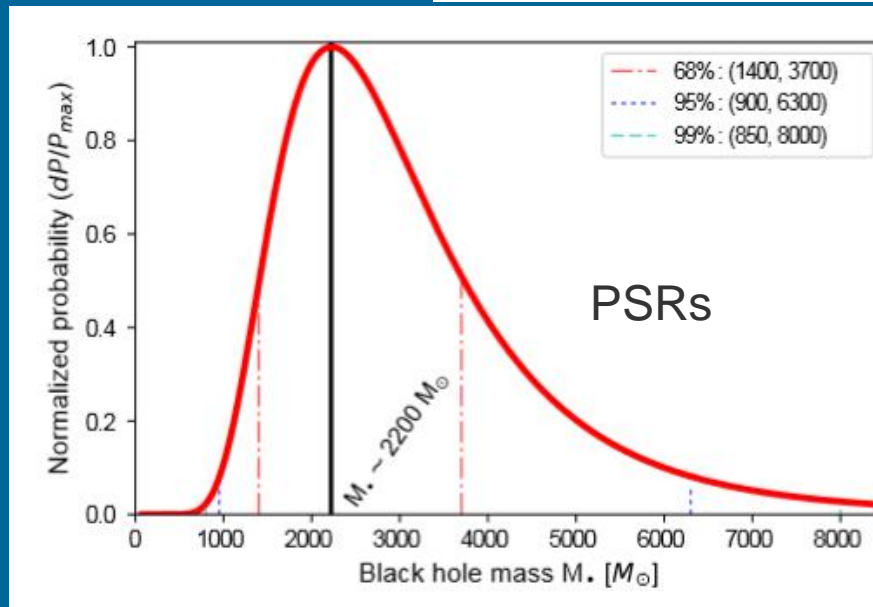
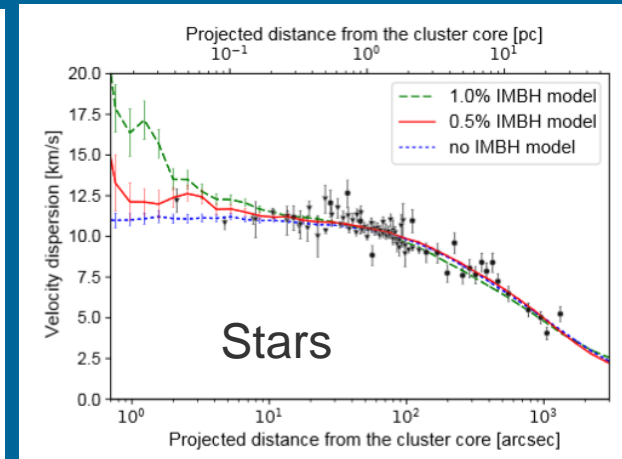
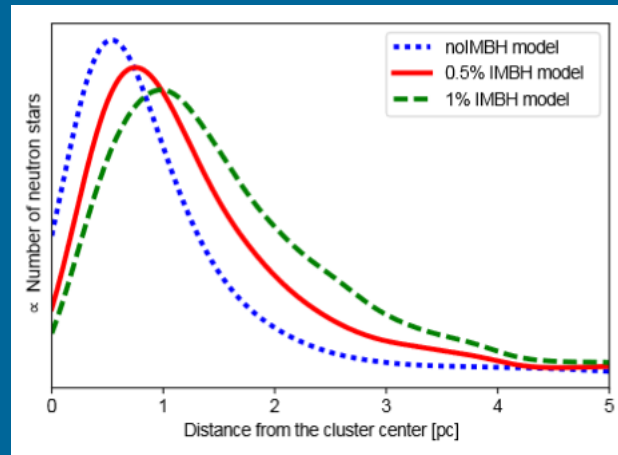
Background sources



Three out of four studied objects appeared to be background AGNs.
The only true ULX is in a spiral galaxy. Two out of false – in ellipticals.

IMBH in 47 Tuc?

Cluster dynamics was probed with radio pulsars.



List of reviews

- Catalogue of LMXBs. Li et al. arXiv:0707.0544
- Catalogue of HMXBs. Li et al. arXiv: 0707.0549
- Modeling accretion: Done et al. arXiv:0708.0148
- Accretion discs: Lasota 1505.02172
- Galactic BH binaries: Paredes arXiv: 0907.3602 
- BH states: Belloni arXiv: 0909.2474; Dunn et al. arXiv: 0912.0142
- X-ray BH binaries: Gilfanov arXiv: 0909.2567
- X-ray observations of ULXs: Roberts. arXiv:0706.2562
- BH binaries and microquasars: Zhang. arXiv: 1302.5485
- BH transients: Belloni. arXiv:1109.3388, 1603.07872
- ULXs: Kaaret et al. 1703.10728, Fabrika 1702.005508
- QPO: Ingram, Motta 2001.08758
- BH spin: Middleton 1507.06153
- IMBHs: Koliapanos 1801.01095, Mezcua 1705.09667
- BH coalescence: Schutz 1804.06308
- BH-BH binaries (stellar and supermassive): Celoria et al. 1807.11489